

FINAL REPORT  
DEVELOPMENT OF IMPROVED GRAPHITE  
FIBER COMPOSITES

14 April 1972 - 11 May 1973

*[Handwritten signature]*  
ADIC USERS ONLY

**DISTRIBUTION STATEMENT A**  
Approved for public release  
Distribution Unlimited

**PHILCO**

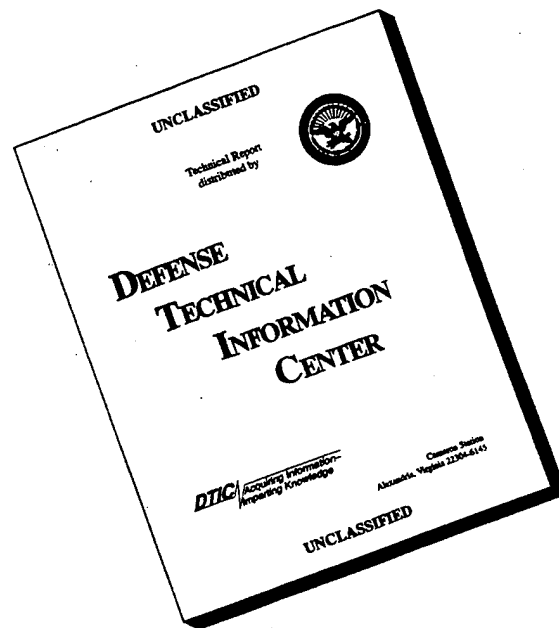


Philco-Ford Corporation  
Aeronutronic Division  
Newport Beach, Calif. • 92663

19960328 090

PLASTIC / 9380

# DISCLAIMER NOTICE



**THIS DOCUMENT IS BEST QUALITY AVAILABLE. THE COPY FURNISHED TO DTIC CONTAINED A SIGNIFICANT NUMBER OF PAGES WHICH DO NOT REPRODUCE LEGIBLY.**

Unclassified

11 May 1973

~~DTIC USERS ONLY~~

FINAL REPORT  
DEVELOPMENT OF IMPROVED GRAPHITE  
FIBER COMPOSITES

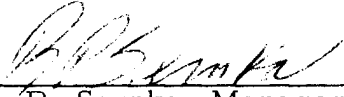
14 April 1972 - 11 May 1973

Prepared for: Naval Air Systems Command  
Washington, D.C.

Under Contract: N00019-71-C-0166

Prepared by: J. L. Perry  
M. L. Damoth  
J. P. Pope

DTIC QUALITY INSPECTED 4

Approved by:   
R. P. Sernka, Manager  
Materials Technology Department

Approved for Public Release: Distribution Unlimited

DISTRIBUTION STATEMENT A  
Approved for public release;  
Distribution Unlimited

**PHILCO** 

Philco-Ford Corporation  
Aeronutronic Division  
Newport Beach, Calif. • 92663

## FOREWORD

This is the final report of work conducted under Naval Air Systems Command Contract No. N00019-71-C-0166 in the area of graphite filament composite materials. It covers the work from April 1972 to May 1973. The Naval Air Systems Command Project Engineer was Mr. M. Stander, Naval Air Systems Command, Department of the Navy, Washington, D.C.

Within Philco-Ford Corporation, management of the contract was assigned to the Aeronutronic Division, Advanced Development Operations, Research Laboratory, Materials Technology Department. Mr. R. P. Sernka was the cognizant department manager. Mr. J. L. Perry, Supervisor, Composites and Graphites Section was the Program Manager. The principal investigators were Mr. John L. Perry, Mr. Michael L. Damoth, and Mr. James P. Pope.

## CONTENTS

SECTION		PAGE
1	INTRODUCTION AND SUMMARY . . . . .	1
2	HYBRID OR MIXED FIBER COMPOSITES . . . . .	4
	2.1 Materials Selection . . . . .	4
	2.2 Panel Fabrication . . . . .	5
	2.3 Panel Characterization . . . . .	11
3	TASK II - FIBER SURFACE TREATMENTS . . . . .	41
	3.1 Experimental Procedure . . . . .	50
	3.2 Discussion of the Experimental Results . . . . .	65
	REFERENCES . . . . .	79
4	CONCLUSIONS AND RECOMMENDATIONS FOR FUTURE WORK . . . . .	81
APPENDICES		
A	MATERIAL SUMMARY . . . . .	A-1
B	MATERIAL PROCESSING PARAMETERS . . . . .	B-1
C	CROSS-SECTIONAL PHOTOMICROGRAPHS, PHOTOMACROGRAPHS OF IMPACT FRACTURE AREAS . . . . .	C-1
D	CHARPY TEST RESULTS AND INTERPRETATION . . . . .	D-1

## ILLUSTRATIONS

FIGURE		PAGE
1	Equipment Set-Up for Fabrication of Test Panels . . . . .	6
2	Application of Weighed Amount of Resin to Winding . . . . .	6
3	Application of Film and Distribution of Resin . . . . .	7
4	Winding in B-Staged Condition . . . . .	7
5	Standard Autoclave Lay-Up . . . . .	9
6	Panel Cutting Diagram . . . . .	10
7	Unidirectional Longitudinal (L) and Transverse (T) Tensile Specimen . . . . .	12
8	Unidirectional Short Beam Shear Specimen . . . . .	12
9	Unidirectional Compression Specimen . . . . .	13
10	Impact Test Setup . . . . .	14
11	Longitudinal Tensile Strengths of Panels . . . . .	20
12	Longitudinal Tensile Modulus of Panels . . . . .	21
13	Longitudinal Strain at Failure of Panels . . . . .	22
14	Transverse Tensile Strength of Panels . . . . .	23
15	Flexural Strength of Panels . . . . .	24
16	Short Beam Shear Strength of Panels . . . . .	25

ILLUSTRATIONS (Continued)

FIGURE		PAGE
17	Flatwise Longitudinal Impact Strength of Panels . . . . .	26
18	Transverse Impact Strength of Panels . . . . .	27
19	Compressive Strength of Panels . . . . .	28
20	200X SEM - Tensile Side of Impact Surface Panel #1, Modulite 5206 . . . . .	34
21	5530X SEM - Fractured Filament on Tensile Side of Impact Surface Panel #1, Modulite 5206 . . . . .	34
22	2210X SEM - Fractured Filament Showing Resin Adherence on Tensile Side of Impact Surface Panel #1, Modulite 5206 . . . . .	35
23	238X SEM - Tensile Side of Impact Surface Panel #2, PRD-49, Type III . . . . .	35
24	1190X SEM - Fractured Filament on Tensile Side of Impact Surface of Panel #2, PRD-49, Type III . . . . .	36
25	238X SEM - Tensile Side of Impact Surface Panel #3, Thornel 400 . . . . .	36
26	2380X SEM - Fractured Filaments on Tensile Side of Impact Surface of Panel #3, Thornel 400 . . . . .	37
27	5950X SEM - Fractured Filament Showing Resin Adherence on Tensile Side of Impact Surface of Panel #3, Thornel 400 . . . . .	37
28	102X SEM - Tensile Side of Impact Surface Panel #4, Boron . . . . .	38
29	535X SEM - Fractured Filament on Tensile Side of Impact Surface, Panel #4, Boron . . . . .	38
30	200X SEM - Tensile Side of Impact Surface of Panel #5, Modulite 5206/PRD-49 . . . . .	39
31	2210X SEM - PRD-49 Filament Showing Mode of Failure on Tensile Side of Impact Surface Panel #5, Modulite 5206/PRD-49 . . . . .	39

ILLUSTRATIONS (Continued)

FIGURE		PAGE
32	Experimental Apparatus for Continuously Coating Graphite Yarn With Carbon . . . . .	42
33	Variation in Interlaminar Shear Strength Resulting From Surface Treatment in Four Different Environments . . . . .	44
34	Effect of the Presence or Absence of Boron on Shear and Tensile Strength . . . . .	46
35	Effect of Dwell Time of the Fiber in the Hot Zone on Shear and Tensile Strength . . . . .	47
36	Comparative Short Beam Shear and Longitudinal Tensile Strength as a Function of the Presence or Absence of Carbon . . . . .	48
37	Effect of Fiber Temperature on Shear and Tensile Strength . . . . .	49
38	Hot Filament Surface Treater . . . . .	53
39	Enclosed Hot Filament Surface Treatment Apparatus . . . . .	56
40	Resistance Furnace Surface Treater . . . . .	58
41	The Free Energy of Formation as a Function of Temperature for Several Reactions Evaluated for CVD Processes . . . . .	66
42	Variation in Yarn Breaking Strength of Control Specimens . . . . .	69
43	Variation in Yarn Breaking Strength Resulting From Heat Treatment in an Inert Environment at Different Temperatures . . . . .	71
44	Effect of Surface Deposited Boron on Yarn Breaking Strength as Function of Deposition Temperature . . . . .	73
45	Apparent Effect of Surface Treatment Apparatus on Resultant Breaking Strength for Two Surface Treatments . . . . .	76
46	Summary and Pattern of the Variation in Yarn Breaking Strength Resulting From Different Surface Treatments . . . . .	77

ILLUSTRATIONS (Continued)

FIGURE		PAGE
C-1	40X Cross-Section of Panel #1 Modulite 5206 . . . . .	C-1
C-2	40X Cross-Section of Panel #2 PRD-49, Type III . . . . .	C-1
C-3	40X Cross-Section of Panel #3 Thornel 400 . . . . .	C-2
C-4	40X Cross-Section of Panel #4 Boron . . . . .	C-2
C-5	40X Cross-Section of Panel #5 Modulite 5206/PRD-49 . . . . .	C-3
C-6	40X Cross-Section of Panel #6 Modulite 5206/PRD-49 . . . . .	C-3
C-7	40X Cross-Section of Panel #7 Modulite 5206/PRD-49 . . . . .	C-4
C-8	40X Cross-Section of Panel #8 Modulite 5206/PRD-49 . . . . .	C-4
C-9	40X Cross-Section of Panel #9 Modulite 5206/Boron . . . . .	C-5
C-10	40X Cross-Section of Panel #10 Modulite 5206/Boron . . . . .	C-5
C-11	40X Cross-Section of Panel #11 Thornel 400/PRD-49 . . . . .	C-6
C-12	40X Cross-Section of Panel #12 Thornel 400/PRD-49 . . . . .	C-6
C-13	40X Cross-Section of Panel #13 S2 Glass . . . . .	C-7
C-14	40X Cross-Section of Panel #14 Modulite 5206/S2 Glass . . . . .	C-7
C-15	40X Cross-Section of Panel #15 Modulite 5206/S2 Glass . . . . .	C-8
C-16	40X Cross-Section of Panel #16 Modulite 5206/PRD-49 . . . . .	C-8
C-17	40X Cross-Section of Panel #17 Modulite 5206/PRD-49 . . . . .	C-9
C-18	40X Cross-Section of Panel #18 Modulite 5206/S2 Glass . . . . .	C-9
C-19	40X Cross-Section of Panel #19 Thornel 400/S2 Glass . . . . .	C-10
C-20	40X Cross-Section of Panel #20 Thornel 400/PRD-49 . . . . .	C-10
C-21	40X Cross-Section of Panel #21 Nomex Nylon . . . . .	C-11
C-22	40X Cross-Section of Panel #22 Modulite 5206/Nomex . . . . .	C-11

ILLUSTRATIONS (Continued)

FIGURE		PAGE
C-23	40X Cross-Section of Panel #23 Modulite 5206/Nomex . . .	C-12
C-24	40X Cross-Section of Panel #24 Modulite 5206/Nomex . . .	C-12
C-25	18X Edge-View of Impact Fracture Area of Panel #1 Modulite 5206 . . . . .	C-13
C-26	18X Edge-View of Impact Fracture Area of Panel #2, PRD-49, Type III . . . . .	C-13
C-27	18X Edge-View of Impact Fracture Area of Panel #3 Thornel 400 . . . . .	C-14
C-28	18X Edge-View of Impact Fracture Area of Panel #4 Boron . . . . .	C-14
C-29	18X Edge-View of Impact Fracture Area of Panel #5 Modulite 5206/PRD-49 . . . . .	C-15
C-30	18X Edge-View of Impact Fracture Area of Panel #6 Modulite 5206/PRD-49 . . . . .	C-15
C-31	18X Edge-View of Impact Fracture Area of Panel #7 Modulite 5206/PRD-49 . . . . .	C-16
C-32	18X Edge-View of Impact Fracture Area of Panel #8 Modulite 5206/PRD-49 . . . . .	C-16
C-33	18X Edge-View of Impact Fracture Area of Panel #9 Modulite 5206/Boron . . . . .	C-17
C-34	18X Edge-View of Impact Fracture Area of Panel #10 Modulite 5206/Boron . . . . .	C-17
C-35	18X Edge-View of Impact Fracture Area of Panel #11 Thornel 400/PRD-49 . . . . .	C-18
C-36	18X Edge-View of Impact Fracture Area of Panel #12 Thornel 400/PRD-49 . . . . .	C-18
C-37	18X Edge-View of Impact Fracture Area of Panel #13 S2 Glass . . . . .	C-19

ILLUSTRATIONS (Continued)

FIGURE		PAGE
C-38	18X Edge-View of Impact Fracture Area of Panel #14 Modulite 5206/S2 Glass . . . . .	C-19
C-39	18X Edge-View of Impact Fracture Area of Panel #15 Modulite 5206/S2 Glass . . . . .	C-20
C-40	18X Edge-View of Impact Fracture Area of Panel #16 Modulite 5206/PRD-49 . . . . .	C-20
C-41	18X Edge-View of Impact Fracture Area of Panel #17 Modulite 5206/PRD-49 . . . . .	C-21
C-42	18X Edge-View of Impact Fracture Area of Panel #18 Modulite 5206/S2 Glass . . . . .	C-21
C-43	18X Edge-View of Impact Fracture Area of Panel #19 Thornel 400/S2 Glass . . . . .	C-22
C-44	18X Edge-View of Impact Fracture Area of Panel #20 Thornel 400/PRD-49 . . . . .	C-22
C-45	18X Edge-View of Impact Fracture Area of Panel #21 Nomex Nylon . . . . .	C-23
C-46	18X Edge-View of Impact Fracture Area of Panel #22 Modulite 5206/Nomex Nylon . . . . .	C-23
C-47	18X Edge-View of Impact Fracture Area of Panel #23 Modulite 5206/Nomex Nylon . . . . .	C-24
C-48	18X Edge-View of Impact Fracture Area of Panel #24 Modulite 5206/Nomex Nylon . . . . .	C-24
D-1	Charpy Testing Apparatus . . . . .	D-2
D-2	Schematic Diagram of the Instrumentation for the Instrumented Charpy Test . . . . .	D-3
D-3	Load-Time and Energy Traces for Modulite 5206, Specimen 26-3 . . . . .	D-6
D-4	Expanded Load-Time Trace of Specimen 26-3 . . . . .	D-6

ILLUSTRATIONS (Continued)

FIGURE		PAGE
D-5	Load-Time and Energy Traces for Modulite 5206/S2 Glass, Specimen 27-2 . . . . .	D-7
D-6	Expanded Load-Time Trace of Specimen 27-2 . . . . .	D-7
D-7	Load-Time and Energy Traces for Modulite 5206/PRD-49, Specimen 28-2 . . . . .	D-8
D-8	Expanded Load-Time Trace of Specimen 28-2 . . . . .	D-8
D-9	Load-Time and Energy Traces for Thornel 400/PRD-49, Specimen 29-2 . . . . .	D-9
D-10	Expanded Load-Time Trace of Specimen 29-2 . . . . .	D-9
D-11	Post Test Specimens Depicting Delamination of Hybrid Panels (27, 28, 29) and Brittle Behavior of Modu- lite 5206 Control Panel (26) . . . . .	D-11

TABLES

TABLE		PAGE
I	Task 1 - Laminate Properties . . . . .	15
II	Hybrid Panel Properties Normalized to Modulite 5206 Data . . . . .	32
III	Typical Chemical Composition of Gas Effluent From Argon-Sealed Surface Treater . . . . .	59
IV	Properties of Materials Evaluated for Task 2 . . . . .	62
V	Properties and Characteristics of Thornel 75S . . . . .	63
VI	Reference Values for Thornel 75S Yarn . . . . .	68
VII	Effect of Heat Cleaning Temperature on Yarn Breaking Strength . . . . .	72
VIII	The Effect of Boron Doping on Thornel 75S Yarn Breaking Strength for Some Deposition Temperatures . . . . .	74
B.1	Laminate Processing Parameters . . . . .	B-1
D.1	Charpy Test Panel Processing Parameters . . . . .	D-4
D.2	Charpy Test Results . . . . .	D-5

## SECTION 1

### INTRODUCTION AND SUMMARY

In many applications of advanced graphite filament composites, the limiting factors in the component design are the transverse tensile, interlaminar shear, or impact properties. These factors restrict the potential use of advanced graphite filament composites in such areas as aircraft surface panels and components and fan blades for advanced air breathing turbine propulsion systems. Their potential use is restricted though other characteristics of the material are competitive or even advantageous over alternate material systems. It was the purpose of this program to explore potential avenues for maximization of these properties. Two technical areas were investigated:

- (1) Hybrid or Mixed Fiber Composites.
- (2) Fiber Surface Treatments.

The first area involved the incorporation of third phase additives in the form of thin reinforcement plies in the composite itself. These reinforcing plies were selected to be of lightweight and of thin construction so they could be incorporated between plies or bundles of graphite filaments without causing significant reductions in graphite filament volume content. Also, investigations were carried out to determine if two relatively new materials, PRD-49, Type III, and Thornel 400 represented a potential for a more balanced combination of composite structural properties. The second area involved the use of boron and boron compounds as a graphite fiber surface treatment to improve interfacial (resin-fiber) bonding properties in the composites.

The following is a summary of the research effort that was accomplished during the program:

- (1) Unidirectional laminates in the combinations listed below were fabricated and tested for determination of longitudinal tensile properties, transverse tensile properties, short beam shear strength, flatwise longitudinal and transverse impact strength, longitudinal flexural strength, and compressive strength.

Base Materials

- (a) Modulite 5206 (M5206)
- (b) PRD-49, Type III
- (c) Thornel 400
- (d) Boron/Tungsten Core
- (e) S2 Glass
- (f) Nomex Nylon

Hybrid Materials

- (g) M5206/PRD-49
- (h) M5206/Boron
- (i) M5206/S2 Glass
- (j) M5206/Nomex
- (k) Thornel 400/PRD-49
- (l) Thornel 400/S2 Glass

- (2) Scanning electron microscope and photomicrographic analyses were performed on selected laminates of the impact fracture surfaces. This revealed evidence for the understanding of the fracture phenomena associated with each material composition.

- (3) The response of the mechanical properties of Thornel 75S (Union Carbide WYJ 160-1/2 yarn) to surface treatment was evaluated. Specimens were prepared in which the surface of the yarn was altered either by heat treatment or by the Chemical Vapor Deposition (CVD) of a suitable surface dopant. The longitudinal tensile strength of the specimen was determined and analyzed to assess the following effects of the process:
- (a) Effect of heat cleaning.
  - (b) Effect of heat cleaning and simultaneous pyrocarbon deposition.
  - (c) Effect of heat cleaning and simultaneous boron deposition.
  - (d) Effect of borocarbon treatment (heat cleaning in presence of boron and carbon).
  - (e) Effect of mechanical degradation as induced by the surface treatment apparatus.
- (4) A limited study was also made of the relative impact characteristics of advanced graphite composites. The particular test employed was a Charpy impact test incorporating an instrumented striker head which provides not only the total amount of energy absorbed by the specimen, but in addition, supplies a load versus time behavior pattern for the specimen. Instrumented impact tests were conducted on Modulite 5206 graphite control specimens and on hybrid composite specimens of 5206/glass, 5206/PRD-49, and Thornel 400/PRD. The load versus time data demonstrated the large energy absorption characteristics of the hybrid composite specimens and identified significant and subtle differences in fracture energy levels.

## SECTION 2

### HYBRID OR MIXED FIBER COMPOSITES

This approach to improvement of impact properties involves the use of third phase additives. An existing two phase system of resin and graphite filaments is purposely modified through the addition of a third phase material which in this program was in the form of thin supplemental reinforcements. The basic reasoning involved in utilizing thin reinforcements as third phase additives in composites is that improved toughness will result without adverse effects on other mechanical properties. This program investigated the effects of selected additives to determine which ones optimized this desired effect.

#### 2.1 MATERIALS SELECTION

##### 2.1.1 BASELINE MATERIAL

The baseline composite composition used throughout this phase of the investigation was Modulite 5206 as manufactured by Whittaker Corporation, Narmco Materials Division. Modulite 5206 consists of collimated Modmor II graphite filaments preimpregnated with Narmco-1004 epoxy resin. The Modmor II filaments with a  $35 \times 10^6$  psi elastic modulus and 350,000 psi tensile strength are manufactured from 10,000 filament end polyacrylonitrile (PAN) precursor tow bundles. The material was procured in meter length grade and certified to specification DMS 1936B written by McDonnell-Douglas Corporation in Long Beach, California. Typical material properties are summarized in Appendix A. The DMS-1936B material results in a cured ply thickness of 0.006 to 0.007 inch.

### 2.1.2 THIRD PHASE MATERIALS

The third phase supplemental reinforcement interply materials selected for evaluation are as listed below:

- (1) PRD-49, Type III
- (2) S2CG Glass
- (3) Nomex Nylon
- (4) Boron/Tungsten Core

These reinforcement materials were considered to be of thin construction so as not to represent a significant volume in the laminate, and thereby effectively minimizing reduction of directional mechanical properties while offering potential for increased composite toughness and impact efficiency. A description and summary of the selected materials appears in Appendix A.

Narmco 1004 epoxy resin was used for all impregnation requirements.

### 2.1.3 ALTERNATE MATERIAL SYSTEM

Additionally, Thornel 400 (WYM 60 1/0), a Union Carbide PAN based yarn, was evaluated individually and in conjunction with several of the above supplemental reinforcements. Its higher strain capability (1.3 percent reported), along with high tensile strength, makes it a candidate for increased impact efficiency.

## 2.2 PANEL FABRICATION

The third phase supplemental reinforcement interply materials were fabricated into plies separately and B-staged with Narmco 1004 epoxy resin with the exception of boron filament reinforcement material. The boron was purchased as a preimpregnated tape from 3M Company identified as SP-272 Epoxy-Boron filament prepreg. The prepreg properties are described in Appendix A. The prepreg resin used by 3M is a high fracture toughness epoxy resin identified as PR-279. The material as cured results in a per ply thickness of 0.005 inch. All remaining interply materials were prepared by drum winding as illustrated in Figures 1 through 4.

The fibers are dry wound over a 0.003-inch thick sheet of Armalon 403F "Teflon" coated glass fabric placed on a drum 25.08 inches in circumference. Fiber tension is controlled as the fiber comes off the spool through the use of a Stearns electric clutch shown in the upper left corner of Figure 1. Drum speed is controlled by utilizing a Bodine dc variable speed drive motor. The Bodine motor also drives a Graham variable speed drive

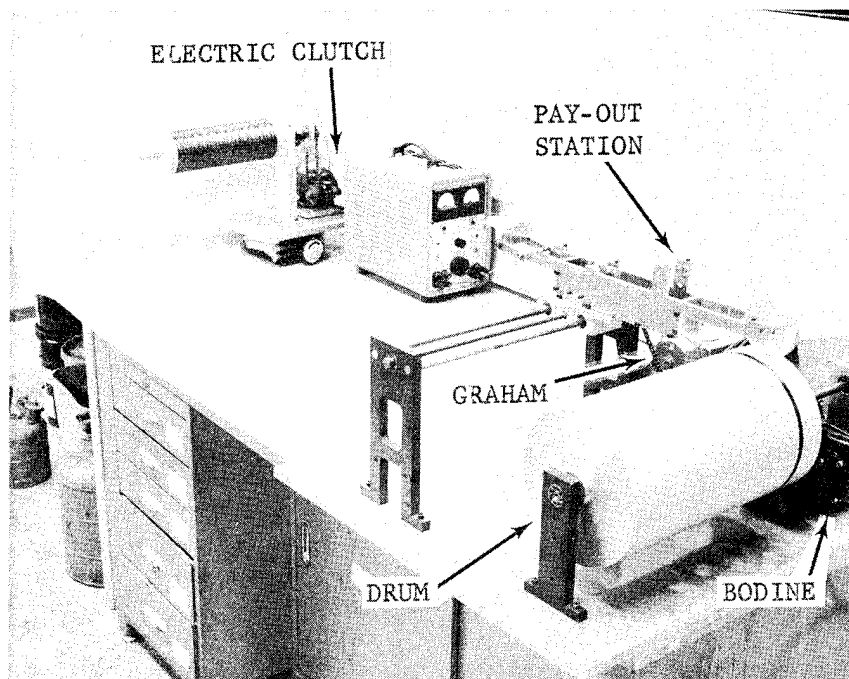


FIGURE 1. EQUIPMENT SET-UP FOR FABRICATION OF TEST PANELS.

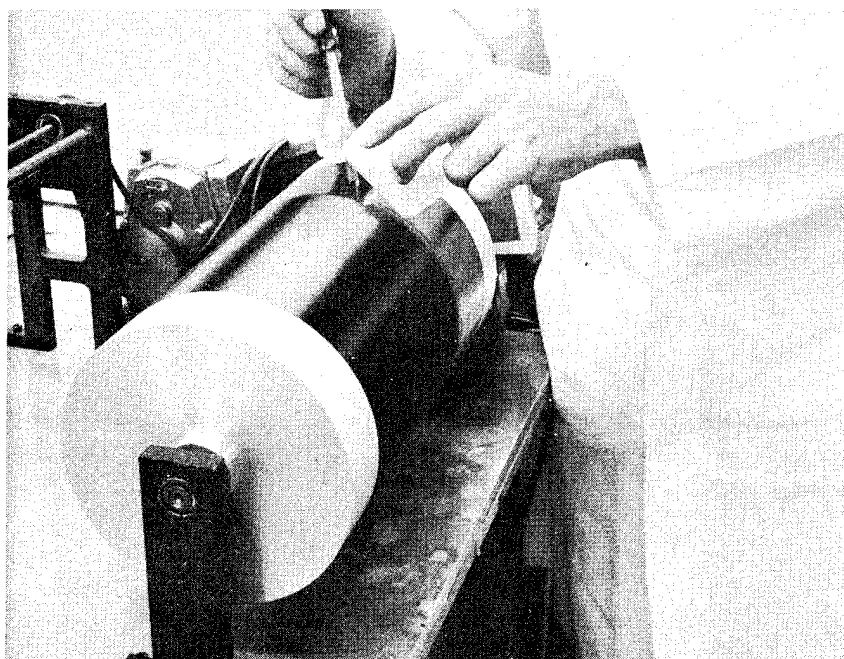


FIGURE 2. APPLICATION OF WEIGHED AMOUNT OF RESIN TO WINDING

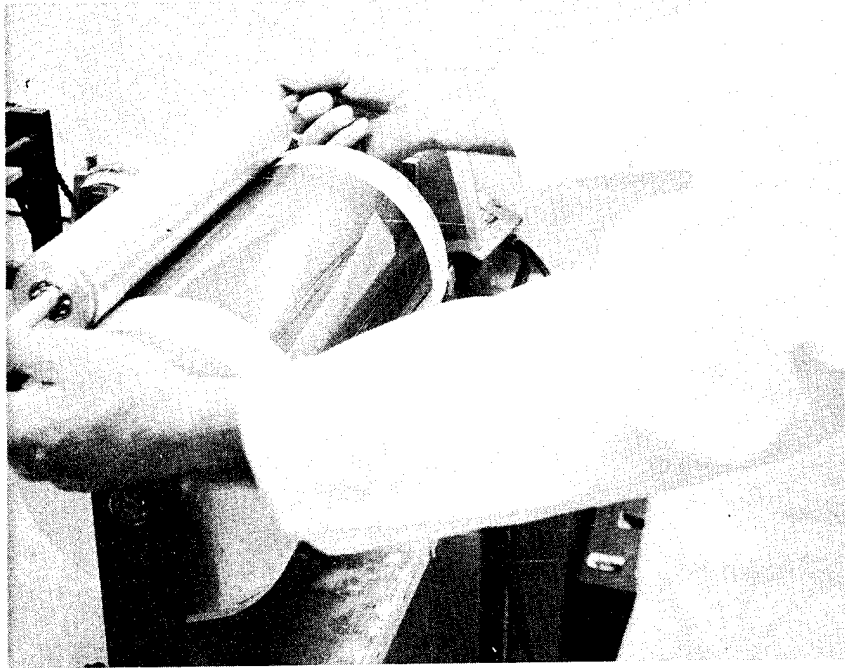


FIGURE 3. APPLICATION OF FILM AND DISTRIBUTION OF RESIN

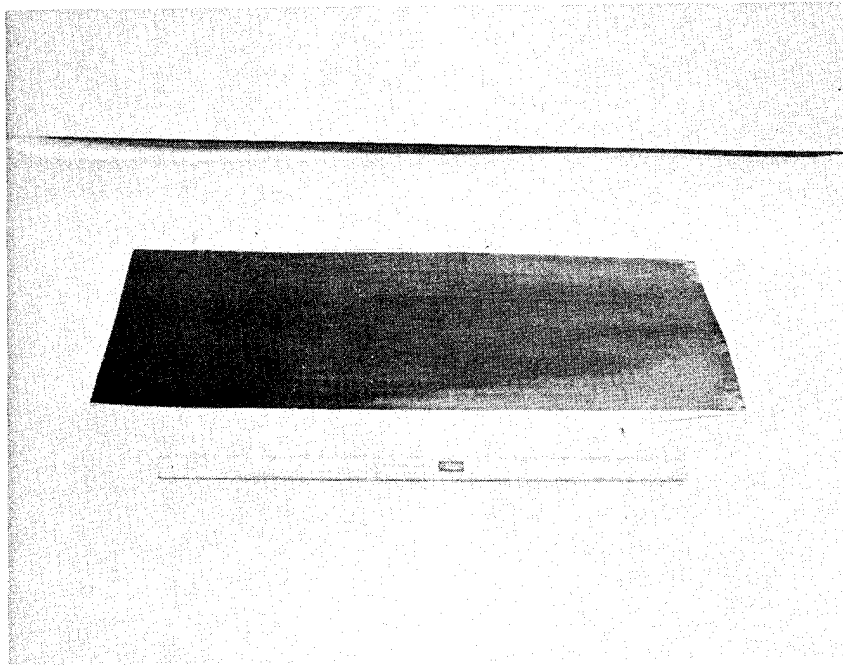


FIGURE 4. WINDING IN B-STAGED CONDITION

mechanism which rotates the lead screw, thereby moving the traversing payout station. Thus, the yarn payout per revolution of the drum (pick count) is controlled and synchronized.

When the required panel width is reached, knowing the weight of yarn per revolution of the drum and the total number of drum revolutions, a measured amount of resin per total weight of yarn is distributed on the fibers while the drum is slowly revolving as shown in Figure 2. A thin transparent sheet of plastic is then placed over the winding to prevent rapid loss of solvent. The winding is then rolled until an even distribution of resin is obtained as shown in Figure 3. The winding is next sliced perpendicular to the fibers, laid out flat, and B-staged at 150°F until the volatile content is lowered to approximately 2 to 5 percent by weight. The B-staged panel is shown in Figure 4.

The panel is next cut into either 3- by 8-inch plies (for thick laminates - 0.090 inch) or 5- by 7-inch plies (for thin laminates - 0.030 inch). The required number of plies are stacked and placed in the standard layup for autoclave curing illustrated in Figure 5. The temperature of the laminate is increased to 275°F and held at that temperature with only vacuum bag pressure applied. At that point, the vacuum is released, the bag vented to the atmosphere, and 100 psig autoclave pressure applied. The laminate temperature is next increased to 355°F and held for 2 hours. The laminates are then allowed to cool to room temperature under pressure. Thin laminates (~0.030 inch) were prepared for all tensile testing and thick (~0.090 inch) laminates were prepared for short beam shear, impact, flexural, and compressive testing as shown in Figure 6. All laminates were fabricated in a unidirectional manner with both primary reinforcement and supplemental interply reinforcement-oriented in the same direction.

Panel configurations were selected to give varying amounts of fiber volume of supplemental reinforcement. The panel configurations are shown below:

- (1) Alternating plies of primary and supplemental reinforcement yielding 25 to 35 percent (of total laminate volume) supplemental fiber volume.
- (2) 3:1:3:1:3:1:3 construction (3 plies of primary reinforcement and 1 ply of supplemental reinforcement) yielding 9 to 15 percent (of total laminate volume) supplemental fiber volume.
- (3) 4:1:4:1:4:1 construction (4 plies of primary reinforcement and 1 ply of supplemental reinforcement) yielding 10 to 16 percent (of total laminate volume) supplemental fiber volume.

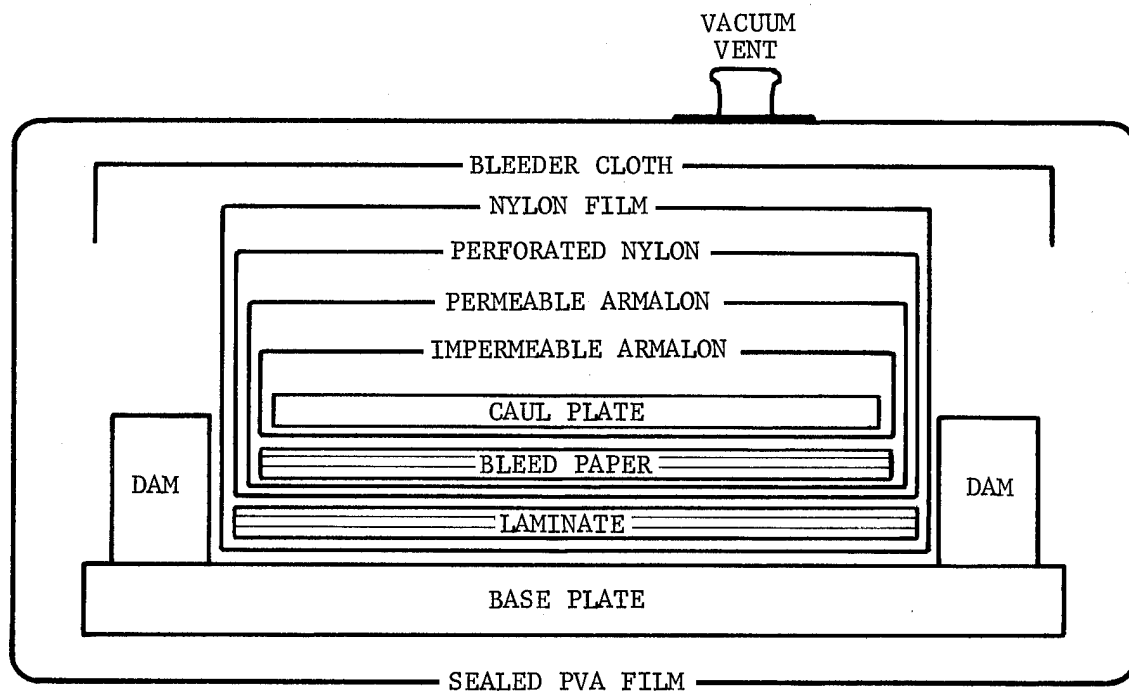
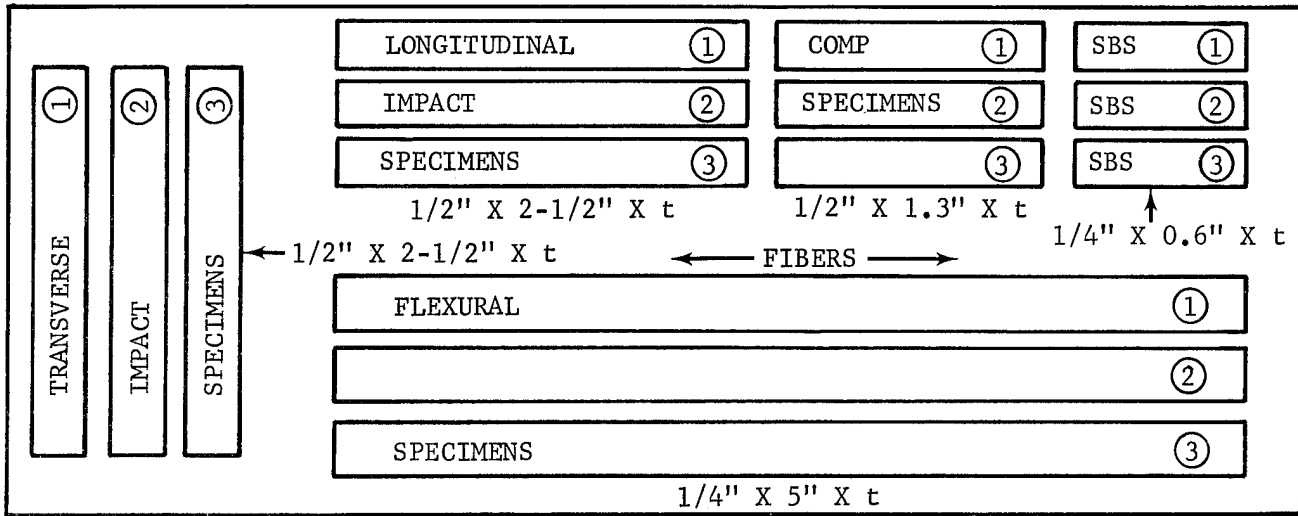


FIGURE 5. STANDARD AUTOCLAVE LAY-UP

3" X 8" PANELS



5" X 7" PANELS

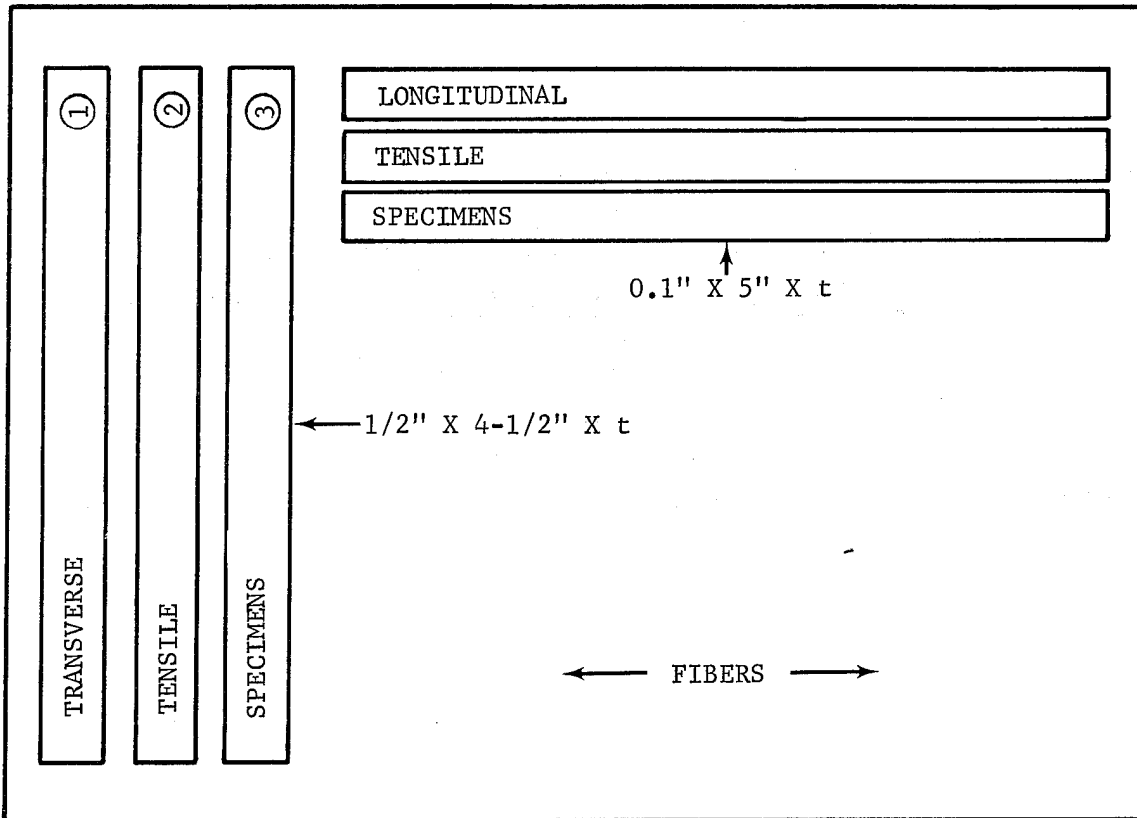


FIGURE 6. PANEL CUTTING DIAGRAM

## 2.3 PANEL CHARACTERIZATION

### 2.3.1 PANEL PROCESSING PARAMETERS

Each panel fabricated was analyzed to determine its processing characteristics. Those results are summarized in Appendix B.

### 2.3.2 TEST METHODS

The following tests were employed to characterize the panels:

- (1) Longitudinal tensile
- (2) Transverse tensile
- (3) Short beam shear
- (4) Compressive
- (5) Flexure
- (6) Izod impact

Longitudinal and transverse tensile specimens were machined from the 0.030-inch laminates in the configuration shown in Figure 7. Glass/epoxy tabs 0.032 inch thick were bonded to each side of each end to facilitate gripping of the specimen. The specimens were tested on a standard Instron test machine with load being measured by load cell and elongation by extensometer via X-Y recorder. Head travel was 0.05 inch per minute.

Short beam shear, impact, compression, and flexural specimens were machined from the 0.090 inch laminates. The short beam shear specimens were machined and tested in the configuration shown in Figure 8. Testing was performed in a standard Instron test machine at 0.05 inch per minute. The ultimate load carried by the specimen was chosen as the point of shear failure. Compression testing was also performed in the Instron test machine at a loading rate of 0.05 inch per minute. The specimens as tested were 0.50 inch wide by 1.30 inches long with a reduced gage section as shown in Figure 9. Each end of each test specimen was contained within an end clamp jig and aligned between flat and parallel loading plates during testing. For the flexural tests, three point loading was employed with a beam span of three inches. Testing was performed on a standard Instron test machine at a speed of 0.05 inch per minute. Specimen deflection was measured by an extensometer probe placed at midspan directly under the center loading point.

The impact testing was conducted at Delsen Corporation. An Izod type specimen was utilized and tested per ASTM-D-256, Method A as shown in

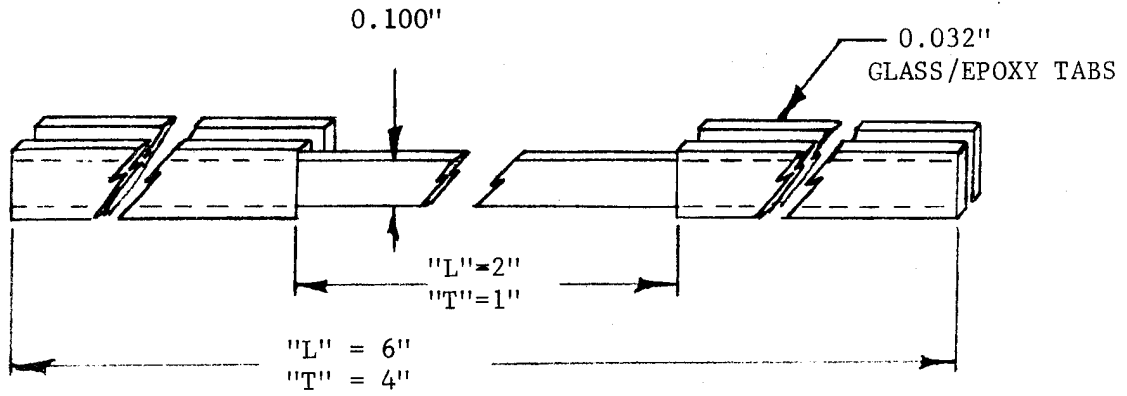


FIGURE 7. UNIDIRECTIONAL LONGITUDINAL (L) AND TRANSVERSE (T) TENSILE SPECIMEN

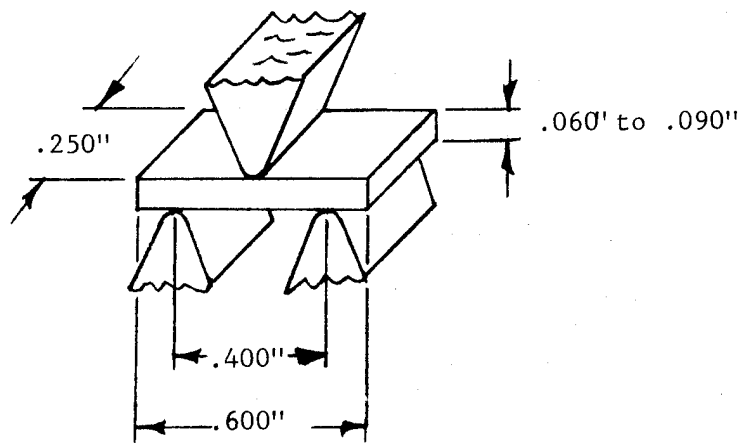


FIGURE 8. UNIDIRECTIONAL SHORT BEAM SHEAR SPECIMEN

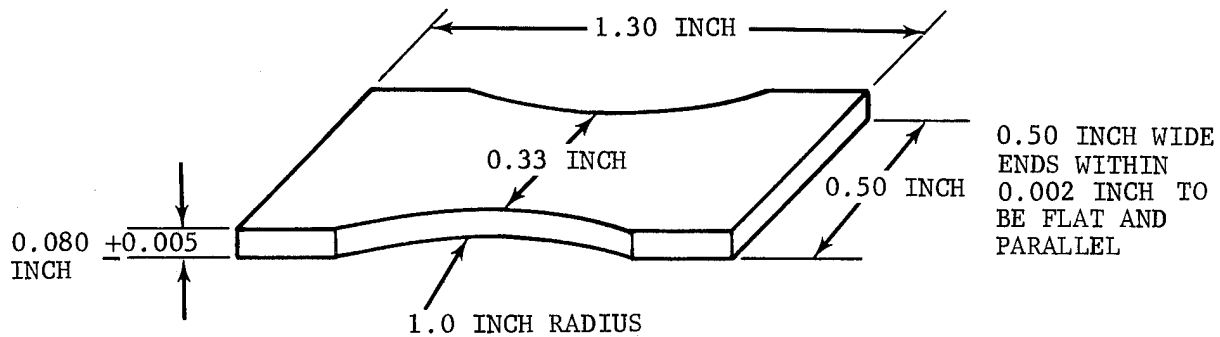


FIGURE 9. UNIDIRECTIONAL COMPRESSION SPECIMEN

Figure 10. An unnotched specimen configuration 0.5 x 2-1/2 inches was used. The specimen is gripped in vise type grips with 1/2 of its length free. The pendulum type striker head is released and impacts the free end of the specimen. The energy absorbed is recorded in foot-pounds. The results are then normalized per inch of width and thickness so that relative analyses can be made. The specimens can be tested in either longitudinal or transverse impact mode. Both were tested in the flatwise condition.

A diamond wafering saw was used to machine all specimens.

### 2.3.3 TEST RESULTS

The test results of all panels fabricated are summarized in Table I. Panels of the basic materials used in the program (no supplemental reinforcement) were fabricated and tested to provide a data base for hybrid panel comparisons. Exceptionally good longitudinal properties were achieved with the Modulite 5206 (panel No. 1) baseline material. The tensile strength was approximately 29 percent higher (240 ksi) than that obtained in the previous years work (Reference 4), along with higher strain at failure (1.1 percent) and higher flatwise longitudinal impact strength (27.8 ft-lb/inch W/inch T).

Two panels were fabricated using PRD-49 III (panels No. 2 and 2A) as primary reinforcement. Higher longitudinal properties were realized with panel No. 2A (versus No. 2) and is attributed to the higher filament volume present (~75 percent versus 59 percent). The PRD-49 III panels are characterized by good strain to failure (1.7 percent), low transverse tensile strength (1.85 ksi) and short beam shear strength (9.4 ksi), low transverse impact strength (1 ft-lb/inch W/inch T), and high longitudinal impact strength (76 ft-lb/inch W/inch T). The longitudinal impact strength is 275 percent greater than a panel composed solely of Modulite 5206. At the target 60 percent fiber volume, the resulting per ply thickness of PRD-49 III is ~3.1 mils.

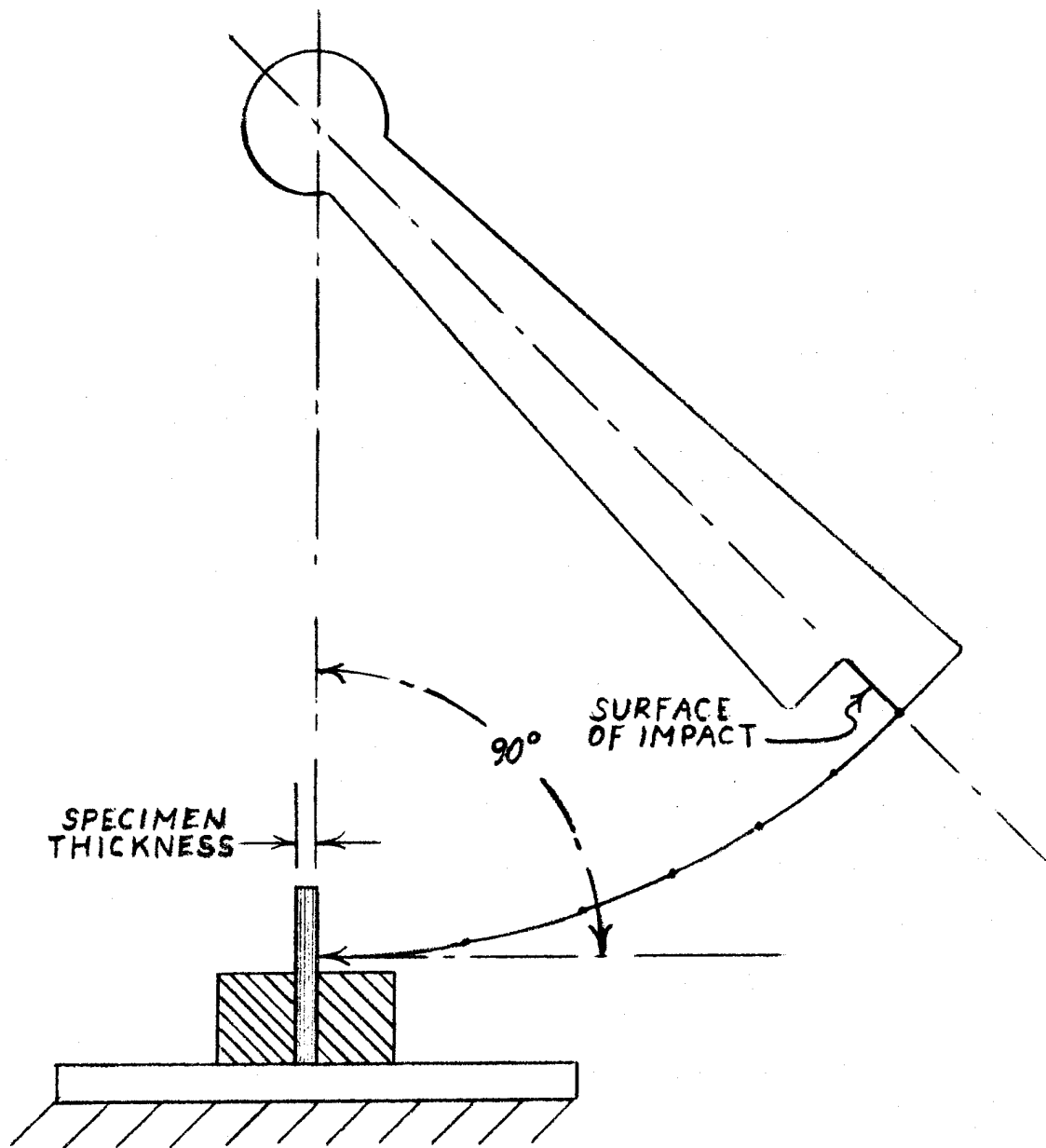


FIGURE 10. IMPACT TEST SETUP

TABLE I. TASK 1 - LAMINATE PROPERTIES

Physical Properties				Mechanical Properties									
Base Material	Interply Material	Interply Orientation	Panel Construction (1)	Long Tensile ksi	Long Modulus PSIx10 <sup>6</sup>	Max Long Strain %	Trans Tensile ksi	Flex Strength ksi	Flexural Modulus PSIx10 <sup>6</sup>	Short Beam Shear Str ksi	Flat Long Impact Str Ft-Lbs/Inch I/Inch W	Trans Impact Str Ft-Lbs/Inch I/Inch W	Comp Strength ksi
1. Modallite 5206	None	-	Thin - 5 plies Thick - 15 plies ~7.0 mils/ply	235.0	18.6	1.1	8.44	221.7	17.2	15.98	30.6	2.39	109.1
				233.0	20.1	1.2	8.49	208.8	18.1	15.96	27.7	2.02	90.5
				231.6	20.2	1.1	8.23	214.7	19.8	16.17	23.2	2.52	130.5
2. PRD-49 III 1004 Epoxy	None	-	Thin - 10 plies Thick - 24 plies ~3.1 mils/ply	239.9	19.7	1.1	8.65	215.1	18.4	16.04	27.8	2.31	110.0
				155.6	10.4	2.4	1.98	ND	ND	9.18	76.8	ND	35.0
				148.6	12.5	1.3	1.71	88.9	11.8	9.53	80.3	5.85	36.5
2A. PRD-49 III 1004 Epoxy	None	-	Thin - 7 plies Thick - 22 plies ~4.3 mils/ply	140.1	11.2	1.4	0.38(2)	88.1	ND	5.94	91.0	1.18	38.8
				148.1	11.4	1.7	0.37	85.5	12.3	6.21	87.1	0.70	--
				155.1	12.5	1.4	0.24	87.5	10.6	6.00	96.2	1.07	--
3. Thorneil 400 1004 Epoxy	None	-	Thin - 5 plies Thick - 15 plies ~6.0 mils/ply	151.2	17.9	0.8	8.71	264.5	9.1	13.5	33.3	1.37	131.5
				208.3	19.6	1.1	8.61	225.0	18.3	13.3	39.5	1.18	121.9
				171.8	19.0	0.9	7.55	254.9	11.4	13.7	42.9	0.79	107.9
4. Boron Tape	None	-	Thin - 6 plies Thick - 18 plies ~4.4 mils/ply	177.1	18.8	0.9	8.29	248.1	13.0	13.5	38.6	1.11	120.4
				184.7	38.5	0.5	6.79	ND	ND	17.5	36.8	1.04	184.6
				198.6	38.7	0.6	6.81	141.8(2)	9.8	17.2	38.3	1.07	195.3
13. S2 Glass 1004 Epoxy	None	-	Thin - 18 plies Thick - 30 plies ~3.0 mils/ply	195.3	36.6	0.6	6.79	275.6	9.2	6.77	167.0	1.48	110.6
				192.9	37.9	0.6	6.80	275.1	9.4	6.53	34.9	2.08	173.2
				233.2	8.96	2.4	6.13	266.3	9.4	6.71	36.7	1.40	184.4
				260.9	9.22	2.7	6.17	266.3	9.4	6.71	17.3	172.0	

NOTES: (1) 0.030" Laminates used for tensile testing, 0.090" Laminates used for short beam shear, impact, and compression testing.

(2) Value not used in average-specimen sub-normal.

(3) Values yet to be determined at time of report.

(4) ND = No Data

TABLE I. TASK 1 - LAMINATE PROPERTIES (Continued)

Physical Properties				Mechanical Properties									
Base Material	Interply Material	Interply Orientation	Panel Construction (1)	Long Tensile ksi	Long Modulus PSIx10 <sup>6</sup>	Max Long Strain %	Trans Tensile ksi	Flex Strength ksi	Flexural Modulus PSIx10 <sup>6</sup>	Short Beam Shear Str ksi	Flat Long Impact Str Ft-Lbs/Inch T/Inch W	Trans Impact Str Ft-Lbs/Inch T/Inch W	Comp Strength ksi
5. Modulite 5206	PRD-49 III	0°	Thin -       Thick -       where   = MOD 5206 : = PRD-49	167.6 174.2 190.8 177.5	15.8 15.2 18.2 16.4	1.0 1.1 1.0 1.0	4.35 4.42 5.00 4.59	ND	ND	13.9 13.3 13.9 13.6	76.2 75.0 85.0 78.7	1.57 1.58 1.72 1.62	101.0 99.7 100.6 100.4
6. Modulite 5206	PRD-49 III	0°	Thin -       Thick -       where   = MOD 5206 : = PRD-49	221.4 208.0 175.6 201.7	20.3 17.9 19.5 19.2	1.1 1.1 0.9 1.0	7.31 7.08 7.10 7.16	ND	ND	13.0 12.0 11.8 12.3	36.2 45.6 42.8 41.5	1.78 2.69 1.71 2.09	105.8 105.8 (2) 103.8 104.8
7. Modulite 5206	PRD-49 III	0°	Long, Impact Specimens Only Thin -       Thick -       where   = MOD 5206 : = PRD-49	ND	ND	ND	ND	ND	ND	ND	62.3 55.4 46.3 54.7	ND	ND
8. Modulite 5206	PRD-49 III	0°	Long, Impact Specimens Only Thin -       Thick -       where   = MOD 5206 : = PRD-49	ND	ND	ND	ND	ND	ND	ND	36.7 38.4 35.2 36.8	ND	ND
9. Modulite 5206	Boron	0°	Thin -       Thick -       where   = MOD 5206 : = Boron	142.7 157.7 142.4 147.6	25.4 26.7 23.2 25.1	0.6 0.7 0.5 0.6	4.24 3.40 3.69 3.78	ND	ND	7.53 8.52 7.25 7.93	58.1 53.7 52.3 54.7	3.33 3.28 2.48 3.03	91.3 101.8 129.1 107.4
10. Modulite 5206	Boron	0°	Thin -       Thick -       where   = MOD 5206 : = Boron	162.3 174.4 188.9 175.2	22.4 22.7 21.8 22.3	0.8 0.9 1.0 0.9	4.86 5.56 5.81 5.41	ND	ND	10.6 10.5 13.1 11.4	40.6 40.9 37.3 39.6	1.70 1.72 1.68 1.70	94.9 112.7 113.9 107.2
11. Thornel 400	PRD-49 III	0°	Thin -       Thick -       where   = Thornel 400 : = PRD-49	273.5 272.3 265.0 270.3	18.5 18.4 18.8 18.6	1.6 1.5 1.5 1.5	5.44 4.85 4.67 4.99	ND	ND	10.6 11.3 11.0 11.0	76.9 (2) 111.7 101.7 106.7	0.83 0.82 1.70 1.12	64.0 69.8 62.1 65.3
12. Thornel 400	PRD-49 III	0°	Thin -       Thick -       where   = Thornel 400 : = PRD-49	216.8 250.8 242.2 236.6	20.5 20.8 20.4 20.6	1.3 1.0 1.1 1.1	6.08 6.19 5.31 5.86	ND	ND	12.5 12.1 12.3 12.3	72.8 83.5 63.6 73.3	0.95 0.93 1.88 1.25	79.1 81.2 83.2 81.2

NOTES: (1) 0.030" laminates used for tensile testing, 0.090" laminates used for short beam shear, impact, and compression testing.  
 (2) Value not used in average, specimen sub-normal.  
 (3) Values yet to be determined at time of report.  
 (4) ND = No Data

TABLE I. TASK 1 - LAMINATE PROPERTIES (Continued)

TABLE I. TASK 1 - LAMINATE PROPERTIES (Continued)

		Physical Properties				Mechanical Properties									
Base Material	Interply Material	Interply Orientation	Panel Construction (1)	Long Tensile ksi	Long Modulus PSiX10 <sup>6</sup>	Max Long Strain %	Trans Tensile ksi	Flex Strength ksi	Flexural Modulus PSiX10 <sup>6</sup>	Short Beam Shear Str ksi	Flat Long Impact Str Ft-Lbs/Inch T/Inch W	Trans Impact Str Ft-Lbs/Inch T/Inch W	Comp Strength ksi		
14. ModuLite 5206	S2 Glass	0°	Thin -  Thick -  where  = MOD 5206 = S2	181.3 196.5 191.8 189.9	17.9 13.3 13.5 14.9	ND 1.1 1.1 1.1	9.17 6.77 9.54 8.49	250.1 230.5 267.2 249.5	15.8 14.6 13.6 14.7	15.8 15.9 15.3 15.7	159.0 155.0 144.0 153.0	1.72 1.89 1.42 1.68	127.6 149.3 138.4 138.4		
15. ModuLite 5206	S2 Glass	0°	Thin -  Thick -  where  = MOD 5206 = S2	223.2 172.6 215.4 203.7	18.2 17.5 19.0 18.2	1.2 0.9 ND 1.1	8.58 8.97 4.50(2) 8.77	209.6 257.5 257.4 241.5	16.7 16.5 18.5 17.3	16.2 15.2 16.1 15.8	74.9 73.8 66.8 71.8	2.06 2.04 1.10 1.73	114.6 113.2 141.1 123.0		
16. ModuLite 5206	PRD-49 III	0°	Thin - None - Impact Specimens Only Thick -  where  = MOD 5206 = PRD-49	ND	ND	ND	ND	ND	ND	ND	45.5 48.0 62.8 52.1	1.26 0.95 1.76 1.32	ND		
17. ModuLite 5206	PRD-49 III	0°	Thin - None (see Panel 6 Data) Thick -  where  = MOD 5206 = PRD-49	220.0 209.0 225.0 218.0	16.7 16.9 17.3 17.0	See Panel 6 Data	See Panel 6 Data	220.0 209.0 225.0 218.0	16.7 16.9 17.3 17.0	13.6 13.9 9.8 12.4	48.5 55.0 46.7 39.2 47.4	0.34 0.67 0.49 0.50	129.0 116.0 124.0 118.0 122.0		
18. ModuLite 5206	S2 Glass	0°	Thin - None (see Panel 15 Data) Thick -  where  = MOD 5206 = S2	165.0 226.0 213.0 201.0	15.4 16.3 16.7 16.1	See Panel 15 Data	See Panel 15 Data	165.0 226.0 213.0 201.0	15.4 16.3 16.7 16.1	15.3 14.5 14.3 14.7	64.7 88.7 62.9 44.4 65.2	0.89 0.84 0.51 0.75	153.0 141.0 125.0 140.0		
19. Thornel 400	S2 Glass	0°	Thin -  Thick -  where  = Thornel 400 = S2	168.4 147.4 155.5 157.1	15.9 15.2 16.0 15.7	1.0 1.0 1.0 1.0	5.78 6.87 7.19 6.61	230.0 210.0 211.0 217.0	14.1 13.9 13.9 14.0	13.6 14.1 13.4 13.7	141.0 148.0 126.0 131.0 137.0	1.21 1.70 1.75 1.55	127.0 143.0 150.0 140.0		

NOTES: (1) 0.030" laminates used for tensile testing, 0.090" laminates used for short beam shear, impact, and compression testing.  
 (2) Value not used in average-specimen sub-normal.  
 (3) Values yet to be determined at time of report.  
 (4) ND = No Data

TABLE I. TASK 1 - LAMINATE PROPERTIES (Continued)

Physical Properties				Mechanical Properties									
Base Material	Interply Material	Interply Orientation	Panel Construction (1)	Long Tensile ksi	Long Modulus PSIx10 <sup>6</sup>	Max Long Strain %	Trans Tensile ksi	Flex Strength ksi	Flexural Modulus PSIx10 <sup>6</sup>	Short Beam Shear Str ksi	Flat Long Impact Str Ft-lbs/Inch T/Inch W	Trans Impact Str Ft-lbs/Inch T/Inch W	Comp Strength ksi
Basic Materials	None	-	Thin - 5 plies Thick - 15 plies ~7.1 mils/ply	216.2	20.7	1.1	5.59	203.0	17.8	14.4	38.2	0.94	121.0
				221.6	20.7	1.0	3.99	227.0	15.1	12.3	38.6	1.22	129.0
Basic Materials	None	-	Thin - 7 plies Thick - 21 plies ~4.2 mils/ply	216.8	22.7	1.1	4.79	248.0	18.1	13.5	40.2	1.08	145.0
				218.2	21.4	1.1	4.79	226.0	17.0	13.4	37.4	1.08	132.0
Basic Materials	None	-	Thin - 7 plies Thick - 21 plies ~4.2 mils/ply	45.4	1.68	>3.2	2.35	52.1	1.7	4.42	88.9	0.77	36.4
				43.5	1.72	>3.2	2.98	53.5	1.8	6.72	72.3	0.62	32.2
Basic Materials	None	-	Thin - 7 plies Thick - 21 plies ~4.2 mils/ply	46.7	1.66	>3.2	2.39	58.9	1.8	4.85	79.4	0.61	35.2
				45.2	1.69	>3.2	2.57	54.8	1.8	5.33	81.2	0.66	34.6
Third Phase Laminates	FRD-49 III	0°	Thin - None (see Panel 12 Data) Thick -       where   = Thornel 400 : = FRD-49	204.0		See Panel 12 Data		204.0	16.8	12.6	77.4	1.00	114.0
				206.0				206.0	15.8	12.6	83.3	1.03	118.0
Third Phase Laminates	Nomex	0°	Thin -       Thick -       where   = MOD 5206 : = Nomex	191.0				191.0	16.3	12.1	60.0	1.46	128.0
				200.0				200.0	16.3	12.5	74.4	1.16	120.0
Third Phase Laminates	Nomex	0°	Thin -       Thick -       where   = MOD 5206 : = Nomex	119.3	13.3	0.9	4.88	184.0	12.1	8.87	33.7	0.85	99.1
				122.6	10.9	1.1	4.77	171.0	11.4	6.79	28.9	0.67	104.0
Third Phase Laminates	Nomex	0°	Thin -       Thick -       where   = MOD 5206 : = Nomex	117.2	12.0	1.0	4.68	176.0	11.2	9.44	41.7	0.83	110.0
				119.7	12.1	1.0	4.77	176.0	11.6	8.37	28.3	0.78	104.0
Third Phase Laminates	Nomex	0°	Thin -       Thick -       where   = MOD 5206 : = Nomex	96.2	16.6	0.9	9.38	225.0	17.7	14.1	20.2	1.75	125.0
				136.0	17.6	0.8	9.65	217.0	18.3	12.6	26.6	1.75	167.0
Third Phase Laminates	Nomex	0°	Thin -       Thick -       where   = MOD 5206 : = Nomex	87.8	16.0	0.5	8.28	219.0	15.7	12.1	19.3	1.05	132.0
				106.7	16.7	0.7	9.10	220.0	17.2	12.9	30.5	1.52	134.0
Third Phase Laminates	FRD-49 III	0°	Thin -       Thick -       where   = Thornel 400 : = FRD-49	203.0		See Panel 23 Data		203.0	14.6	9.13	17.9	1.53	117.0
				219.0				219.0	15.9	8.39	26.3	1.53	136.0
Third Phase Laminates	FRD-49 III	0°	Thin -       Thick -       where   = Thornel 400 : = FRD-49	189.0				189.0	12.2	7.31	18.5	1.03	126.0
				204.0				204.0	14.3	8.28	19.5	1.36	126.0
Third Phase Laminates	FRD-49 III	0°	Thin -       Thick -       where   = Thornel 400 : = FRD-49	17.1	17.1	1.0	2.74	174.0	14.9	11.8	110.0	1.10	38.8
				214.8	16.8	1.3	2.98	206.0	18.6	12.3	110.0	1.44	95.1
Third Phase Laminates	FRD-49 III	0°	Thin -       Thick -       where   = Thornel 400 : = FRD-49	245.0	19.1	1.4	2.96	199.0	16.8	12.5	104.0	0.93	38.8
				229.9	17.7	1.3	2.89	193.0	16.8	12.2	105.0	1.16	38.8

NOTES: (1) 0.030" laminates used for tensile testing, 0.090" laminates used for short beam shear, impact, and compression testing.  
 (2) Value not used in average-specimen sub-normal.  
 (3) Values yet to be determined at time of report.  
 (4) ND = No Data

Two panels were fabricated using Thornel 400 as the primary reinforcement (panels 3 and 3A). A higher longitudinal tensile strength was achieved with panel No. 3A (218 ksi versus 177 ksi for panel No. 3) and again can be attributed to the higher filament volume of the panel (68 percent versus 57 percent). The longitudinal impact strength of the Thornel 400 panels is 39 percent higher than the panel fabricated of Modulite 5206. The resulting per ply thickness of a Thornel 400 ply is ~6.0 mils.

The boron (panel No. 4) purchased as a prepreg exhibited high longitudinal tensile strength and modulus (193 ksi and  $38 \times 10^6$  psi), low strain at failure (0.6 percent), and high short beam shear strength (17.3 ksi). The boron panel offers an increase in longitudinal impact strength of 32 percent over the Modulite 5206 panel. The resulting per ply thickness is ~4.4 mils.

The panel fabricated of S2 glass (panel No. 13) exhibited high longitudinal tensile strength and strain at failure (261 ksi and 2.7 percent), and low transverse tensile and short beam shear strengths (6.2 and 6.7 ksi). The S2 glass panel also exhibited an extremely high longitudinal impact strength of 172 ft-lb/inch W/inch T (620 percent greater than the Modulite 5206 impact strength). The resulting per ply thickness is ~3.0 mils.

The panel fabricated using Nomex Nylon (panel No. 21) was characterized by low longitudinal tensile strength and modulus (45 ksi and  $1.7 \times 10^6$  psi), high strain at failure (>3.2 percent), and low short beam shear strength (5.3 ksi). The longitudinal impact strength was 290 percent higher than the Modulite 5206 panel. The resulting per ply thickness is ~4.2 mils.

Hybrid panels using the above materials in conjunction with Modulite 5206 as the primary reinforcement in varying configurations as illustrated in the panel construction column of Table I, were then fabricated and characterized. Figures 11 through 19 illustrate, through the use of bar graphs, the relative property variances of the panels.

a. PRD-49 III Reinforced Modulite 5206. Panels fabricated using Modulite 5206 as the primary reinforcement and PRD-49 III as the supplemental reinforcement were characterized by increased longitudinal impact strength when compared to the Modulite 5206 panel. The PRD-49 III reinforced Modulite 5206 panels are No. 5 (alternating plies with 24 percent PRD-49), No. 6 (3131313 configuration with 9 percent PRD-49), Nos. 7 and 17 (414141 configuration with 11 and 15 percent PRD-49), No. 8 (~10 percent PRD-49 uniformly distributed between Modulite 5206 plies),\* and No. 16 (17 percent PRD reinforcement between varying numbers of Modulite 5206 plies - impact specimens only were evaluated).

\*This was the only panel fabricated of this configuration. It was fabricated by laying PRD-49 yarns dipped in 1004 resin at 1/16 inch intervals between each Modulite 5206 ply. Impact specimens only were evaluated.

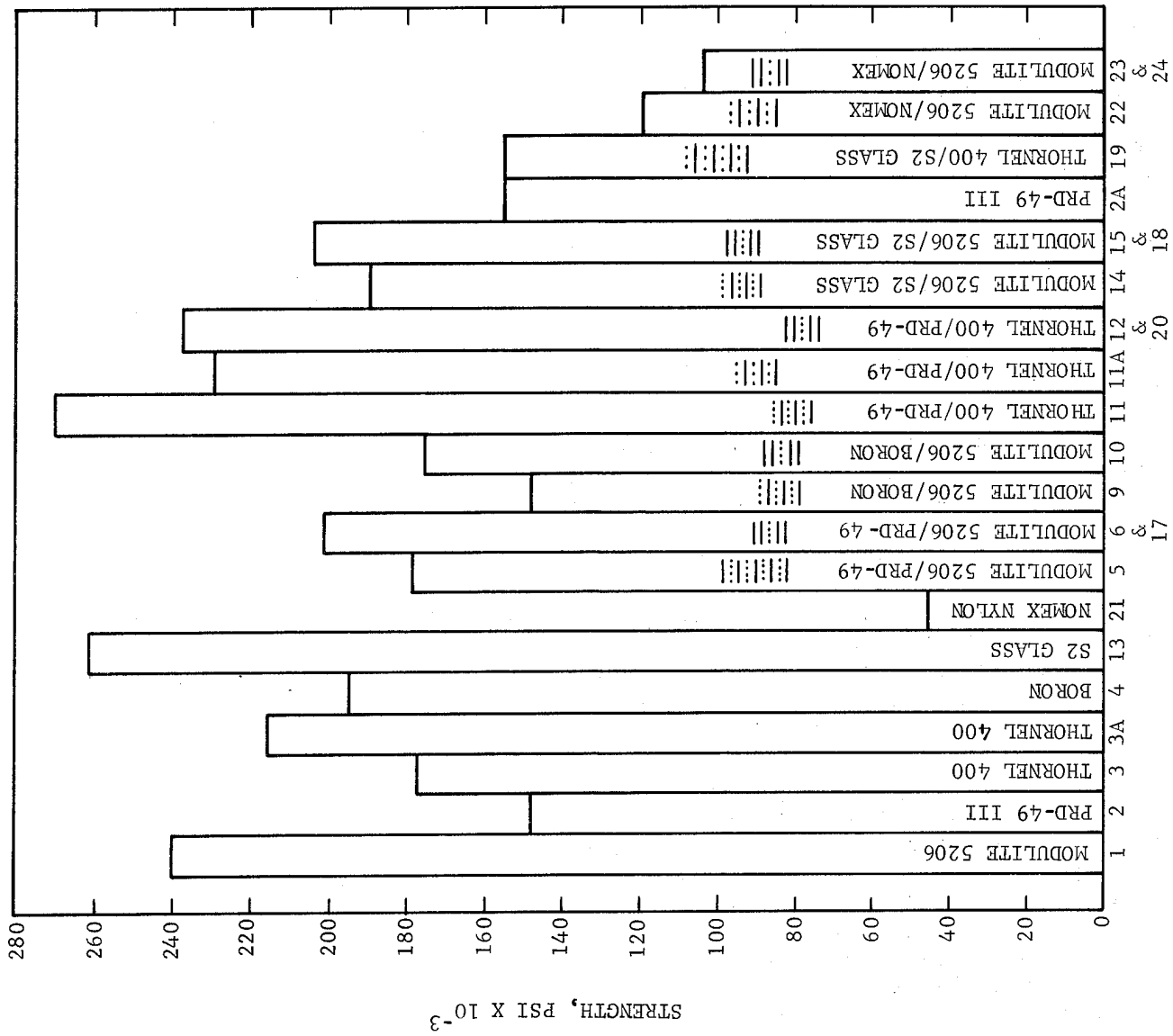


FIGURE 11. LONGITUDINAL TENSILE STRENGTHS OF PANELS

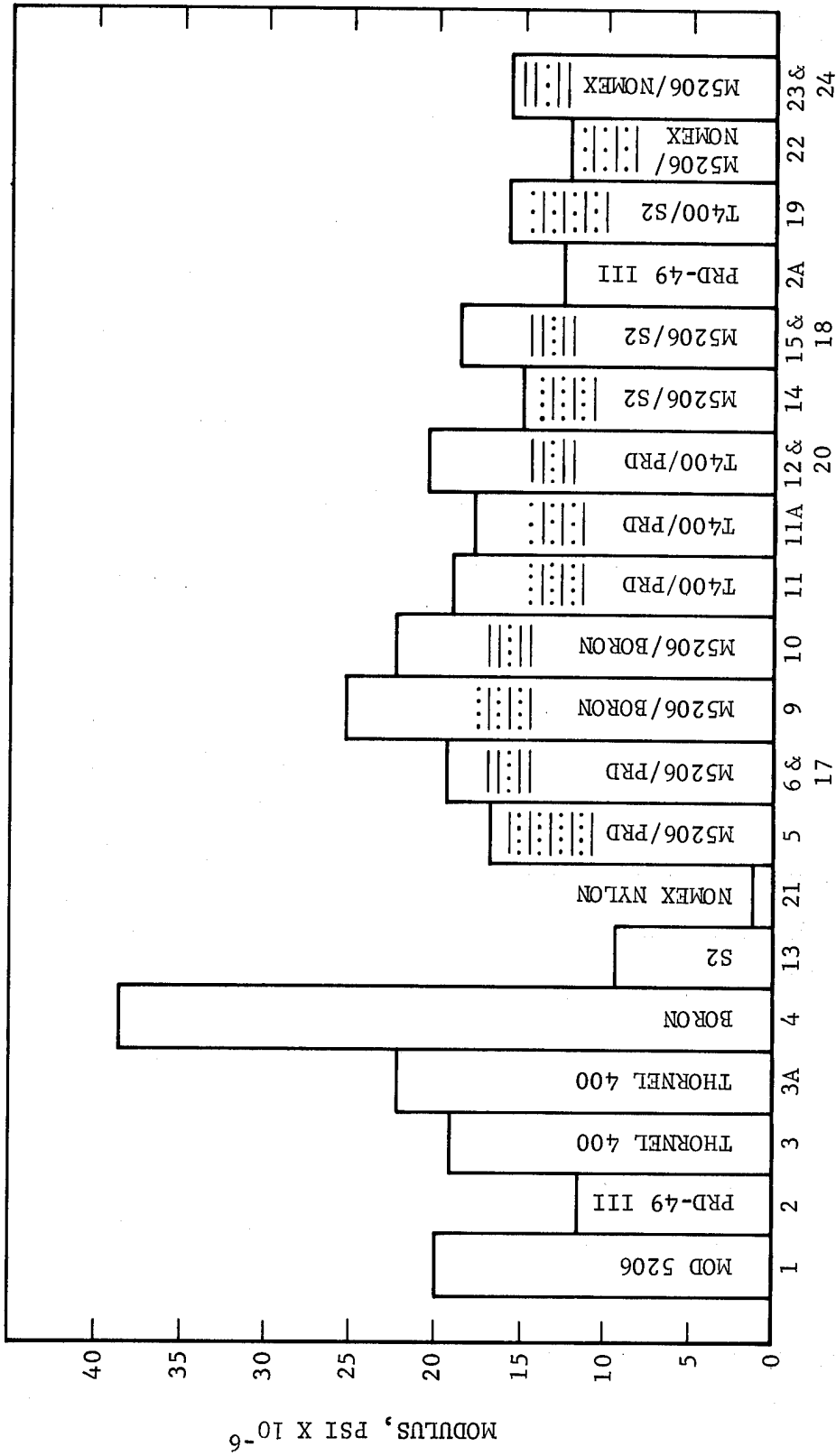


FIGURE 12. LONGITUDINAL TENSILE MODULUS OF PANELS

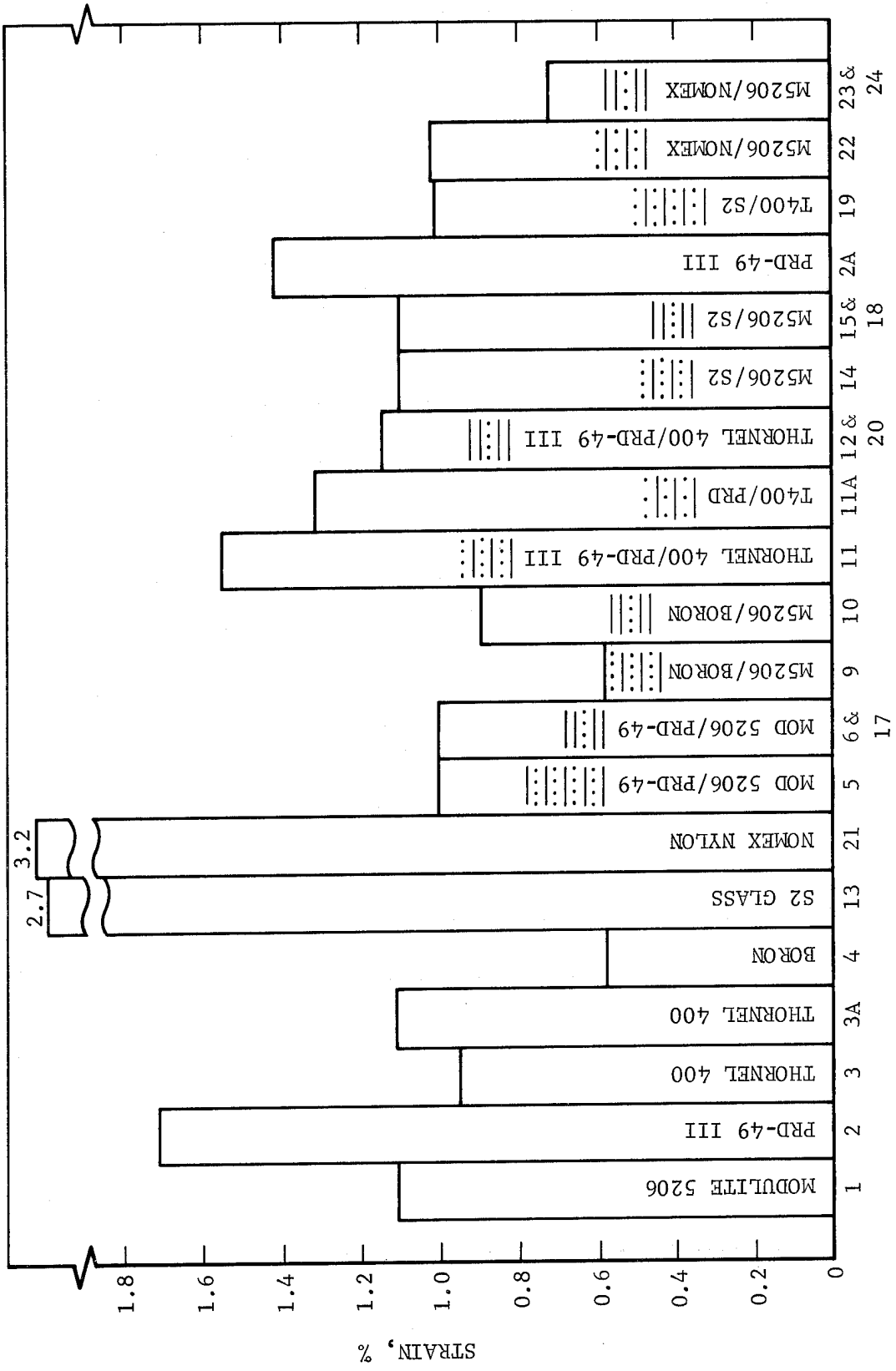


FIGURE 13. LONGITUDINAL STRAIN AT FAILURE OF PANELS

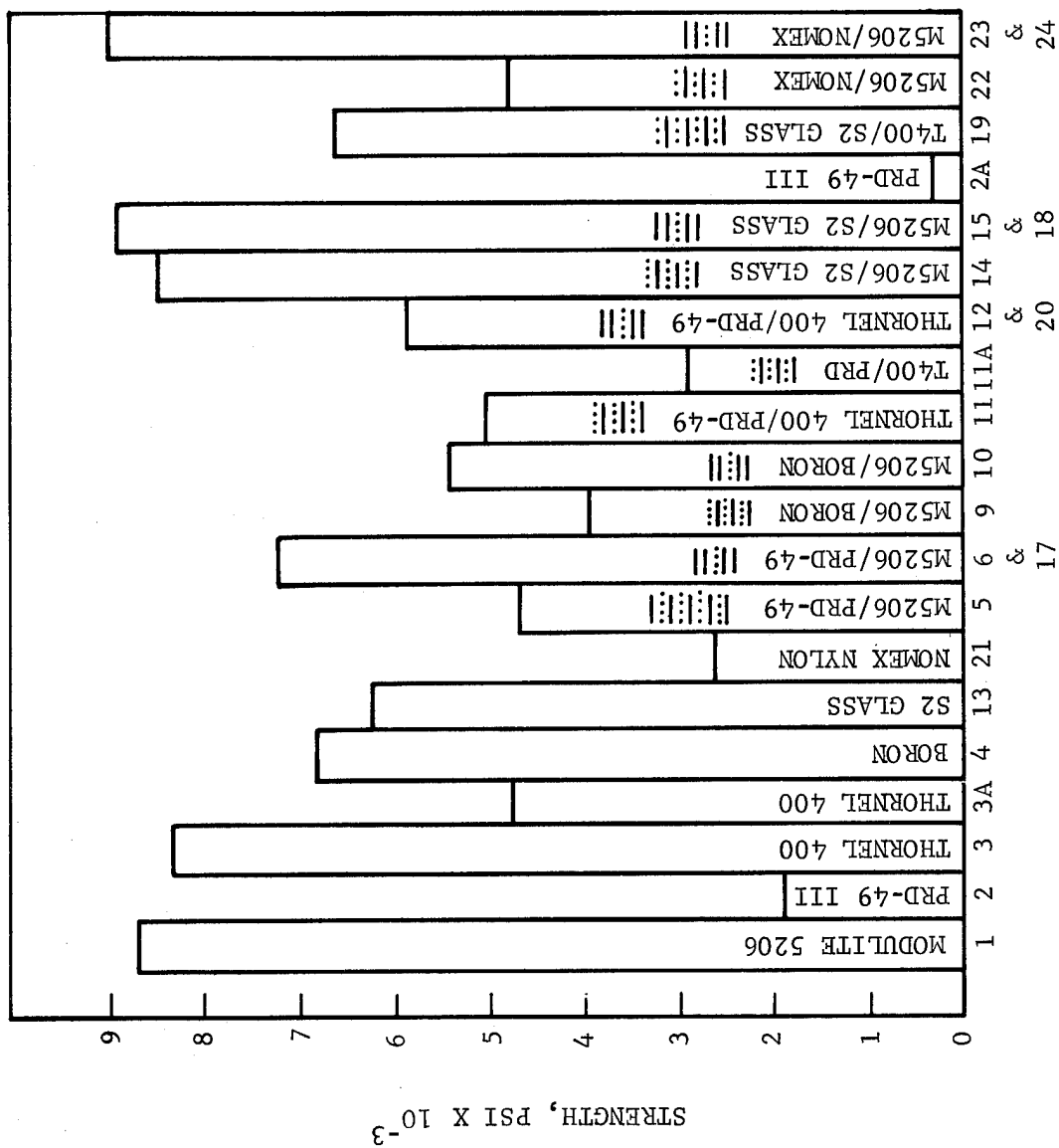


FIGURE 14. TRANSVERSE TENSILE STRENGTH OF PANELS

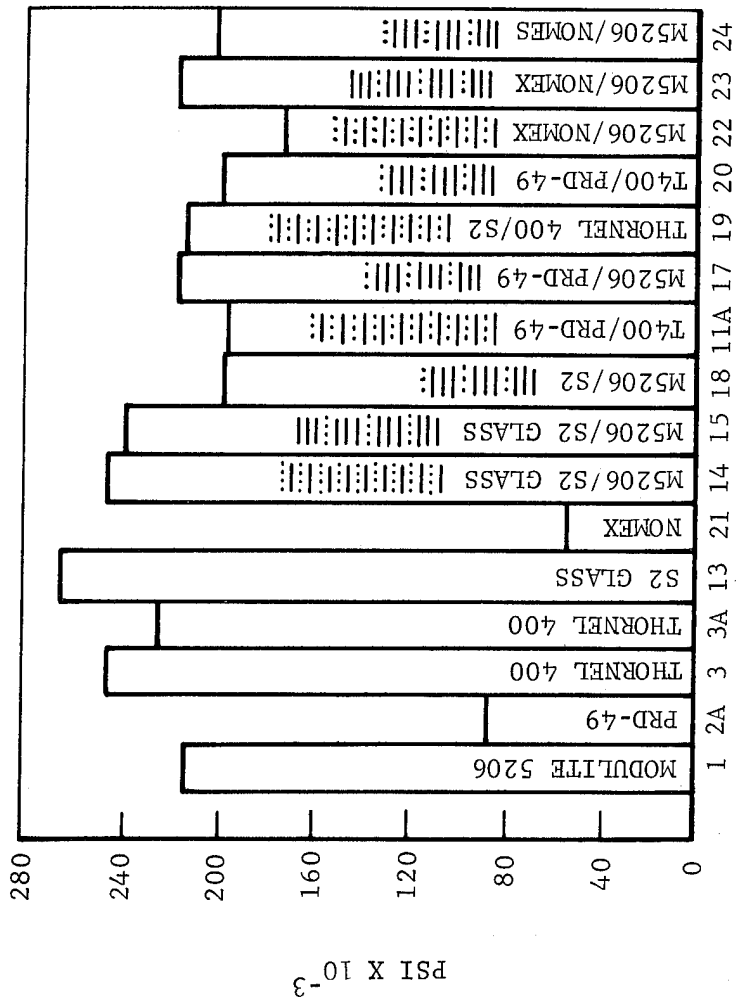


FIGURE 15. FLEXURAL STRENGTH OF PANELS

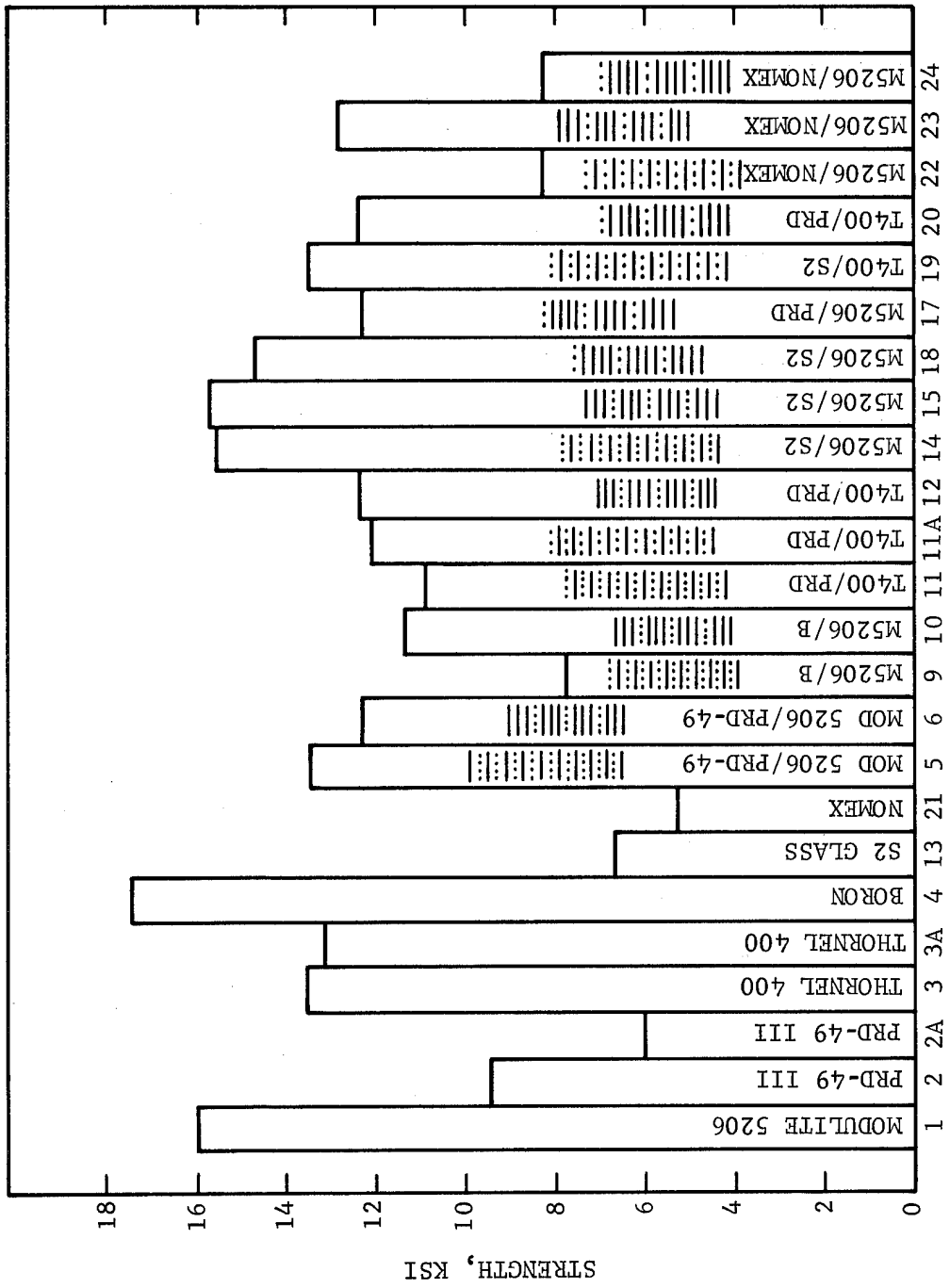


FIGURE 16. SHORT BEAM SHEAR STRENGTH OF PANELS

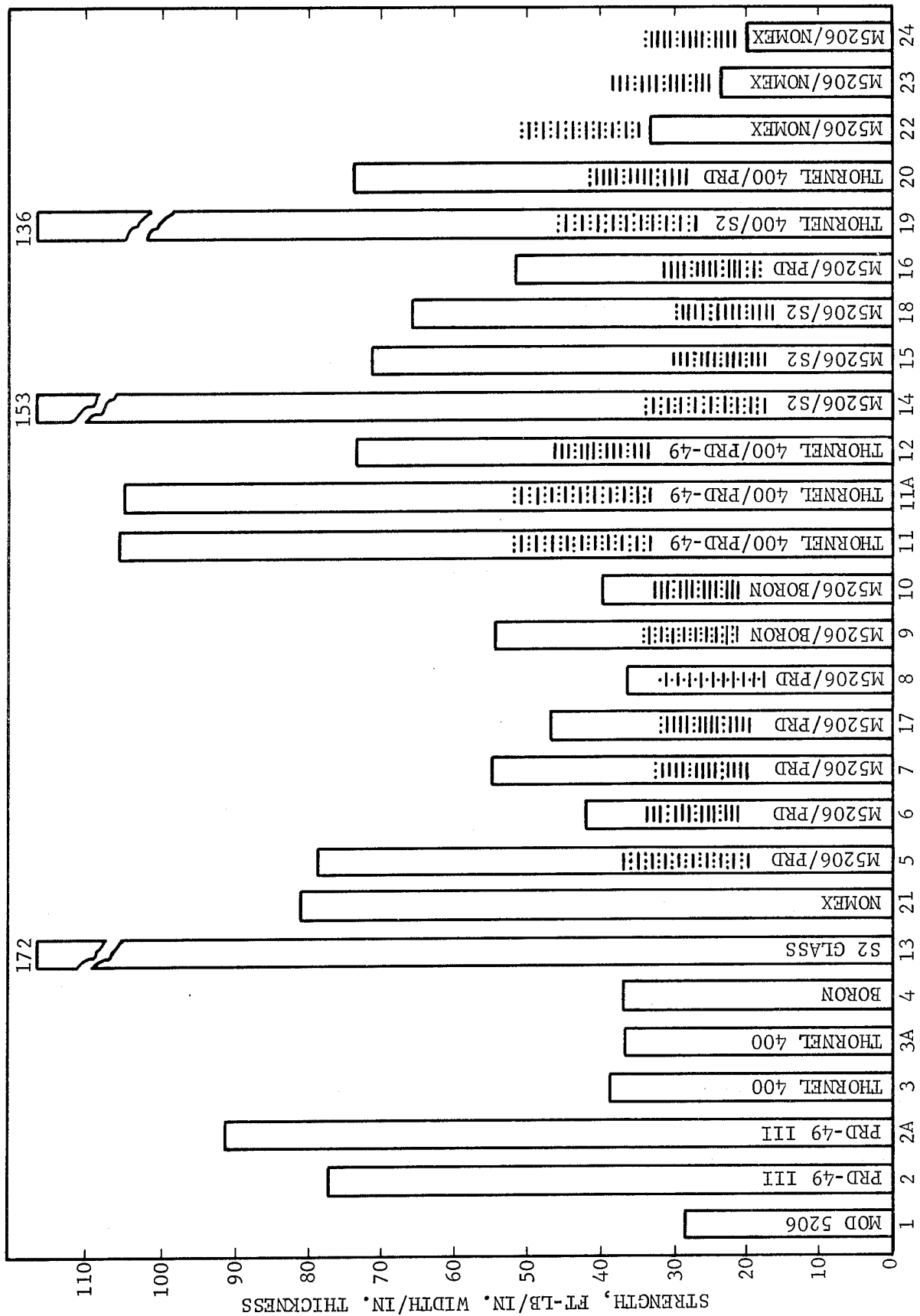


FIGURE 17. FLATWISE LONGITUDINAL IMPACT STRENGTH OF PANELS

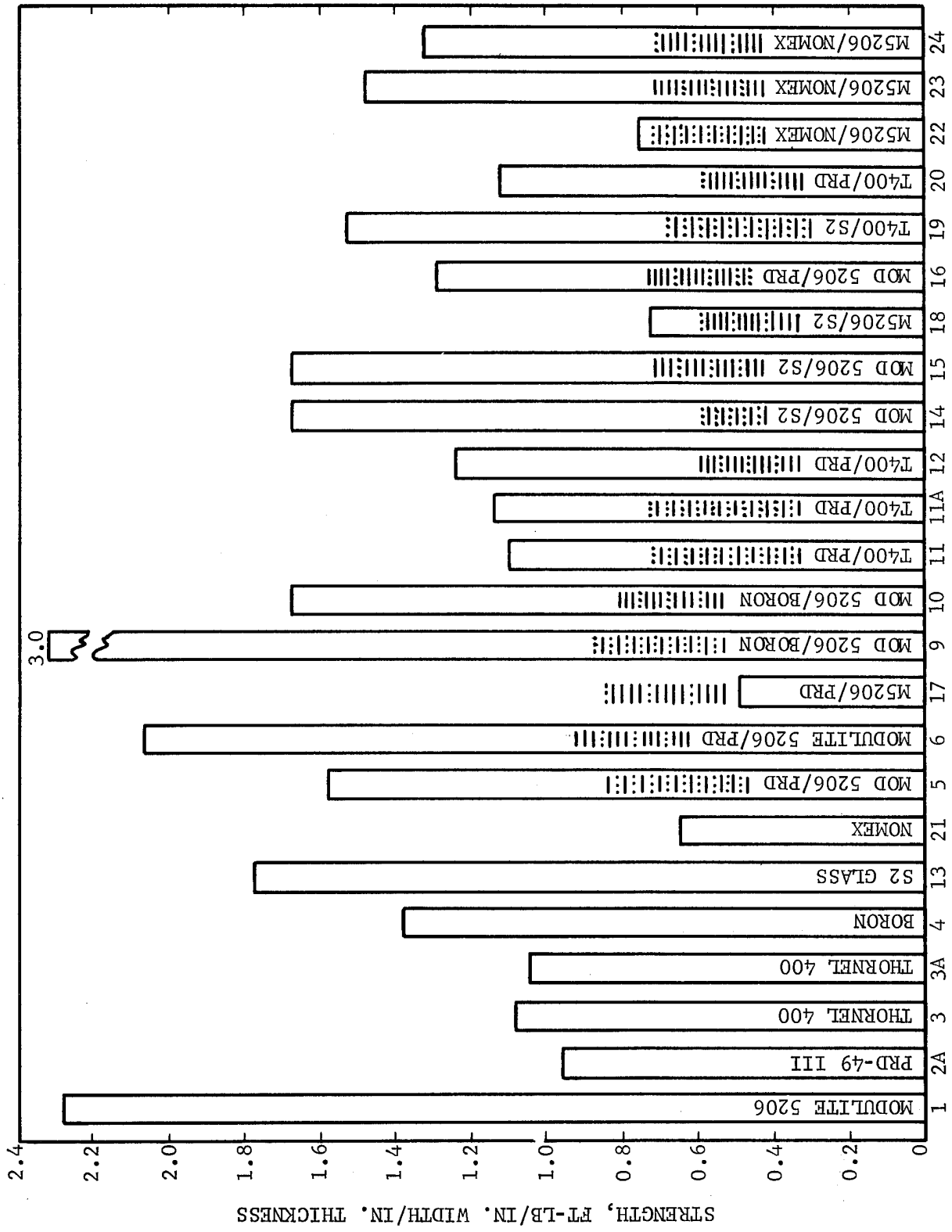


FIGURE 18. TRANSVERSE IMPACT STRENGTH OF PANELS

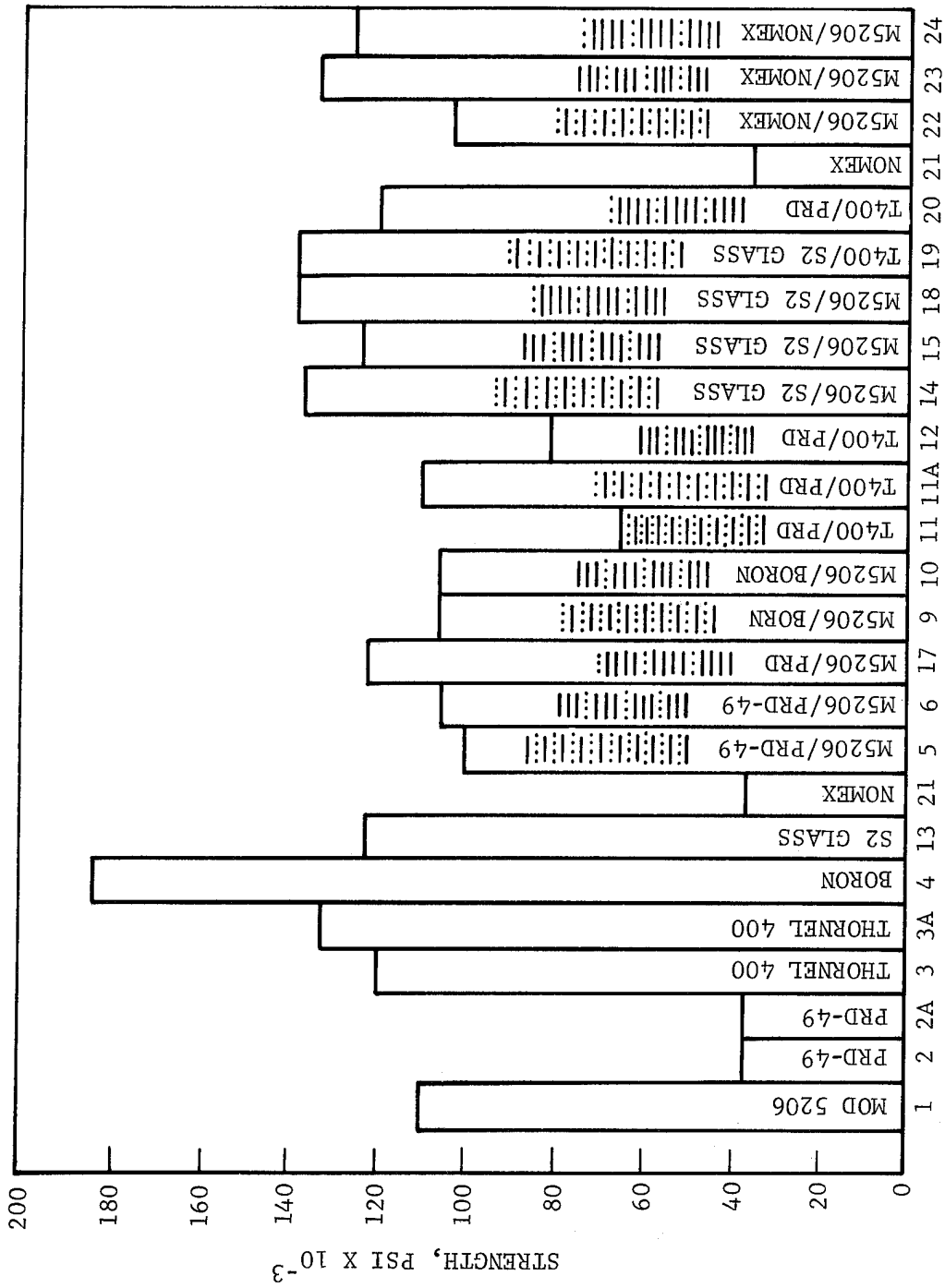


FIGURE 19. COMPRESSIVE STRENGTH OF PANELS

By alternating plies of PRD-49 and Modulite 5206 (panel No. 5), an increase in longitudinal impact strength of 185 percent over a panel fabricated solely of Modulite 5206 was realized (79 ft-lb/inch W/inch T versus 28 ft-lb/inch W/inch T) with only a 25 percent reduction in tensile strength. Transverse tensile strength dropped 47 percent while short beam shear decreased 15 percent compared to the Modulite 5206 laminate.

Of the three laminates with ~10 percent PRD-49 supplemental reinforcement (panels 6, 7 and 17, and 8), the 414141 configuration (Nos. 7 and 17) exhibited the highest longitudinal impact strength (95 percent greater than the Modulite 5206 panel). The 10 percent PRD-49 uniformly distributed between the 5206 plies exhibited the lowest impact efficiency of the 10 percent configuration. Evidently, 10 percent of supplemental reinforcement uniformly distributed is not a sufficient amount of material to allow the impact energy to distribute along the fibers. The energy impacted to the material is concentrated to a small localized area and a cleavage type fracture characteristic of graphite laminate ensues.

It was felt that the configuration employed in panel No. 16 (17 percent PRD-49) would result in high impact efficiency approaching that of a panel composed solely of PRD-49. This result was expected if the impact specimens when impacted were struck on the PRD-49 rich side, thus yielding a higher strain capability on the tensile side of the specimen. The impact results proved this not to be the case with the impact value (52 ft-lb/inch W/inch T) falling in between panels No. 5 (24 percent PRD-49) and No. 6 (9 percent PRD-49) and approximately the same as panel No. 7 (11 percent PRD-49).

PRD-49 as a supplemental reinforcement, increases the impact efficiency of Modulite 5206.

b. Boron Reinforced Modulite 5206. Two panels were fabricated using boron as a supplemental reinforcement between Modulite 5206 plies. One panel (No. 9) was fabricated by alternating plies of boron and Modulite 5206 (26 percent supplemental boron fiber volume) while the other panel (No. 10) had a 3131313 pattern (10 percent supplemental boron fiber volume). Both panels offered only slight increases in impact efficiency when compared to a panel composed solely of Modulite 5206. This was expected because boron as a primary reinforcement in panel No. 4, exhibited only a slightly greater impact strength than Modulite 5206 (37 versus 28 ft-lb/inch W/inch T). Short beam shear strength of the two panels (7.9 and 11.4 ksi) was much lower than the short beam shear strength of the panels composed solely of boron (17.3 ksi) or Modulite 5206 (16 ksi). Boron as a third phase supplemental reinforcement appears to offer little in the way of increased impact efficiency.

c. S2 Glass Reinforced Modulite 5206. Three panels were fabricated using S2 glass as a supplemental reinforcement between Modulite 5206 plies.

Panel No. 14 was fabricated by alternating plies of S2 and Modulite 5206 (26 percent S2 glass supplemental fiber volume). Panel No. 15 employed a 3131313 configuration (10 percent S2 glass supplemental fiber volume) and panel No. 18 employed a 414141 configuration (10 percent S2 glass supplemental fiber volume). Highest in longitudinal impact strength was panel No. 14 (153 ft-lb/inch W/inch T). This is 550 percent greater than a panel composed solely of Modulite 5206. Panel No. 15 and 18 also exhibited high impact strength (258 percent and 235 percent greater than Modulite 5206). Excellent longitudinal properties with high strain (1.1 percent) at failure was also a characteristic of these panels. S2 glass offers high impact efficiency as a supplemental reinforcement for Modulite 5206.

d. Nomex Nylon Reinforced Modulite 5206. Although as a primary reinforcement (panel No. 21) Nomex nylon exhibited high longitudinal impact strength (81 ft-lb/inch W/inch T), as a supplemental reinforcement in Modulite 5206 the impact capability of the fiber did not dominate. Panel Nos. 22, 23, and 24 show little if any increase in longitudinal impact strength over a panel fabricated solely of Modulite 5206. Panel No. 22 with alternating plies of nylon and Modulite 5206 (36 percent supplemental nylon fiber volume) was only 20 percent higher in longitudinal impact strength than the Modulite 5206 panel while panel No. 23 (3131313 construction with 15 percent supplemental nylon fiber volume) and No. 24 (414141 construction with 14 percent supplemental nylon fiber volume) actually showed reduced impact strength. Both panels, Nos. 23 and 24, were characterized by high transverse tensile strength (9.1 ksi) indicating good fiber to matrix bonding. All three panels exhibited much reduced longitudinal tensile strength compared to Modulite 5206.

Nomex nylon, as a supplemental reinforcement, offers only slight potential for increased composite toughness at high supplemental fiber volumes.

e. PRD-49 III Reinforced Thornel 400. Because of the higher impact capability (compared to Modulite 5206) shown by Thornel 400 (panel Nos. 3 and 3A), it was felt that its combination with PRD-49 III would be of interest. Three panel configurations were fabricated with Thornel 400 as the primary reinforcement; panels 11 and 11A with alternating plies of Thornel 400 and PRD-49 (37 percent supplemental PRD-49 fiber volume), panel No. 12 with a 3131313 layup pattern (16 percent supplemental PRD-49 fiber volume), and panel No. 20 with a 414141 layup pattern (16 percent supplemental PRD-49 fiber volume).

Both panels 11 and 11A with alternating ply configuration show higher longitudinal impact characteristics than either of their constituent materials laminates (panels No. 2 and No. 3). This particular combination of materials appear to alter the impact failure mode so that higher energy levels can be absorbed. The impact level was 107 ft-lb/inch W/inch T or 385 percent greater than a panel composed of Modulite 5206. These panels also exhibited very high tensile strengths (>230 ksi) and strain at failure (>1.3 percent).

Panel Nos. 12 and 20 exhibited increased impact strength (260 percent greater than Modulite 5206); however, both were lower than a panel composed solely of PRD-49 III fiber.

The combination of Thornel 400 and PRD-49 III in the alternating ply configuration offers great increases in longitudinal impact strength with no change in longitudinal tensile properties when compared to Modulite 5206.

f. S2 Glass Reinforced Thornel 400. One panel was fabricated using Thornel 400 as primary reinforcement and S2 as supplemental reinforcement. Panel No. 19, with alternating plies of Thornel 400 and S2 glass (27 percent supplemental S2 fiber volume) was characterized by high longitudinal impact strength (136 ft-lb/inch W/inch T and reduced tensile strength (157 ksi). The impact strength, however, was lower than the corresponding value determined for Modulite 5206 and S2 in the alternating ply configuration (panel No. 14).

Summarized in Table II are the test values of selected hybrid panels normalized to the program standard Modulite 5206. In each case, the value obtained for the selected panel was divided by the corresponding value obtained for the Modulite 5206 panel. By adding the normalized data, some indication of the total performance of each laminate can be determined. It can also be seen where low values and high values affect the total. The normalized flexural data are included in the table for interest; however, the totals for each panel do not include the normalized flexural values because the test was not performed on all panels. The total performance for normalized Modulite 5206 is 8.

S2 glass, as a supplemental reinforcement in Modulite 5206, produced the greatest effect on total laminate performance (13.16 for 25 percent S2 glass and 9.22 for 10 percent S2 glass). It can be seen that the high impact strengths of these panels greatly influenced the totals. The S2 reinforced panels show superior performance to the Modulite 5206.

The next highest totals (of the Modulite 5206 panels) were registered by panels reinforced with PRD-49 III fiber (7.30 for 25 percent PRD-49 and 7.69 for 10 percent PRD-49). For practically each property, the PRD-49 III values are lower than the corresponding value obtained for the S2 glass panels. Again, the impact strengths had the greatest influence on the total. The PRD-49 III reinforced panels are slightly inferior to Modulite 5206 in total performance.

The boron reinforced Modulite 5206 was only slightly lower in total performance than those reinforced with PRD-49 III (7.61 for 25 percent boron and 6.88 for 10 percent boron). The higher moduli of the panels along with low transverse tensile strengths and slightly higher longitudinal impact strengths most influenced total performance. The boron reinforced panels were inferior to Modulite 5206 in total performance.

TABLE II. HYBRID PANEL PROPERTIES NORMALIZED TO MODULITE 5206 DATA

TABLE II. HYBRID PANEL PROPERTIES NORMALIZED TO MODULITE 5206 DATA

Modulite 5206		Modulite 5206 With Supplementary Reinforcement										Thornel 400 With Reinforcement				
		PRD-49 III		Boron		S2 Glass		Nomex		PRD-49 III		S2 Glass				
		25% (1) (Panel 5)	10% (1) (Panel 6)	25% (1) (Panel 9)	10% (1) (Panel 10)	25% (1) (Panel 14)	10% (1) (Panel 15)	36% (1) (Panel 22)	15% (1) (Panel 23)	36% (1) (Panel 11)	16% (1) (Panel 12)	28% (1) (Panel 19)				
Property	Normalized Value															
• Longitudinal Tensile Strength	1	0.74	0.84	0.62	0.73	0.79	0.85	0.50	0.45	1.12	0.98	0.65				
• Longitudinal Modulus	1	0.83	0.98	1.27	1.13	0.76	0.92	0.62	0.85	0.94	1.05	0.80				
• Longitudinal Strain (maximum)	1	0.91	0.91	0.55	0.81	1.00	0.88	0.91	0.64	1.36	1.00	0.91				
• Transverse Tensile Strength	1	0.53	0.83	0.44	0.62	0.98	1.01	0.55	1.05	0.59	0.68	0.76				
• Flexural Strength	1	-	-	-	-	1.16	1.12	0.82	1.02	-	-	1.01				
• Short Beam Shear Strength	1	0.85	0.77	0.49	0.71	0.98	0.99	0.52	0.81	0.69	0.77	0.86				
• Flat Longitudinal Impact Strength	1	2.83	1.49	1.97	1.42	5.50	2.58	1.20	0.87	3.85	2.64	4.93				
• Transverse Impact Strength	1	0.70	0.91	1.30	0.49	0.73	0.75	0.34	0.66	0.49	0.54	0.67				
• Compressive Strength	1	0.91	0.96	0.97	0.97	1.26	1.12	0.95	1.22	0.59	0.74	1.27				
TOTAL (2)	8	7.30	7.69	7.61	6.88	13.16	9.22	5.59	6.55	9.63	8.40	10.85				

NOTES: (1) Percentage of total laminate volume. See Appendix B.

(2) Total for each panel minus flexural strength value (not determined for all panels).

The Nomex nylon reinforced Modulite 5206 were lowest in total performance of all the hybrid panels (5.59 for 36 percent Nomex and 6.55 for 15 percent Nomex). The low strength and modulus of the fiber in conjunction with little improvement in longitudinal impact strength most influenced the total performance.

Both the S2 glass and PRD-49 III reinforced Thornel 400 configurations exhibited superior total performance to Modulite 5206 (10.85 for 28 percent S2 glass, 9.63 for 36 percent PRD-49 III and 8.40 for 16 percent PRD-49 III). To be noted are the near unity longitudinal tensile properties and high longitudinal impact properties of the PRD-49 III reinforced Thornel 400. Both configurations were only inferior in overall performance to the S2 glass reinforced Modulite 5206.

#### 2.3.4 POST-TEST ANALYSIS

It is generally conceded that graphite or carbon filament reinforced plastics exhibit a degree of crack sensitivity and brittleness with accompanying low impact strength or "toughness." One objective of this program was to acquire a basic understanding of the phenomena associated with the various reinforcements and layup patterns with regard to their level of resistance to impact damage. Post-test analysis consisting of photomicrographic and scanning electron microscopic examination was employed in an attempt to determine what failure behavior was characteristic of each fiber/matrix type.

The investigation was conducted on the longitudinal impact specimens. Photomicrographic cross sections of each panel type were prepared by sectioning a small piece from the end of a selected longitudinal impact specimen. These photomicrographs appear as representative panel cross sections shown as Figures C-1 through C-24 in Appendix C. An edgewise photomicrograph was prepared of a selected longitudinal impact specimen from each panel type to show the associated mode of fracture. These photomicrographs appear as Figures C-24 through C-48 in Appendix C. In general, the graphite and boron panels exhibit a brittle, cleavage type fracture appearance with little or no evidence of fiber pullout. The PRD-49 reinforced panels, in turn, indicate a high degree of fiber debonding with ensuing fiber pullout. It has been shown (Reference 5) that energy absorbed by debonding is two orders of magnitude higher than the energy absorbed in cleavage, indicating considerable improvement in composite impact efficiency when fiber tensile failures are coupled with debonding or pullout. With the introduction of the third phase interply reinforcement of PRD-49 between the graphite plies, the cleavage, "brittle" type behavior is changed to multimode fracture behavior consisting of both the "brittle" fracture associated with the graphite and "ductile" fracture associated with the PRD-49.

The particular phenomenon associated to each fiber type was further studied through the use of scanning electron microscopy. Selected longitudinal impact specimens were prepared and the fracture surface studied and photographed. The photographs appear as Figures 20 through 31. Figures 20, 21, and 22 show the fracture surface associated with Modulite 5206, panel No. 1. Little evidence of fiber pullout is evident in Figure 20. The fibers have

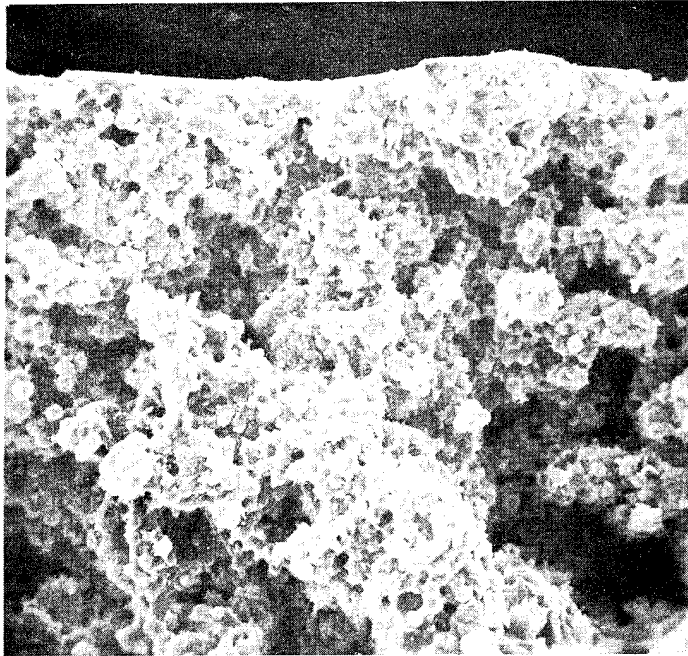


FIGURE 20. 200X SEM - TENSILE SIDE OF IMPACT SURFACE PANEL #1, MODULITE 5206

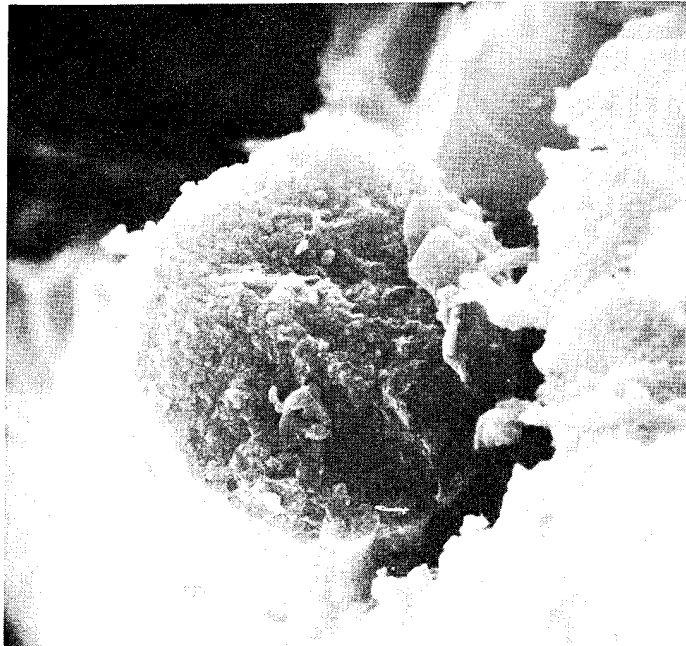


FIGURE 21. 5530X SEM - FRACTURED FILAMENT ON TENSILE SIDE OF IMPACT SURFACE PANEL #1, MODULITE 5206

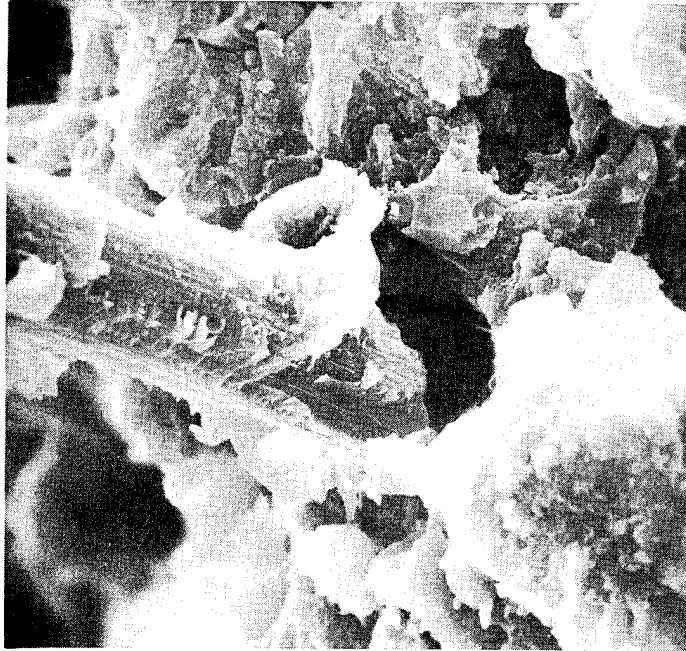


FIGURE 22. 2210X SEM - FRACTURED FILAMENT SHOWING RESIN ADHERENCE ON TENSILE SIDE OF IMPACT SURFACE PANEL #1, MODULITE 5206



FIGURE 23. 238X SEM - TENSILE SIDE OF IMPACT SURFACE PANEL #2, PRD-49, TYPE III

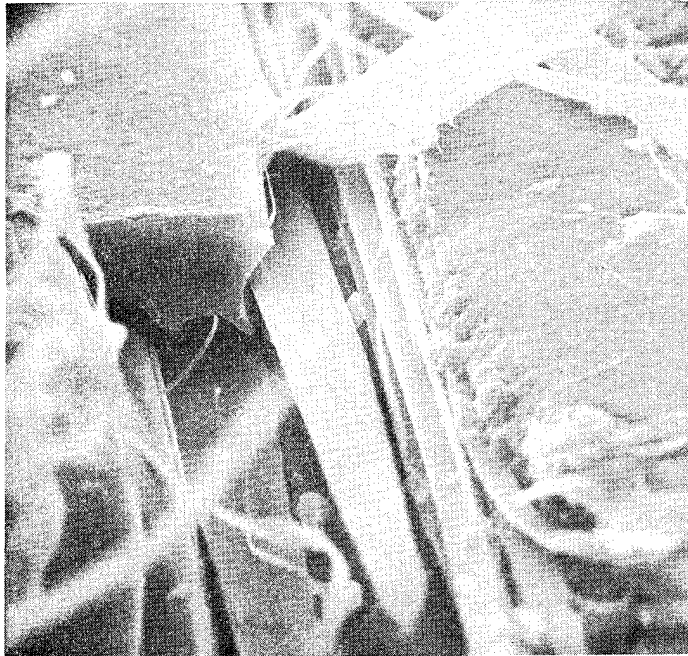


FIGURE 24. 1190X SEM - FRACTURED FILAMENT ON TENSILE SIDE OF IMPACT SURFACE OF PANEL #2, PRD-49, TYPE III

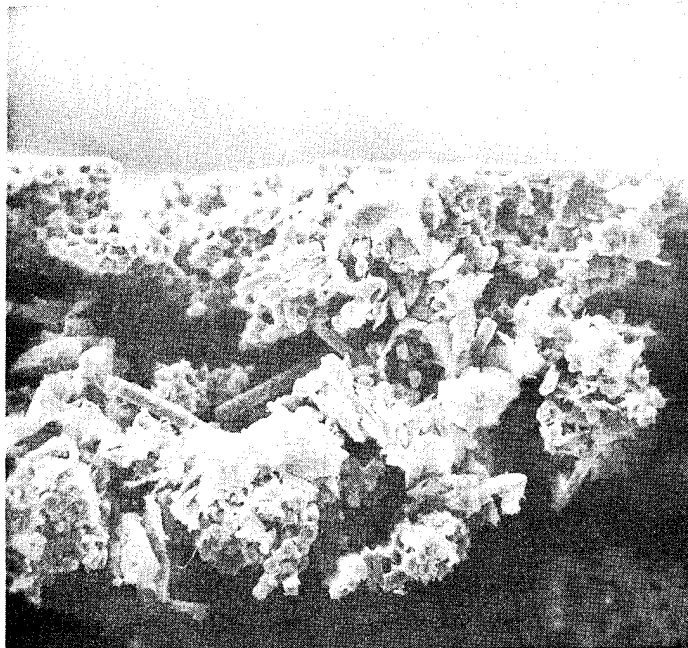


FIGURE 25. 238X SEM - TENSILE SIDE OF IMPACT SURFACE PANEL #3, THORNEL 400

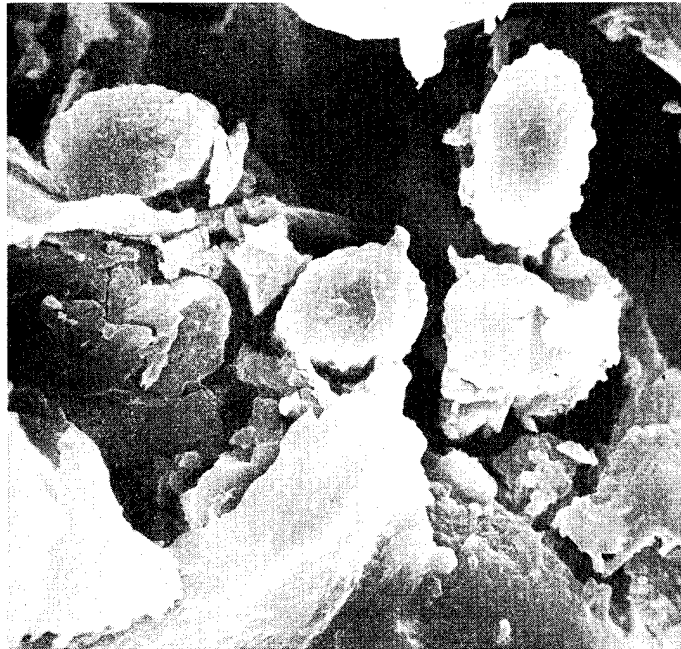


FIGURE 26. 2380X SEM - FRACTURED FILAMENTS ON TENSILE SIDE OF IMPACT SURFACE OF PANEL #3, THORNEL 400

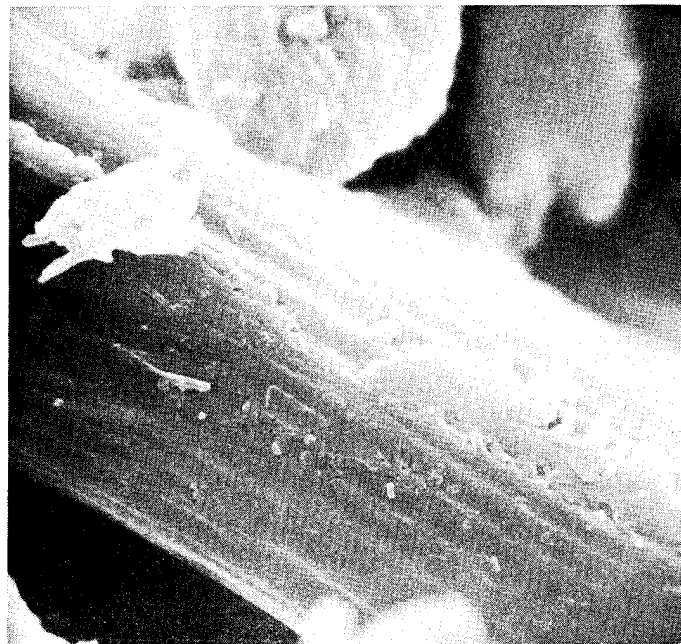


FIGURE 27. 5950X SEM - FRACTURED FILAMENT SHOWING RESIN ADHERENCE ON TENSILE SIDE OF IMPACT SURFACE OF PANEL #3, THORNEL 400

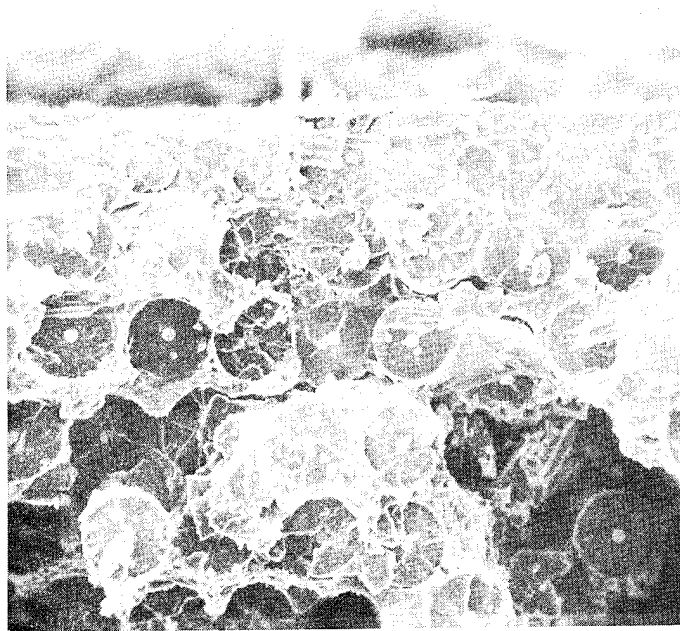


FIGURE 28. 102X SEM - TENSILE SIDE OF IMPACT SURFACE PANEL #4, BORON

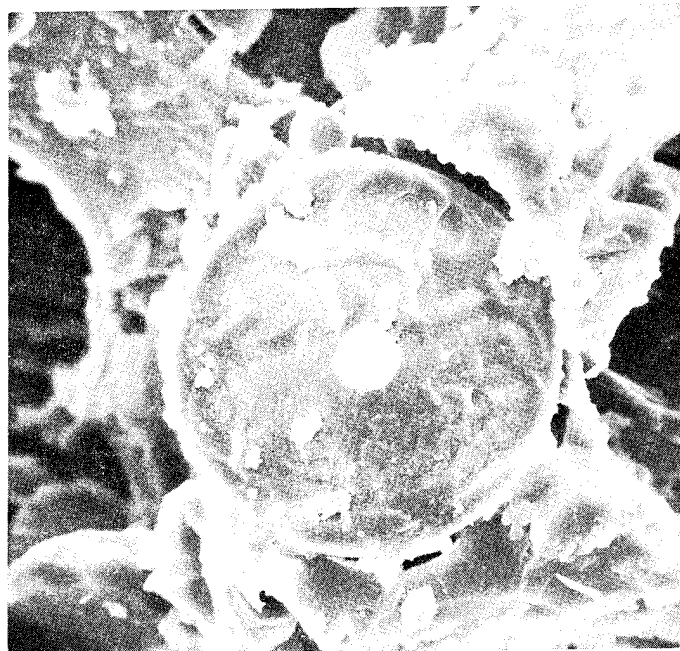


FIGURE 29. 535X SEM - FRACTURED FILAMENT ON TENSILE SIDE OF IMPACT SURFACE, PANEL #4, BORON

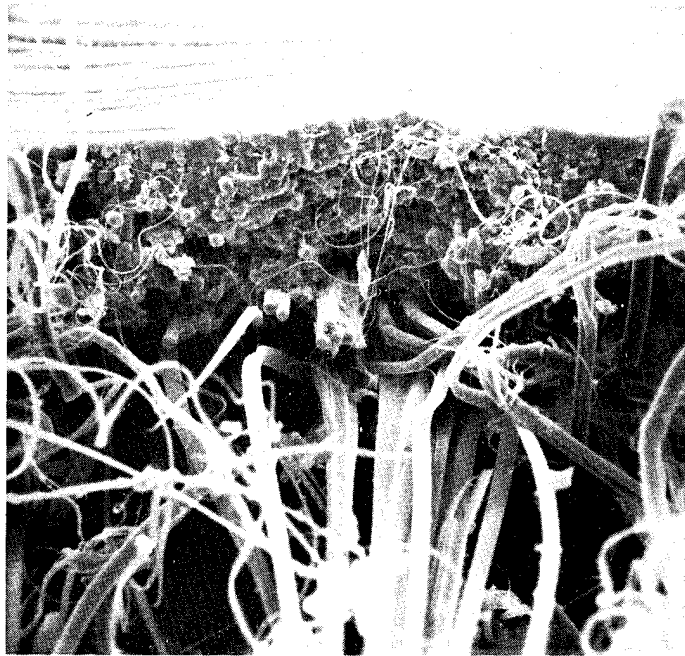


FIGURE 30. 200X SEM - TENSILE SIDE OF IMPACT SURFACE OF PANEL #5, MODULITE 5206/PRD-49



FIGURE 31. 2210X SEM - PRD-49 FILAMENT SHOWING MODE OF FAILURE ON TENSILE SIDE OF IMPACT SURFACE PANEL #5, MODULITE 5206/PRD-49

undergone tensile failure promoting cleavage of the matrix normal to the fiber axis. This failure sequence is normal for composites with high filament volumes exhibiting high fiber/matrix bonding characteristic of the surface treated graphite fibers. Strain energy released by a broken fiber must be absorbed locally to prevent propagation of an unstable crack. Failed graphite fibers in Figures 21 and 22 show the adherence of resin to fiber and the fluted nature of the fiber surface thus helping to promote the adherence of the matrix.

Figures 23 and 24 depict the impact fracture surface associated with PRD-49 III, panel No. 2. A high degree of fiber debonding and pullout in Figure 23 is present. A close examination of a fractured PRD-49 fiber in Figure 24 shows that the fiber has undergone a complete catastrophic failure over a considerable length of the fiber. In addition to absorbing energy by debonding, the PRD-49 fiber shows an ability to absorb relatively larger amounts of energy during fracture because of the very nature of its type of failure. The smooth appearance of the impression left by the PRD-49 fiber in the matrix at the left edge of the fractured fiber should be noted. Figure 31 also shows the smooth surface associated with a PRD-49 fiber. This smoothness of the PRD-49 fiber surface prevents the high degree of mechanical interlocking of fiber to matrix and subsequently is a cause for the reduced transverse tensile and interlaminar shear strengths (the other principal cause being a relatively lower degree of chemical bonding).

Figures 25, 26, and 27 show the impact fracture surface associated with Thornel 400, panel No. 3. Some fiber debonding and pullout is evident although the specimens still underwent a cleavage-type fracture. The higher initial strain energy capability of the fiber relative to the Modmor II filament is believed to be the reason why the impact resistance of the Thornel 400 is higher than the Modulite 5206 panel. A fluted surface is also associated with the Thornel 400 fiber, shown in Figures 26 and 27, thus resulting in relatively higher interlaminar shear strengths. The impact fracture surface of the boron epoxy, panel No. 4, is shown in Figures 28 and 29. Its surface exhibits a very brittle, cleavage mode of failure. High interlaminar shear strengths indicate good chemical bonding of fiber to matrix as shown in Figure 29.

Scanning electron microscopic examination was not made of the S2 glass and Nomex nylon panels because their principal mode of failure was delamination as shown in Figures C-37 and C-45 of Appendix C.

The fracture surface of a hybrid panel impact specimen fabricated from Modulite 5206 and PRD-49 III is shown in Figures 30 and 31. Figure 30 shows the multimode fracture associated with the hybrid. The graphite ply underwent its characteristic "brittle" failure and the PRD-49 ply underwent its characteristic "ductile" failure. Figure 31 depicts the smooth surface associated with the PRD-49 fiber and the splitting of the fiber due to fracture. Other hybrid panels not shown, fractured in multimode fashion with variations of brittle, cleavage fracture, fiber debonding and pullout, and delamination as shown in Appendix C.

A limited amount of testing was conducted to determine the relative impact characteristics of selected panel configurations utilizing an instrumented Charpy impact testing apparatus. A detailed description of the test method, specimen composition, test results and mode of failure are discussed and documented in Appendix D, pages D-1 through D-11.

## SECTION 3

### TASK II - FIBER SURFACE TREATMENTS

Task II comprises an experimental program to investigate and evaluate the feasibility of obtaining gross improvements in the impact toughness of graphite fiber composites by surface treatment of the individual fiber. This effort is a continuation of research conducted at Philco-Ford over three years. In the fall of 1969, Philco-Ford investigated the effect of surface treatments as a means of improving the performance of high-modulus graphite filaments in epoxy composites. The effort was part of Naval Air Systems Command Contract No. N00019-68-C-0475 which emphasized other aspects in the development of graphite-fiber-reinforced composites. Only a few cursory experiments involved surface treatment. Coating Thornel\* yarn with pyrolytically deposited carbon was found to enhance the interlaminar shear strength of composites.<sup>(1)</sup> Carbon was applied by heating the graphite yarn to about 1000°C in the presence of toluene vapor. Continuous lengths of yarn were treated in the experimental apparatus schematically illustrated in Figure 32.

Yarn was transported through a covered glass jar as shown in Figure 32. An electrical current was caused to flow through a section of yarn suspended above a pool of toluene. The incandescent yarn was quenched in the toluene pool and the liberated heat utilized to form toluene vapor. Above 1000°C, toluene thermally decomposes and forms carbon. Consequently the incandescent yarn was coated with carbon as it passed through the jar. There were some

---

\*Thornel is a trademark of Union Carbide Corporation for graphite filaments made from rayon precursors. The preparation and characteristics of these fibers have been described by Epreman.<sup>(6)</sup>

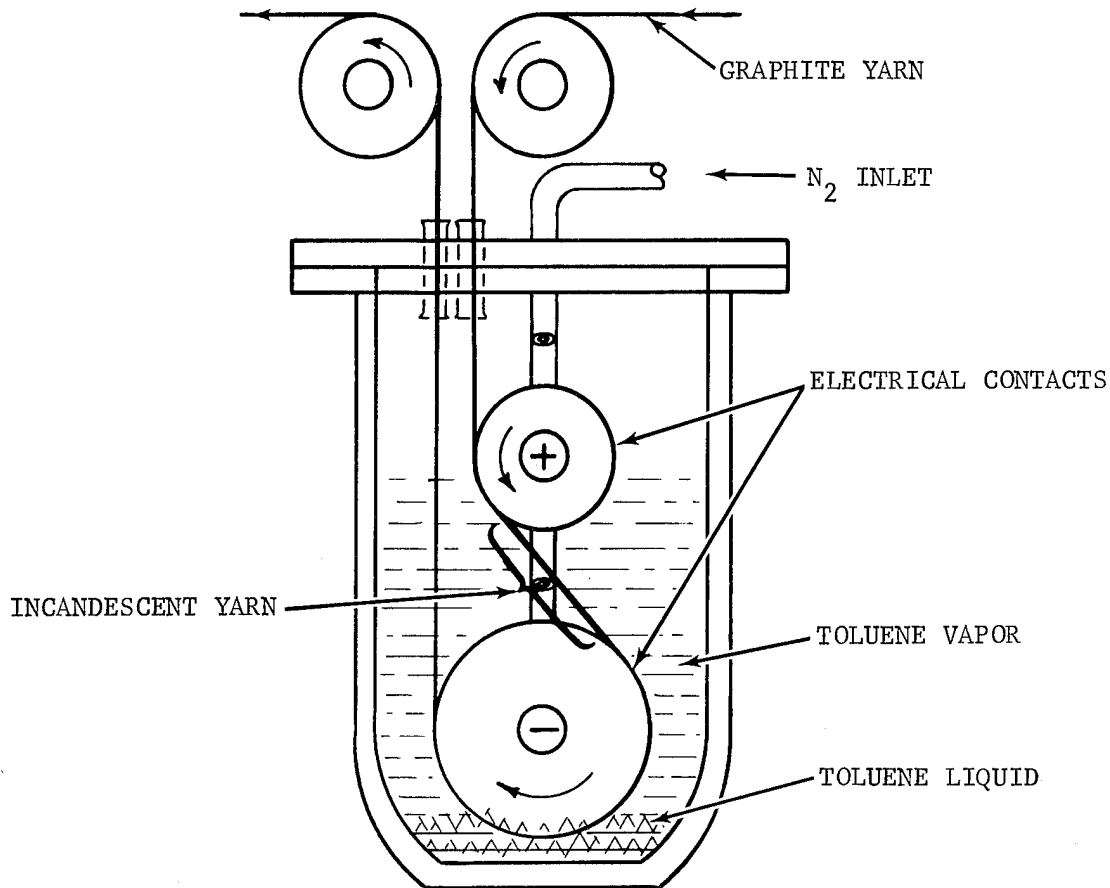


FIGURE 32. EXPERIMENTAL APPARATUS FOR CONTINUOUSLY COATING GRAPHITE YARN WITH CARBON

indications that the addition of boron trichloride to the toluene further enhanced the interlaminar shear strength of epoxy composites reinforced with treated Thornel yarn, but the results were inconclusive.

During 1970, carbon coating as described in the last paragraph was extensively used as a surface treatment during the performance of Contract No. N00019-69-C-0135. The process was demonstrated to yield composites with improved mechanical properties.<sup>(2)</sup> Interlaminar shear strength was enhanced without the degradation in tensile strength that occurred in some surface treatments. Boron was not used in these experiments.

During 1971, Philco-Ford conducted under Contract No. N00019-70-C-0301, research specifically concerned with the development of surface treatments for high-modulus graphite filaments. Experiments were conducted to evaluate surface treatments in which Thornel yarn was coated with carbon, boron,

or a mixture of the two. The effects of heat cleaning or heat treating were also studied. Composites were prepared from treated yarn and epoxy resin. The interlaminar shear strength and tensile strength were determined and compared with results from other surface treatments. These experiments were performed utilizing different apparatus than previous research employed.

The changes in equipment were motivated by the desire to control more effectively gaseous reactants such as boron trichloride. In the original work, graphite fibers were heated to incandescence by an electric current in a closed vessel containing a vapor phase of boron trichloride and toluene. The treatment improved the shear strength of composites compounded of the modified fibers and epoxy without degrading tensile strength.<sup>(1)</sup> However, the results were highly inconsistent and only small quantities of improved fiber could be made. The apparent reason for the inconsistencies was that the concentration of boron trichloride in the toluene solution changed rapidly and this caused a wide variation in the boron trichloride content in the vapor phase.

The modified apparatus resembled that used in the production of boron monofilament by chemical vapor deposition (CVD).<sup>(7)</sup> Methane was used as a carbon precursor in place of toluene. According to Brown and Watt<sup>(8)</sup>, deposits of carbon formed from hydrocarbon like methane are nearly identical to those formed from aromatic compounds like benzene. Substitution of methane for toluene greatly facilitated metering the carbon precursor and enabled its gaseous concentration to be varied more precisely over a wide range of concentration.

The modified apparatus clearly demonstrated an improvement in surface treatment methods during the performance of Contract No. N00019-70-C-0301. Reproducibility was calculated to be 90 percent for interlaminar shear specimens emanating from a wide variety of processing experiments.<sup>(3)</sup> Long continuous lengths (up to 500 feet) of fiber were routinely processed. The combination of reproducible results and the ability to fabricate substantial numbers of specimens were integrated with a carefully conceived 2<sup>4</sup> factorial experiment to determine the effects on fiber strength of several process parameters.

The most conclusive observations were the effect of environment and temperature upon the short beam shear strength of composites fabricated from surface altered fiber. Those results, for treated Thornel 75S yarn, are presented in Figure 33. Note that treatment in an inert environment is akin to heat cleaning as practiced by past investigators.<sup>(9)</sup> Consequently, Figure 33 presents the experimental results in such a manner that one can at a glance ascertain the improvement made by the four alternative methods: heat cleaning, boron treatment, carbon treatment and borocarbon treatment.

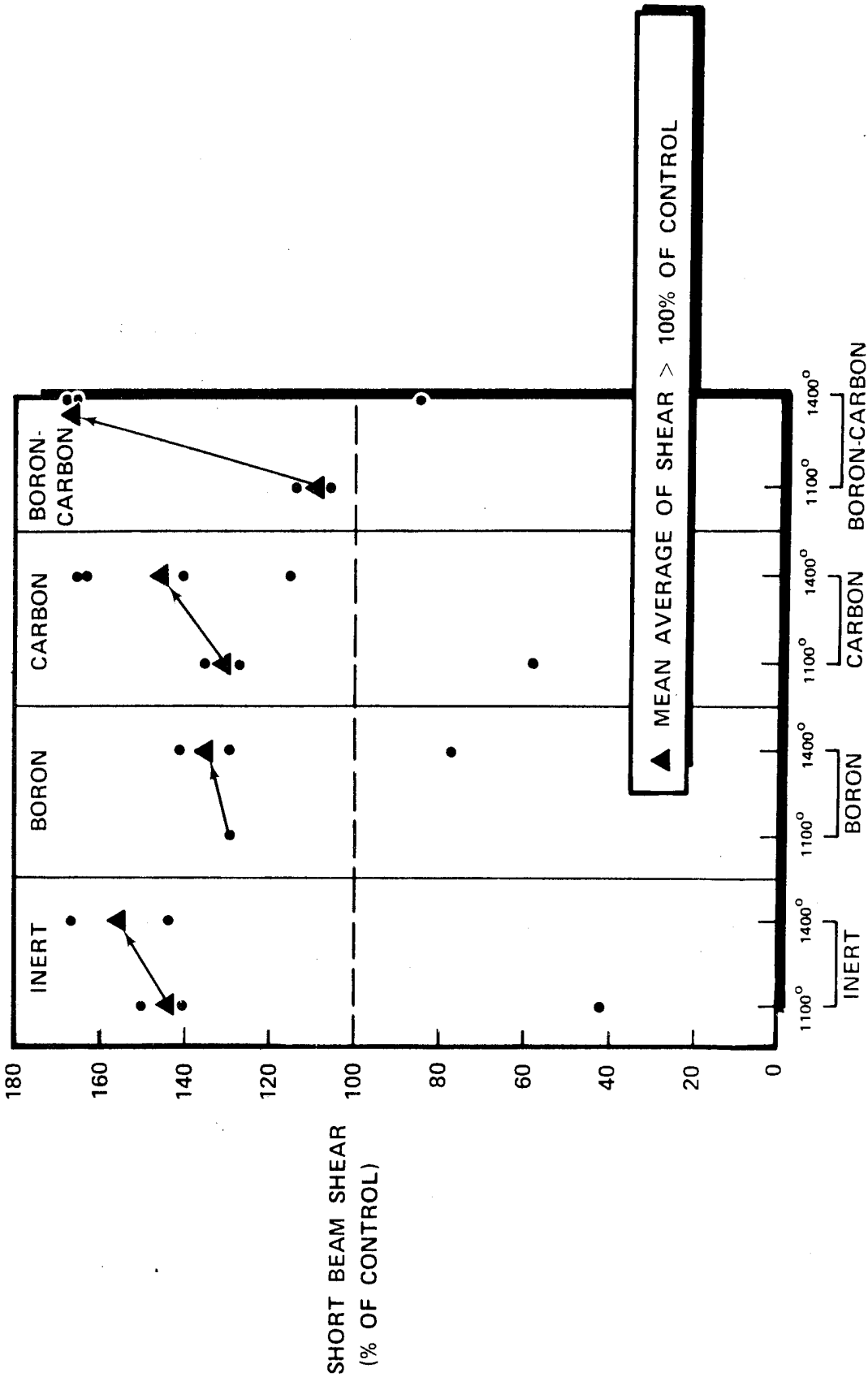


FIGURE 33. VARIATION IN INTERLAMINAR SHEAR STRENGTH RESULTING FROM SURFACE TREATMENT IN FOUR DIFFERENT ENVIRONMENTS

(Reference 3)

The following general observations and conclusions seem appropriate from examination of Figure 33:

- (1) Borocarbon treatment is statistically superior to the other treatments.
- (2) The effect of temperature is the greatest in the case of the borocarbon treatment. (All treatments are more effective at the higher temperature than at the lower temperature.)
- (3) Boron treatment (in the absence of carbon) is the least effective treatment.
- (4) Heat cleaning is nearly as effective as any of the other treatments.

The second observation--that concerning temperature--may be the most significant. The data appear to indicate that borocarbon treatment at temperatures above those investigated may result in substantial improvements in shear strength; whereas heat cleaning and carbon treatment may result in less improvement, and boron treatment in no significant increase at all.

The reproducibility between test specimens for a given set of process variables in the interlaminar shear measurements was not matched by the results of the longitudinal tensile specimens. Specimens processed in separate experiments but under identical levels of the four process factors varied by as much as 50 percent in tensile strength. However, with few exceptions, the modulus of those specimens very closely compared with the mean modulus of the four controls. Modulus variation between similarly processed specimens was only a few percent for most conditions.

Figures 34, 35, 36, and 37 present a summary of processing experiments which yielded both interlaminar shear and longitudinal tensile data. In those figures, the measured short beam shear strength is plotted against the longitudinal tensile strength and is presented as a function of four interacting process factors, respectively.

Several of the specimens exhibit improved interlaminar shear strength gained with little expense in tensile strength. This is the exception not the rule. Most specimens demonstrate significantly higher shear strength than the control but at a cost in longitudinal tensile strength. Significantly, no combination of process parameters (factors and levels) interact more favorably or less favorably than any other toward the retention of the tensile strength of as-received fiber.

In this respect, the data substantiate a conviction that was impressed early in the program on the investigators: "the degradation in tensile strength is partially, if not totally, mechanical in nature.(3)" "The yarn

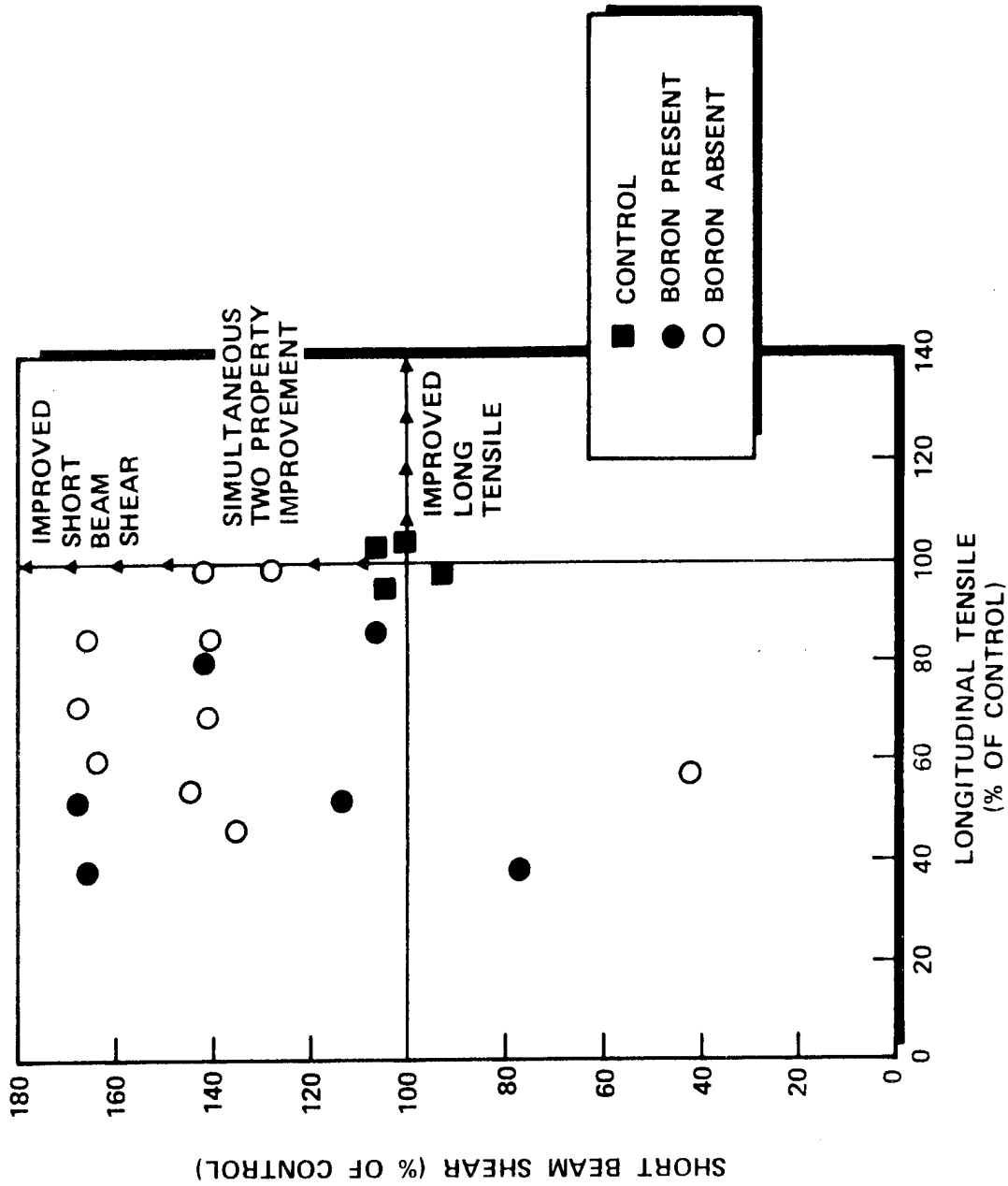


FIGURE 34. EFFECT OF THE PRESENCE OR ABSENCE OF BORON ON SHEAR AND TENSILE STRENGTH

(Reference 3)

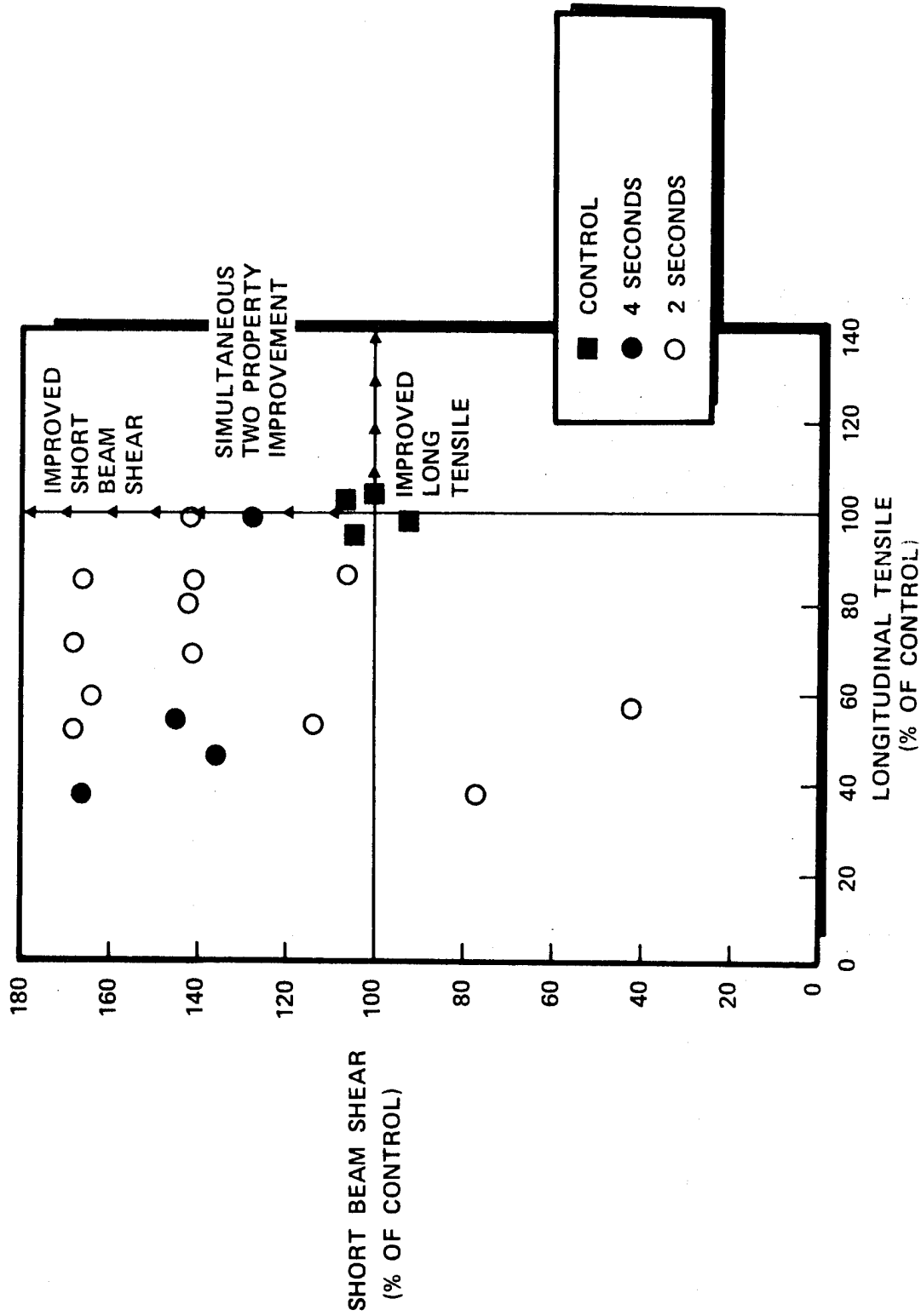


FIGURE 35. EFFECT OF DWELL TIME OF THE FIBER IN THE HOT ZONE ON SHEAR AND TENSILE STRENGTH (Reference 3)

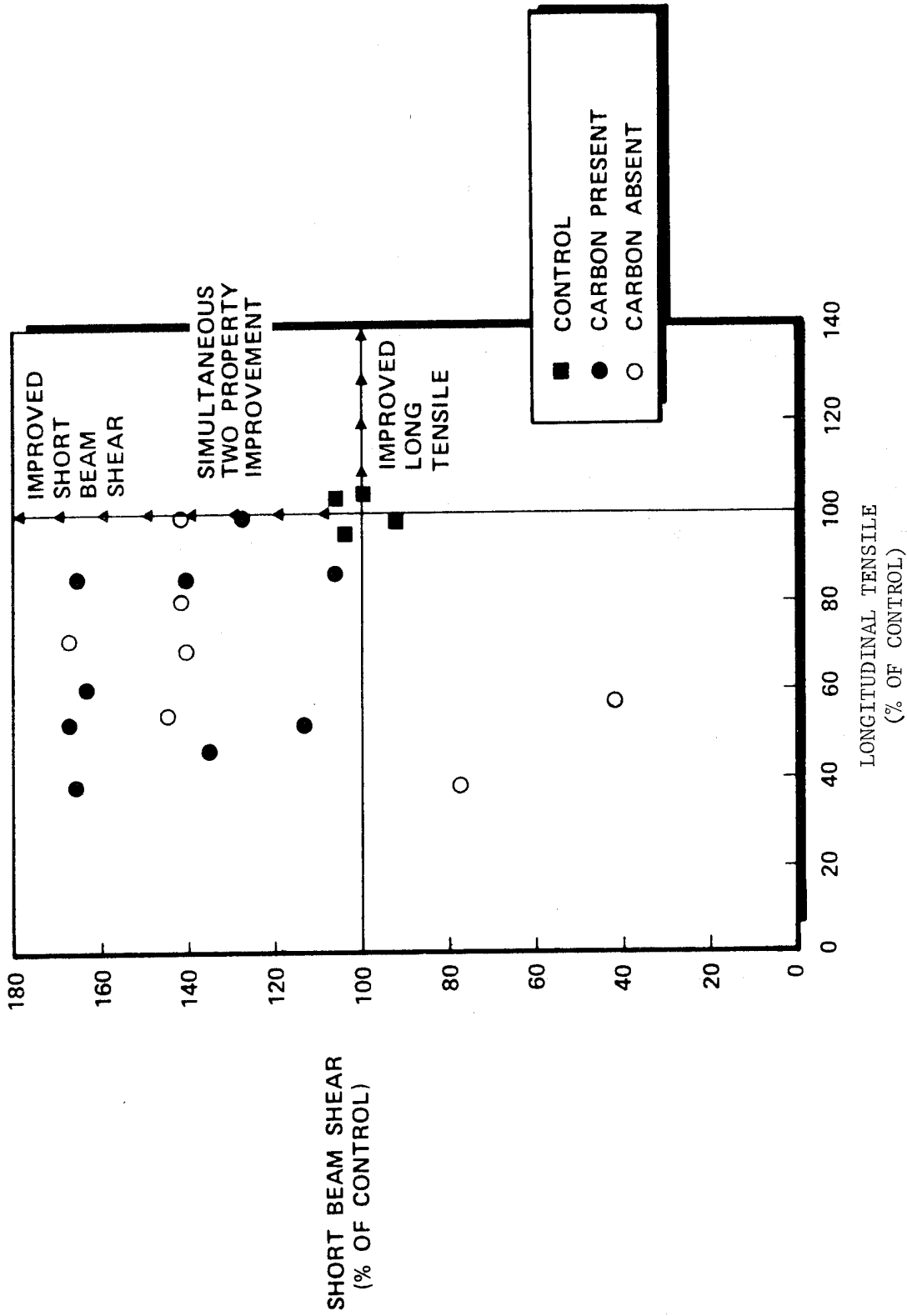


FIGURE 36. COMPARATIVE SHORT BEAM SHEAR AND LONGITUDINAL TENSILE STRENGTH AS A FUNCTION OF THE PRESENCE OR ABSENCE OF CARBON

(Reference 3)

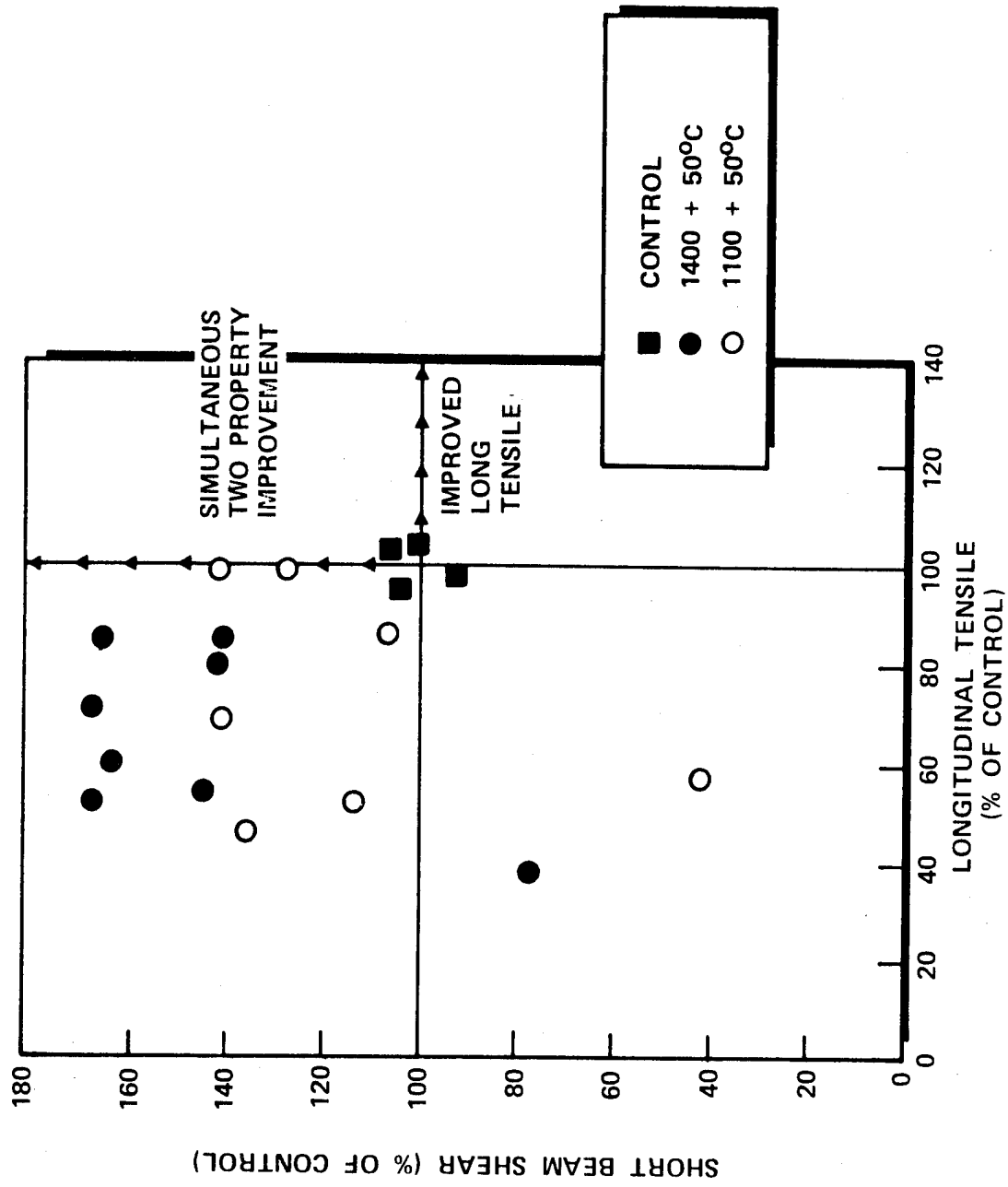


FIGURE 37. EFFECT OF FIBER TEMPERATURE ON SHEAR AND TENSILE STRENGTH

(Reference 3)

was often mechanically degraded while being transported through the surface treater. Those areas which inflict the most physical abuse on the fiber are between the removal of the protective sizing and the impregnation of the resin. The fiber undergoes fraying or splintering in the longitudinal direction. This mechanical degradation was never completely eliminated. Composites were prepared from the least damaged portions of yarn. Many runs were aborted because of excessive mechanical degradation."<sup>(3)</sup>

Based on the data presented in Figures 34, 35, 36, and 37, the following observations were deemed appropriate:

- (1) Retention of tensile strength is greatest in treatments in which boron was absent.
- (2) Retention of tensile strength is greatest in treatments at the low dwell time.
- (3) Retention of tensile strength is greatest in treatments in which carbon was present.
- (4) Retention of tensile strength is greatest in treatments at the low temperature.

Although the experimental data may be too insignificant to warrant a general conclusion, if one were made, it would be that retention of tensile strength is favored by carbon treatment at the low temperature whereas enhancement of shear strength is promoted by borocarbon treatment at the high temperature.

Task II is a continuation of the experimental effort to determine and characterize the effect of fiber surface treatment methods upon the mechanical strength of graphite composites. Under Task II, Philco-Ford has conducted research specifically to ascertain and characterize the thermochemical effect of surface treatments and the mechanical effect of apparatus upon the tensile strength of Thornel yarn. This approach was prompted by the results of completed Contract No. N00019-70-C-0301 and is intended to augment and compliment that effort by providing information on the cause of the negative results in regard to tensile properties of otherwise enhanced composites.

### 3.1 EXPERIMENTAL PROCEDURE

Experimental design is especially important in investigations of surface phenomena, because the extent of improvement must generally be measured by indirect means. For instance, in the previous program<sup>(3)</sup>, the effect of the surface treatment was assessed by incorporating the treated fiber

into a resin matrix and then measuring the mechanical properties of the resulting composite. There are many variables associated with the preparation of advanced composites that are difficult to control; consequently mechanical properties may vary significantly for reasons other than the effect of surface treatment on graphite filaments unless considerable care is exercised.

Moreover, there are other thermal treatments known to improve the mechanical properties of graphite filaments in epoxy composites. According to Epreman<sup>(6)</sup> various oxidizing and etching thermal treatments have been found to be beneficial. Friedlander and Calfee<sup>(9)</sup> and Bridges and Pope<sup>(3)</sup> report that an improvement in shear strength without loss in fiber strength can be accomplished by simple heat cleaning, i.e., heating the fiber above 1000°C in a nitrogen atmosphere. There are aspects of these reported processes which are embodied in the surface treatments previously referred to and the subject of this investigation. For instance, all are conducted at elevated temperatures in the presence of gases that can coat, oxidize, etch or otherwise alter the filaments dependent on partial pressures and other parameters. There is no simple way to design experiments in which the effects of each treatment are ascertained separately.

In view of the foregoing, a method of approach was adopted based somewhat judiciously on expediency. Time and monies did not permit the careful separation of variables necessary for a complete statistical analysis on the nature of surface treatment effects upon the tensile strength of graphite yarns. Therefore, the options of the investigation were arbitrarily narrowed to those variables which the investigators believed would yield the most fruitful information within the framework of the effort.

Specifically, the investigative options were narrowed down to four essential questions to be answered by the experiments. These questions embody an epitome of the investigation. The experiments that follow were conducted mainly to answer these questions.

- (1) HOW EFFECTIVE IS HEAT CLEANING (HEAT-TREATING) IN IMPROVING FIBER TENSILE STRENGTH?
- (2) HOW EFFECTIVE IS BORON DEPOSITION IN IMPROVING FIBER TENSILE STRENGTH?
- (3) WHAT IS THE EFFECT OF TEMPERATURE ON THE ABOVE TWO PROCESSES?
- (4) WHAT IS THE DEGRADATION EFFECT OF THE PROCESSING APPARATUS?

In order to expedite test results and to isolate the effect of surface treatment on discrete sections of treated yarn, the standard longitudinal tensile test was deleted from these investigations. In place of the tensile test, an ASTM strand breaking strength test was utilized. Individual and discrete sections of continuous treated yarn were tested for breaking strength in gauge lengths from 1 to 8 inches, to be compared to control specimens. This method facilitates the elimination of variations in results associated with the preparation of graphite fiber composites, and provides more descriptive data regarding the individual yarn.

### 3.1.1 EXPERIMENTAL EQUIPMENT AND METHODS

Three separate and distinct types of surface treaters were utilized in these investigations. Two of the surface treaters are designated as "hot filament" types in which the graphite fiber is brought to incandescence by applying current to the section of the fiber to be treated. The third surface treater employed a "resistance tube furnace" to heat the fiber by radiation. All three units utilized a common network of rotometers, manometers, valves, and manifolds to control and monitor pressure and gaseous combinations within the reaction chamber. All three systems utilized the concept of gas-seals to permit the entrance and exit of fiber while insulating the reaction chamber from the surrounding atmosphere. In general, the experimental apparatus used to treat the graphite filaments is identical to that commonly used in chemical vapor deposition. The surface treaters resemble that employed in industry to produce boron monofilament<sup>(7)</sup> and that used experimentally by Monsanto in the heat cleaning of graphite filaments.<sup>(9)</sup> Both heat cleaning and boron deposition experiments were performed in all three surface treaters.

a. Surface Treater - Hot Filament Type. The surface treater which emerged from exhausting efforts in the previous contract is presented as a schematic in Figure 38. Although some aspects of the design and a few components retain certain negative characteristics, the apparatus incorporates the best of component materials and functional design that evolved by trial and error from earlier designs. The surface treater is capable of processing continuously over 500 feet of fiber (500 feet being the maximum attempted to date). The unit has been operated at 1500°C for periods up to 2 hours and is capable of operating in partial vacuum or in slight positive pressures. This surface treater was used to process most of the test panels of surface-treated graphite-fiber laminates which is reported in Reference 3.

The surface treater is constructed of inconel and monel metals, both of which have relatively high resistance to corrosion by chlorine. The unit consists of essentially three basic parts: a 2.5 inch diameter, 9-inch long cylinder and two end caps onto which electrodes, fiber guide wheels, and gas-sealing curtains are mounted. The end caps which are sealed to the

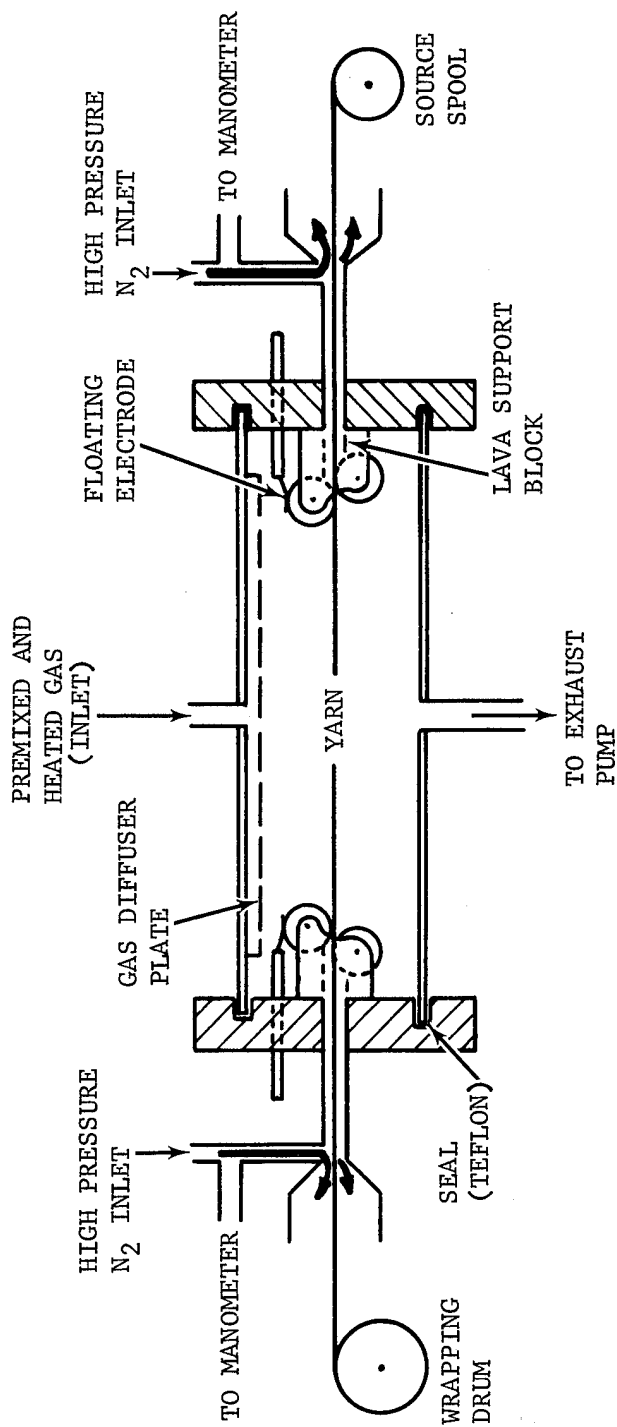


FIGURE 38. HOT FILAMENT SURFACE TREATER

cylinder by Teflon are removable for cleaning and fiber threading operations. The chamber is equipped with a gas inlet capillary which attaches onto a gas-diffuser plate. The latter is welded to the interior of the chamber at its seams and contains 20 equally spaced small holes. Incoming gas can only enter into the deposition chamber through these small holes. Thus, a fairly uniform mixture of fresh gas and reacted gases is insured throughout the length of the chamber. Although not shown in Figure 38, the exhaust capillary is also covered by a gas-diffuser plate to enhance the uniformity of the gas flow pattern. A pumping station is provided downstream on the exhaust line to permit greater control of gas flow rates of reaction.

The chamber is equipped with a 3 by 1/2 inch I.D. extension tube covered with a quartz window for optically viewing the incandescent fiber. The temperature of the fiber is monitored through this view port with an optical pyrometer. (Appropriate corrections for emissivity and absorption must be applied to the recorded temperatures.)

The electrodes by which electrical current is transferred to the moving fiber consists of two freely suspended inconel rotating wheels, one mounted on each end cap via an electrical insulation block of lava. The outer perimeter of the wheels are concaved toward the center axis and the surfaces finely polished. This design permits the fiber to travel in close intimate contact with the surface of the wheel without being mechanically grabbed (and, hence, shredded) by either a geometric pinching effect or by a coarse metal finish.

Electrical current, provided by an external dc power supply, is conducted to the wheel by insulated power leads on both end caps which transfer the current to a floating electrode. The latter is a copper spring with a electrical-transfer disc of graphite which contacts the rotating wheel. The concept of the floating electrode is to provide intimate contact between the electrical source and the transfer wheel without inducing mechanical drag on the wheel. Hence, the wheel is free to rotate with the traveling fiber and thus allowed to cool with resonant frequency. This prevents the buildup of localized hot spots which could damage incoming fibers either through spurious overheating or by a welding effect causing attachment between the fiber and the wheel. A secondary, but very important feature of the floating electrode concept, is the fact that the energy transfer occurs on the surface or the skin of the wheel. Thus, overheating of the axial area or hub of the wheel, which could stop or impede the rotation of the wheel, is averted since energy is not directed toward the center. The effect of a nonrotating or interrupted wheel is to induce mechanical drag to the traveling fibers.

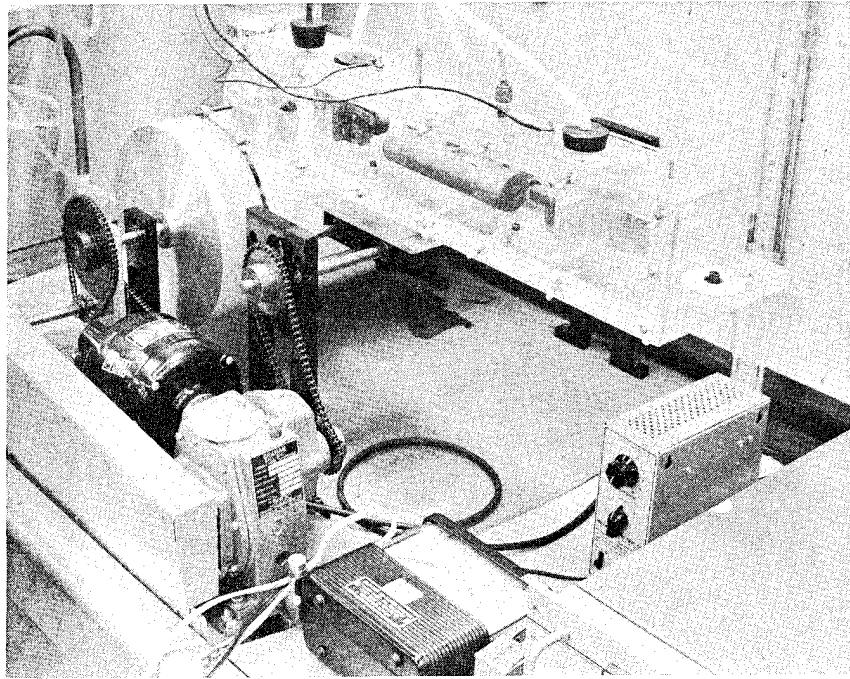
The traveling fiber is guided off the exit electrode of the electrical transfer wheels by narrow inert versions of the former. These wheels are slightly offset with respect to fiber axis. Therefore, they act to press

the fiber onto the transfer wheels, thereby insuring nearly steady-state electrical transfer. The electrical transfer system described above has operated continuously for 2 hours under a supplied power load of 70 volts and 3 amps (1500°C fiber temperature over 6 inches of incandescence) with only minor current fluctuations. The latter was observed to be due to undampened harmonic oscillations in the long fiber rather than spurious electrical system defects. Peak power loads of 100 volts and 12 amps causing a fiber temperature of 1600°C over 12 inches of fiber have been tested with the electrode design.

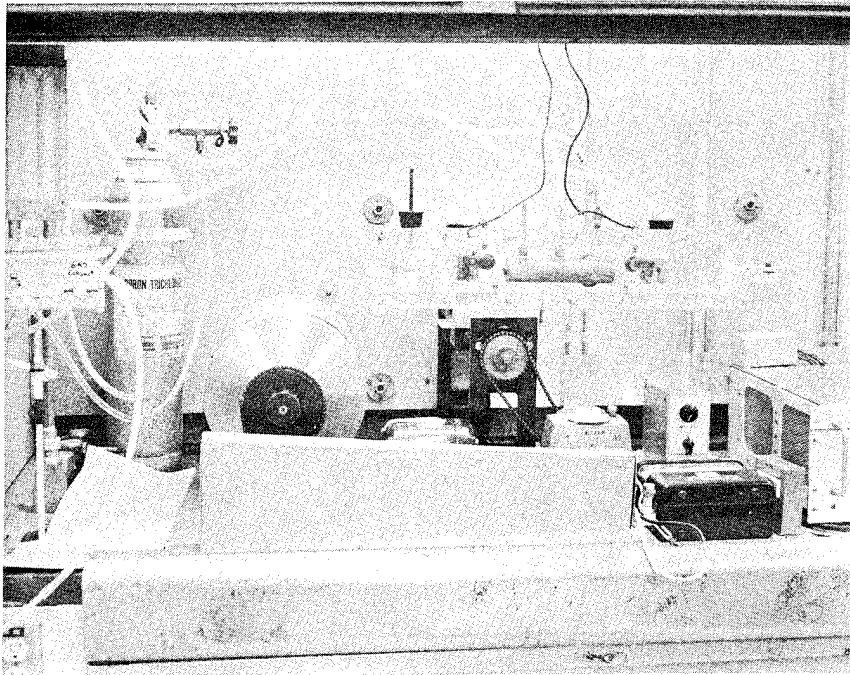
b. Surface Treater - Enclosed Hot Filament Type. This unit was developed during the program in an attempt to improve surface treatment processing equipment. Two goals fostered the development of this unit; (1) reduction of induced mechanical degradation which effects tensile strength of treated fiber; and (2) improved efficiency in the boron trichloride reaction governing boron deposition. The unit incorporates many of the concepts and materials and several components from the "hot filament type surface treater" described above. The unit is pictured in Figures 39a and 39b.

Two major changes distinguish this unit from the above hot filament surface treater concept. They are:

- (1) All integral components of the actual surface treatment process are housed inside a lucite dry box. The components include the electrodes, reaction chamber, and resin impregnation tank. The lucite dry box traverses along the yarn takeup wheel to facilitate fabrication of panels. An inert atmosphere is maintained inside the dry box thereby insuring the complete processing under conditions which retard external effects such as oxidation, water absorption and thermal etching.
- (2) The current electrodes are moved outside the gaseous reaction chamber and are located fore and aft of the same. Thus, the heat cleaning operation which necessarily precedes the boron deposition in the boron trichloride reduction process is performed before the fiber enters the reaction chamber. Therefore, vapor phases of the thermally evolved sizing and impurities in the graphite yarn do not interfere with the combination of gases in the reaction chamber. An additional advantage to this electrode location is the incorporation of an inert gas jet which sweeps the current electrode wheels with a cleaning stream of gas thereby retarding the accumulation of foreign material. Electrode impurity



(a)



(b)

FIGURE 39. ENCLOSED HOT FILAMENT SURFACE TREATMENT APPARATUS

accumulation has been observed to cause physical degradation which severely reduces the tensile strength of the treated fibers.(3)

c. Surface Treater - Resistance Furnace Type. The high temperature resistance heated deposition furnace used in this program for radiation heating of the filament is shown in Figure 40. The heating zone was 1-1/2 inches in diameter by 9 inches in length. A quartz tube designed from previous CVD experience was fabricated to serve as the reaction chamber. Temperature of the reaction zone was monitored by means of Pt-Pt+10% Rh thermocouples imbedded into the quartz. Temperature of the filament was calculated from radiation heat equations which consider wall temperature and emissivity, specific heats, and convective heat losses. The temperature of the filament was also estimated by viewing the hot filament at an oblique angle through the transparent ends of the quartz tube reactor. The furnace pressure can be reduced to less than one-half atmosphere and was equipped with rotometers, manometers, valves, and manifolds to allow the desired combination of gases to be admitted into the furnace during operation.

The resistance furnace technique had the disadvantage that processing of continuous filaments required the gas curtain seals shown in Figure 40. Those seals are necessary to isolate the reaction chamber from the ambient and yet permit the filament to move in and out of the chamber. Thus convective cooling within the chamber and along the axis of the filament was encountered due to the turbulence of the system. Also, the large area of the hot wall which formed the radiation surface also served to heat and react the incoming gaseous mixture. This in turn led to three effects; (1) the hot wall became a very large sink for boron deposition as compared to the substrate, (2) the substrate was coated only very slowly, and (3) boron solids were observed near the exhaust end of the reactor tube.

The advantages of the resistance furnace type surface treater are, of course, the elimination of mechanical and electrical contact between the current electrodes and moving fiber. Thus, mechanical degradation to the tensile properties was severely restricted. This permitted separation of that variable for purposes of ascertaining the effects of heat cleaning and partially in assessing the effect of boron deposition on fiber tensile strength.

d. Common Gas Flow and Pressure Control Network

(1) Gas Seals. The gas-seal curtains have proven quite effective and were arrived at as the best design which would permit the fiber to enter and exit the deposition chamber with a minimum of wear to the fibers, while concurrently insulating the chamber from the presence of air. The concept is one of capillary impedance in which pressure differentials and capillary cross sections are used to cause a directional gas-flow pattern.

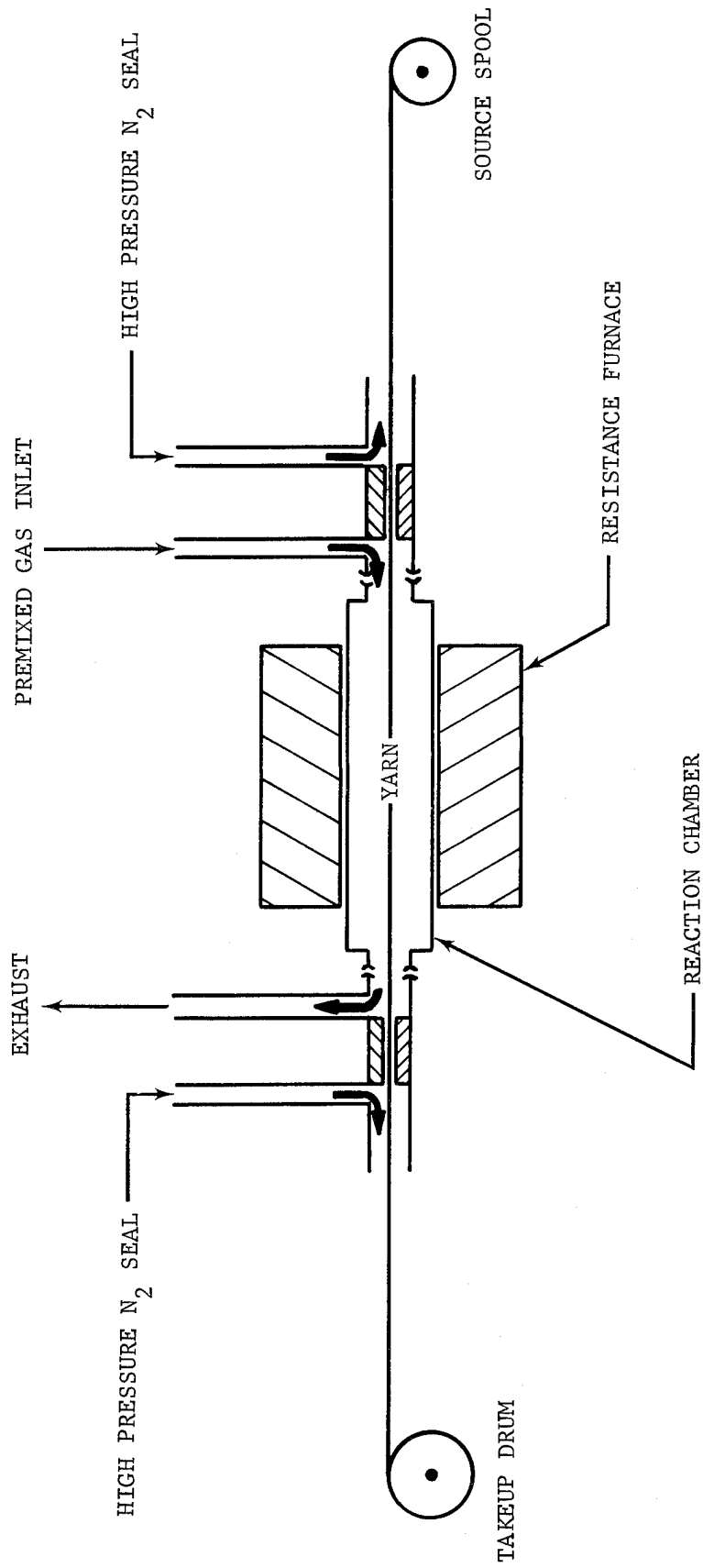


FIGURE 40. RESISTANCE FURNACE SURFACE TREATER

Nitrogen or argon are injected at the fiber entrance and exit ports at pressures greater than atmospheric and directed away from the deposition chamber which is isolated from the ports by flow-resistant capillaries. Thus, air is prevented from entering the chamber, and the graphite fiber can enter and exit without encountering mechanical parts or by immersion in a liquid seal.

The reliability of the gas curtain seals was demonstrated by chemical analysis of samples of effluent gases from the deposition chamber. Typical results as determined by mass spectrography are presented in Table III.

TABLE III. TYPICAL CHEMICAL COMPOSITION OF GAS EFFLUENT FROM ARGON-SEALED SURFACE TREATER

Reactants Seal and Exhaust Pressures:	CH <sub>4</sub> + H <sub>2</sub> + BCl <sub>3</sub> Argon - 800 mm Exhaust - 750 mm	H <sub>2</sub> + BCl <sub>3</sub> Argon - 800 mm Exhaust - 700 mm
Reaction Temperature:	1300°C	1300°C
Species	Mole Percent	Mole Percent
H <sub>2</sub>	18.89	8.55
CH <sub>4</sub>	13.65	0.01
H <sub>2</sub> O	0.03	0.02
C <sub>2</sub> H <sub>6</sub> (ethane)	0.20	0
Hydrocarbons (as butane) C <sub>4</sub> H <sub>10</sub>	0.02	0
N <sub>2</sub>	0.30	0.23
O <sub>2</sub>	0.03	0.05
CO <sub>2</sub>	0.05	0
HCl	5.53	0.76
1, 2-BIS-2-chloroethoxyethane	0.59	0
BCl <sub>3</sub>	5.92	0.01
Argon	54.79	90.37

(2) Reactant Gases - Sources and Metering System. Commercially available cylinders of various gas species were utilized as the source of boron, carbon, and hydrogen. Cylinder gas was vented through standard tank regulators to control valves whereby the rate of flow was further checked. The volume flow rate of the respective gas was then controlled by the valve and monitored with a Brooks Rotameter Series R-2-15 flow meter. The gas then entered into a one-liter mixing chamber where it combined with other reactant gases. The temperature of the premixing chamber was maintained at 250°C.

The gas mixture was then valved from the premixing chamber to the deposition chamber through another flow meter which monitored the total gas volume flow rate. The gas transport system was maintained at 250°C to guard against cold-wall losses, particularly cold-wall reaction with the boron trichloride.

(3) Monitoring Network. In addition to the gas-flow-rate monitors mentioned in the above subsection, a series of U-tube mercury manometers were used to monitor pressure and pressure differentials. These were employed in the deposition chamber and in the exhaust capillary which ventilated the chamber. Manometers also were employed to establish and maintain the proper pressure differential in the gas sealing curtains.

### 3.1.2 PREPARATION OF FIBER STRENGTH TEST SPECIMENS

As treated yarn emerged from the surface treater described in Paragraph 3.1.2a, b, or c, it was passed through a shallow trough containing epoxy resin. Narmco 1004 resin was used as the impregnant. The impregnated yarn was wound onto the takeup drum at a spacing of about 66 yarn bundles per inch. Generally, about 1 inch width of 66 bundles per inch yarn was processed before terminating the run. The 1-inch (nominal) wide bundle was then split, removed from the drum, and stretched flat to cure.

Breaking strength specimens were removed from the flat panel and placed on 3x5 or 5x10 index cards. The gauge length of the breaking strength specimen was varied between 1 and 8 inches by design. The index cards were used to support the specimen and thereby restrict physical or mechanical degradation due to handling. Prior to the breaking strength test, the index support card was split in half in the gauge length area.

The breaking strength test fixture consists of a mechanical force gauge, a variable speed drive bodine motor, and two noncrimping end clamps. The unit is mounted in a horizontal plane such that the treated yarn specimen is supported by the index card until an applied tension causes the suspended yarn to support itself. The range of pulling speed can be varied from 0.01 to 0.50 inch/minute. The mechanical force gauge was calibrated in Philco-Ford's Metrology Laboratory.

### 3.1.3 SELECTION OF BASELINE MATERIALS

Four commercially available graphite yarns were evaluated in the initial stages of this effort. The four materials and their associated properties are presented in Table IV. The four yarns are Thornel 50, Thornel 75S, Modmor I, and Modmor II. Cursory surface treatment experiments indicated that little was to be gained by processing two grades of the same yarn, i.e., data extracted from one grade was comparable with the other for similar surface treatments. Distinct differences in the apparent effect on tensile strength were observed in some cases for identically processed Thornel and Modmor yarns. In other cases, insignificant differences were observed. This discrepancy is directly attributable to the random physical degradation induced by the processing equipment.

Modmor yarn did appear to have a greater propensity for induced physical degradation in the processing equipment employed in these investigations. As a result, and in order to keep the investigation in line with the previous effort (Contract No. N00019-70-C-0301), the Thornel 75S graphite yarn was selected as the baseline fiber for the remainder of the experimental effort.

Thornel 75S graphite yarn is a patented continuous length high modulus graphite fiber in a two-ply construction. It is fabricated by the Union Carbide Corporation, Carbon Products Division. The surface of the fiber has been treated to increase the interlaminar shear strength in a resin matrix composite. Specific properties and characteristics of Thornel 75S Yarn Grade WYJ 160-1/2 is presented in Table V.

### 3.1.4 REACTION CHEMISTRY OF THE BORON EXPERIMENTS

Boron can be alloyed with graphite as a substitutional material replacing a carbonation or as an interstitial material locating between the carbon laminae. The first small quantities of boron add substitutionally, but the point at which the additions change to interstitial locations is not clear. Recent work on the codepositions of pyrolytic graphite and boron from mixtures of methane and boron trichloride indicate the interstitial additions begin at about 1 weight percent of boron.<sup>(10)</sup> The amount of interstitial boron that can be added is not known but some experiments went as high as 7 percent. The substitutional boron acts as a graphitizing agent, increases density, decreases electrical resistivity and increases the oxidation rate. Interstitial boron acts inversely of substitutional boron, i.e., decreases graphitization, decreases density, increases electrical resistivity and decreases oxidation.

The interstitial boron in a pyrolytic graphite deposition has been suggested to be boron carbide ( $B_4C$ ).<sup>(11)</sup> Flexural samples of pyrolytic graphite decrease in strength to about 0.5 percent boron and increase strength substantially after 0.5 percent to a maximum of 2.5 percent. The increase in strength was attributed to dispersion hardening by the interstitial boron carbide.

TABLE IV. PROPERTIES OF MATERIALS EVALUATED FOR TASK 2

Property or Characteristic	Unit	Thornel 50	Thornel 75S	Modmor I	Modmor II
Sizing or Coating		PVA	Resin?	Treatment/ Resin?	Treatment/ Resin?
Filaments per ply		720	720	10,000	10,000
Plies per yarn		2	2		
Yarn Diameter	Microns	6.0	6.0	7.8	8.1
Yarn Twist	Twist per foot	18	18		
Breaking Strength (10 in. gauge)	lb	8.8	10.5		
Tensile Modulus	( $10^6$ psi)	78	78	56	39
Ultimate Tensile Strength	( $10^3$ psi)	380	345	340	360
<u>Composite Properties</u>			Typical for ERLB 4617/ MPDA	Typical for Shell 828/ NMA/BDMA	Typical for Shell 828/ NMA/BDMA
Tensile Modulus	$10^6$ psi		44		
Tensile Strength	$10^3$ psi		214		
Flexural Modulus	$10^6$ psi		41	28	20
Flexural Strength	$10^3$ psi		115	170	222
Interlaminar Shear Strength	$10^3$ psi		6.0	10.0	12.5
Fiber Volume	%		57	60	60

TABLE V. PROPERTIES AND CHARACTERISTICS OF THORNEL 75S

Average Properties and Characteristics "Thornel" Yarn Grade WYJ 160-1/2				
Property	Unit	Value		
Tensile Strength (10 in. Gauge)	lb/in. <sup>2</sup>	345,000		
Tensile Modulus	x 10 <sup>6</sup> lb/in. <sup>2</sup>	78		
Density	g/cc	1.80		
Yield	yd/lb	8,200		
Yarn Denier/Ply	g/9000 M	270		
Breaking Strength (10 in. Gauge)	lb	10.5		
Elongation at Break	%	0.53		
Plies/Yarn	--	2		
Filaments/Ply	--	720		
Yarn Twist	TPI	1.5(S)		
Yarn Diameter	in.	0.015		
Yarn Cross Sectional Area	x 10 <sup>-5</sup> in. <sup>2</sup>	4.9		
General Properties "Thornel" 75S Graphite Filaments				
Property	Unit	Value		
Elongation at Break	%	0.5		
Elastic Recovery	%	100		
Equivalent Diameter	μ	6.0		
Carbon Assay	w/o	99.9		
Surface Area	m <sup>2</sup> /g	1		
Thermal Conductivity	Btu-ft/hr (ft <sup>2</sup> )(°F)	90		
Specific Heat	70°F	0.17 (mean 70° to 2700°F = 0.40)		
Manufacturing Specification				
Property	Acceptance Limits			
	Nom	Min	Max	Std Dev
Strand Modulus, psi x 10 <sup>6</sup>	76*	70	82	2.48
Strand Breaking Strength, psi	360,000*	300,000	--	31,000
Torsion Shear Strength, psi	7,200	6,000	--	910
Yield, ft/lb, 2 ply	25,800	24,300	27,300	657
Density, gms/cc (lot average)	1.82	1.77	1.88	0.02
Splices/lb	8	--	15	2.9

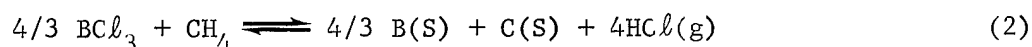
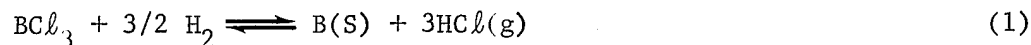
\*Average of five measurements

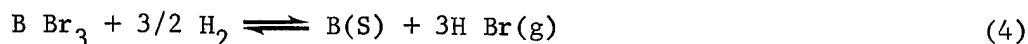
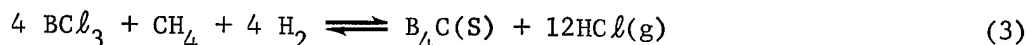
Similar experiments to the alloying of pyrolytic graphite with boron have been conducted on high modulus graphite fibers.<sup>(12)</sup> Graphite crucibles doped with different levels of boron were used to anneal PAN precursor high modulus fibers at temperatures of 1900 to 3000°C. The boron from the crucibles formed a vapor phase and diffused into the graphite fibers. Final boron concentrations in the fibers were 0.05, 0.25 and 1.0 percent. The electrical resistivity decreased and the modulus increased both as the boron concentration increased and as the annealing temperature increased. The best modulus values were between 90 and 100 x 10<sup>6</sup> psi. The strength determinations were more widely scattered and the change with boron was not as pronounced as resistivity and modulus. There was definite trends toward higher values, particularly with the higher modulus fibers. The highest strengths were 450,000 psi. X-ray diffraction produced a slight sharpening of the diffraction lines with increasing boron concentration, but no new lines. The boron was believed to increase modulus and strength by improving crystallinity and acting as a solid solution hardening element, preventing shear in the crystallites.

The first successful boron treatment to improve bonding properties of graphite fibers was combined with a deposit of pyrolytic graphite. The source of the pyrolytic graphite, toluene, was added to the reaction atmosphere around the incandescent fiber as a reactant to remove the chlorine released by the decomposition of boron trichloride. The concentration of the boron was not determined, but it was known to be much lower than the added carbon. The use of pyrolytic graphite appears to be a needed part of the process and this is the logical place to begin additional work. However, at this time there is no logic to explain a need for additional carbon and any continuation of a boron fiber modification should thoroughly evaluate boron deposits alone.

A hot filament will reduce a boron halide and hydrogen to boron and the hydrogen halide or decomposes diborane to boron and hydrogen. The chemistry is simple, but a uniform deposition contains the same problems as a boron/pyrolytic graphite coating. The reduction of a boron halide has widespread application in industry and has been extensively employed at Philco-Ford in research concerning boron deposition.

Since the effect of boron deposition on tensile strength was to be investigated semi-qualitatively, it was desirable to use simple chemical reactions in which the inlet gas flow could be readily controlled to maintain boron concentration in the reaction chamber. The four following reactions exemplified that requirement.





The free energy of formation,  $\Delta F_f^0$ , of the four reactions is presented in Figure 41. Equations (1) and (2) were used exclusively throughout the experimental phase as the formation of  $\text{B}_4\text{C}$  in Equation (3), though requiring investigation, contained another variable which the scope of this effort could not permit. The same condition was true in the reduction of boron tribromide in Equation (4).

### 3.2 DISCUSSION OF THE EXPERIMENTAL RESULTS

The response of Thornel 75S (Union Carbide WYJ 160-1/2 yarn) to heat cleaning or boron doping surface treatment was evaluated by data analysis and experimental observation. Experiments were conducted in which two parameters, temperature and boron content were varied. The latter parameter, boron content, was assigned the values of "presence" or "absence" within the reactor. When experimentally called for, the boron content was a constant throughout as governed by the input flow rate, the volume of the reaction chamber, and the length of incandescent yarn. Temperature was allowed to vary for both types of surface treatment between  $800^\circ \pm 50^\circ\text{C}$  to  $1400^\circ \pm 75^\circ\text{C}$ .

The dwell time of the incandescent yarn within the reaction chamber was maintained at a constant 4 seconds for all experiments. The gas seals (Paragraph 3.1.1.d) of the three types of surface treaters described in Paragraph 3.1.1 were operated with Argon gas at constant flow rates. The type of resin, Narmco 1004, and its solid content (37.5 percent) were maintained as constants.

Duplicate experiments were conducted in the three surface treater units (Paragraph 3.1.1) and, therefore, the type of apparatus can be construed as a qualitative parameter. Each type of reactor contained design features which were observed to act negatively or positively in relation to each other. Experimental observations from the experience of the three units will be discussed in Paragraph 3.2.4.

Each treatment was performed at least twice in duplicate runs; some treatments were repeated several times. This replication served two purposes: It provided a check of reproducibility; and for several treatments, it was essential to assure overall preparation of sufficient material to determine the true average strength of that treatment. In all, replication resulted in over 40 different runs.

Yarn breaking strength data was derived from these 40 experiments. The tensile strength, as characterized by the breaking strength, was significantly improved in several of the treated yarns as in otherwise identical

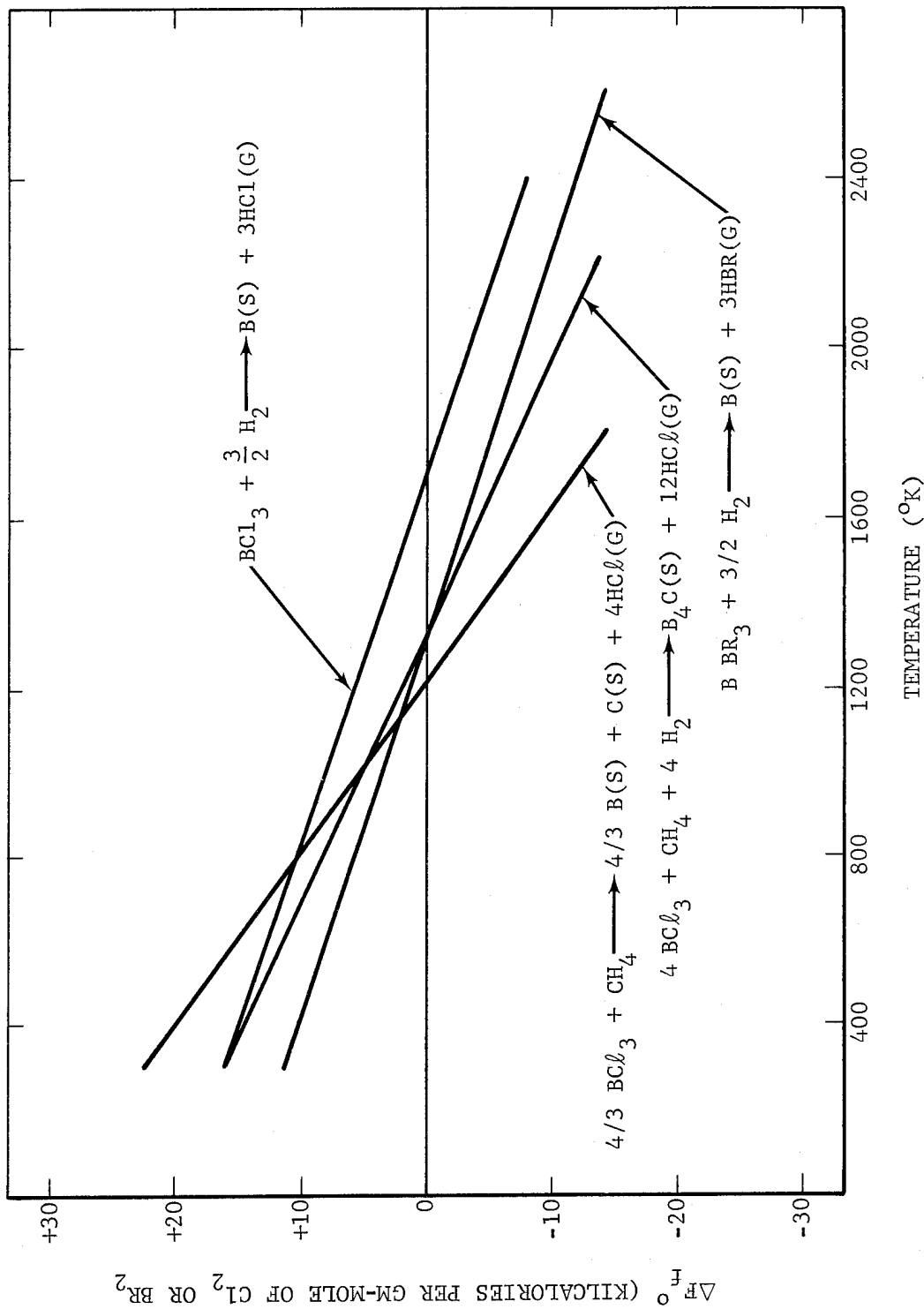


FIGURE 41. THE FREE ENERGY OF FORMATION AS A FUNCTION OF TEMPERATURE FOR SEVERAL REACTIONS EVALUATED FOR CVD PROCESSES

untreated control yarns. This was particularly the case for some yarns heat cleaned in an argon atmosphere between  $1000^{\circ} \pm 50^{\circ}\text{C}$  and  $1300^{\circ} \pm 75^{\circ}\text{C}$ . Above and below these temperatures, most treated yarns were unchanged or reduced in strength as in the otherwise identical control. The boron doped yarns did not produce the same results but did tend to establish a pronounced relationship between the yarn incandescence temperature and the strength of the resultant treated yarn.

In general, a notable lack of consistency and reproducibility was evidenced in both the processing characteristics and the resultant treated yarn strength.

### 3.2.1 CONTROL SPECIMEN AND RESIN IMPREGNATION ENHANCEMENT OF STRENGTH

In order to determine the relative effect of the surface treatments upon the strength of the yarn, an accurate determination of the breaking strength of untreated yarn was required. Complicating the issue, is the fact that degradation induced by the surface treater apparatus must be assessed. Obviously, mechanical degradation at ambient or cold temperatures will be different from the thermally boosted degradation at the higher incandescent temperatures. Intuitively, this statement remains reasonable for all conceivable and more perfected surface treatment apparatus and processing methods. Thermochemical splitting of individual filaments at high temperatures would be expected because of rapid reactions which evolve impurity vapors from the depths of the bundle, to say nothing of the reaction at the yarn surface caused by the host gases of the chamber. Electrostatic splitting of individual filaments must also be anticipated at elevated temperatures.

The problem at hand then became one of which is the proper reference level; (1) strength of as-received material; (2) strength of yarn mechanically degraded at ambient temperature; or (3) the strength of yarn degraded at temperatures slightly below the surface treatment temperature. Obviously the latter two conditions would more accurately serve as a reference point by which the true enhancement of strength due to the surface treatment could be assessed. However, from an applied stand both (2) and (3) would yield inflated values of relative strengths for treated yarns.

The problem resolved itself, however, when repeated measurements revealed an insignificant difference ( $\leq 5$  percent) in yarn breaking strength between the "as-received" Thornel 75S yarn and yarn pulled through the surface treater at low temperatures when both conditions of yarn were resin impregnated. This was true even though a significant difference (20 percent nominally) was observed between the "as-received" material and yarn pulled through the surface treater when neither was resin impregnated.

Three of the described conditions are presented in Figure 42. The data in Figure 42 are average values taken from up to 20 measurements for each condition. The condition of "resin impregnated as-received" yarn is approximately the same values as shown for yarn "pulled through the surface treater and resin impregnated." The former is nominally 5 percent greater.

The contradiction in the values of breaking strength presented in Figure 42 for different conditions of yarn reference material highlights the effect of resin impregnation. Though the as-received material was degraded in strength up to 20 percent when subjected to mechanical abuse in the surface treatment apparatus, the same absolute difference was not observed in repeated measurements when the two conditions of yarn were resin impregnated. The suggested answer appears to be that the resin matrix and cure cycle has a healing effect upon the mechanically abused yarn for (at least) short gauge lengths. The mechanism of healing affected by the resin could be similar to that of heat cleaning wherein voids caused by the twist and stretching action of the surface treater to the yarn bundle are filled in by straightening of the filaments comprising the yarn.

The scope of this phase of the program did not permit further exploration of reference values. Therefore, the very highest values of resin impregnated yarn from both the as-received material and mechanically abused yarn were accepted, and the rest of the data discarded. These highest values contained a mean deviation of approximately  $\pm 5$  percent. They were accepted as the control value or reference value for Thornel 75S yarn and are used for analysis on the effect of surface treatments to follow. The established highest reference values are presented in Table VI.

TABLE VI. REFERENCE VALUES FOR THORNEL 75S YARN

Gauge Length (inches)	Breaking Strength (pounds)	Average Corresponding Tensile Strength (psi)
1	14.1	287,000
3	13.9	284,000
5	13.5	276,000
7	12.9	263,000

Repeated control measurements throughout the experimental period failed to produce higher values.

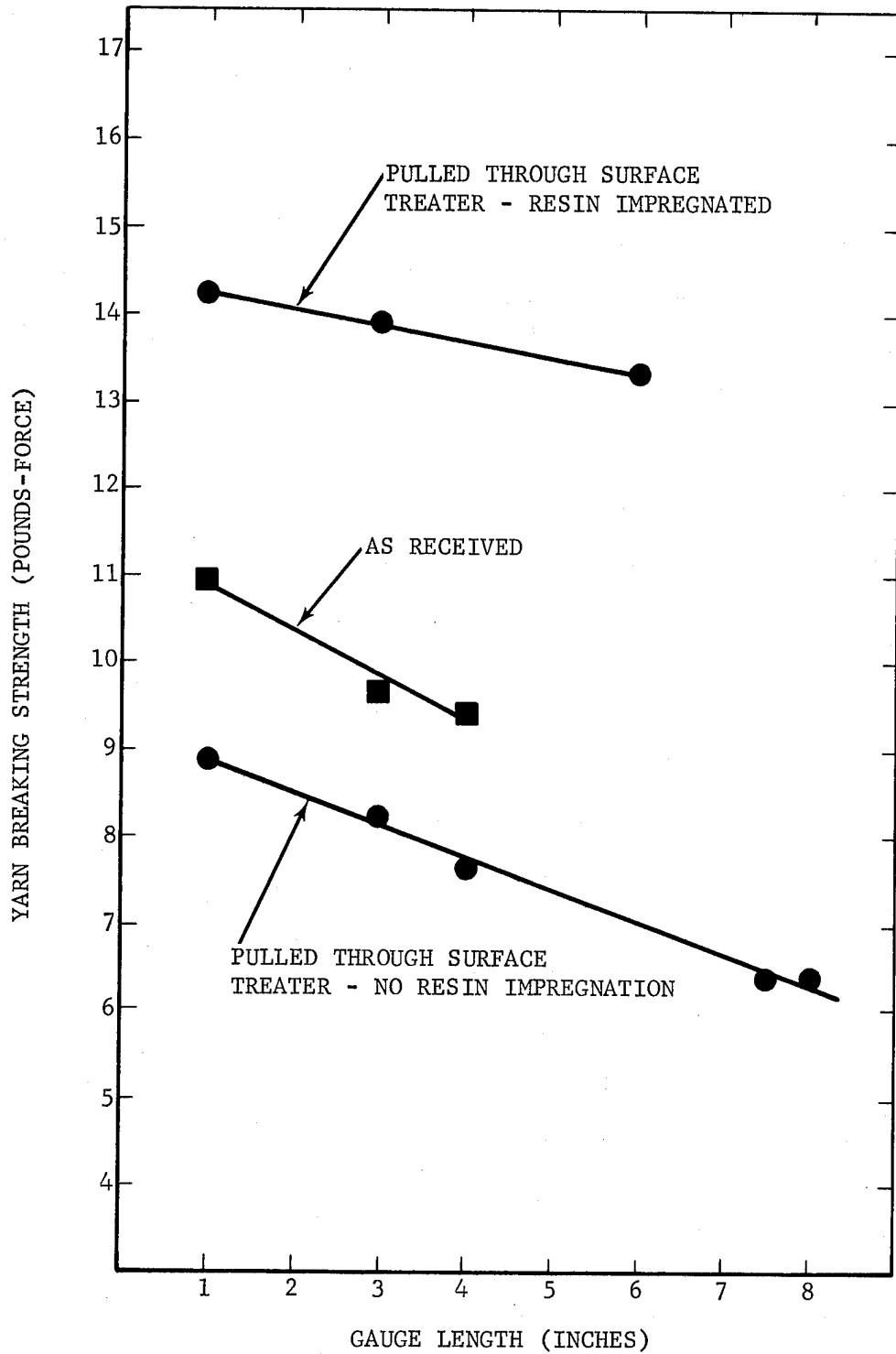


FIGURE 42. VARIATION IN YARN BREAKING STRENGTH OF CONTROL SPECIMENS

### 3.2.2 EFFECT OF HEAT CLEANING

The effect of heat cleaning on yarn breaking strength as a function of temperature is presented in Figure 43 and in Table VII. The data in Figure 43 represents an array of average data from many measurements. The data are not identified in Figure 43 as to the type of surface treatment apparatus (Paragraph 3.1.1). This is because of little significant difference in breaking strengths derived from specimens processed by the different surface treatment apparatus (see Paragraph 3.2.4 for elaboration). The complete data identification is presented in Table VII. All of the data is not presented in Figure 43 for purposes of clarity since many data points are duplicated. The horizontal line through the data represents the variation in, and accuracy of determination, of the incandescent temperature of the yarn.

In general, heat cleaning in an inert environment (argon) had a beneficial effect on yarn breaking strength where the incandescent temperature of the yarn was above 1000°C and below 1350°C for hot filament type surface treaters. The same statement is generally true for the radiation type heating of the resistance tube furnace (Paragraph 3.1.1c) where the calculated temperature of the filament was in the above temperature regime. However, improvement in breaking strength was less pronounced for the latter type of heating. Rapid and periodic convective cooling of the filament is the suspected cause of this effect.

Above 1350°  $\pm$ 75°C and below 1000°  $\pm$ 50°C the resultant breaking strength was either unchanged or slightly degraded as in otherwise identical specimens of untreated yarns (reference value). The latter are depicted in Figure 42 by the inset pair of data points corresponding to room temperature (R.T.).

### 3.2.3 EFFECT OF BORON DEPOSITION

The effect on yarn breaking strength as affected by boron doping is presented as a function of deposition temperature in Figure 44 and Table VIII. The data were derived from experiments conducted in the surface treatment apparatus described in Paragraph 3.1.1b; the inert gas surrounded (enclosed) hot filament surface treater. Data derived from specimens prepared with the other two types of apparatus revealed lower and substantially more deviating (between the same specimen) values of breaking strength. Additionally, the yarn was observed to be more physically abused during processing for the other two types of surface treaters.

The data in Figure 44 are average values of several measurements from a single processing run. The horizontal lines through the data points represent the variation in, and accuracy of determination, of the incandescent temperature of the yarn during boron deposition. All data are from identical

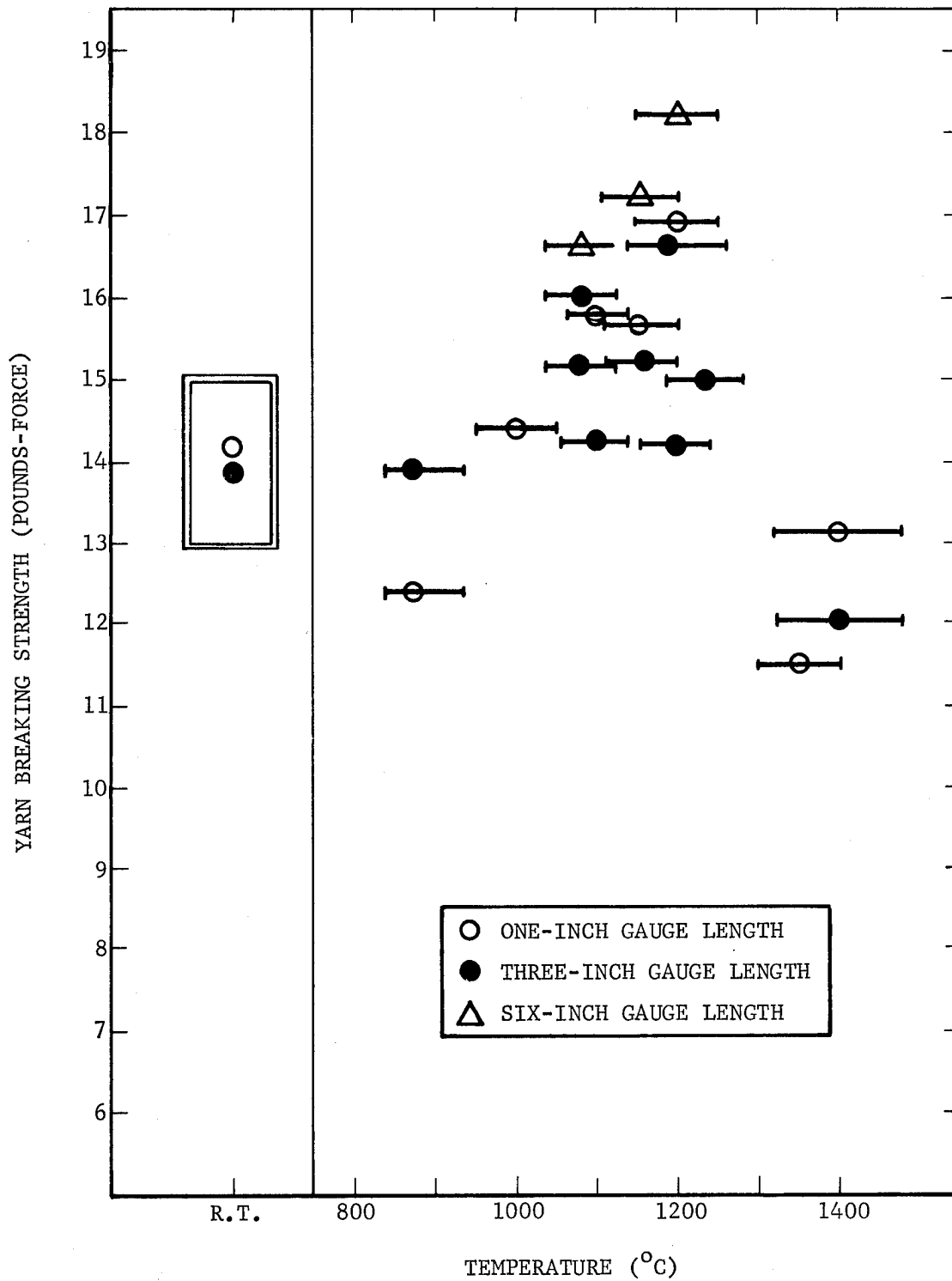


FIGURE 43. VARIATION IN YARN BREAKING STRENGTH RESULTING FROM HEAT TREATMENT IN AN INERT ENVIRONMENT AT DIFFERENT TEMPERATURES

TABLE VII. EFFECT OF HEAT CLEANING TEMPERATURE ON YARN BREAKING STRENGTH

Surface Treater	Temperature (°C)	Breaking Strength, Pounds																			
		Pull Rate = 0.05 Inch/Minute						Pull Rate = 0.25 Inch/Minute						Pull Rate = 0.25 Inch/Minute							
		1 in. Gauge		3 in. Gauge		6 in. Gauge		1 in. Gauge		3 in. Gauge		6 in. Gauge		1 in. Gauge		3 in. Gauge		6 in. Gauge			
High	Low	High	Low	High	Low	High	Low	Ave	High	Low	High	Low	Ave	High	Low	High	Low	Ave			
Type I	870° ±50°	--	--	15.0	10.9	14.1	--	--	--	--	--	--	--	--	16.9	6.4	12.2	14.7	5.5	10.5	
Type II		12.9	10.2	17.8	8.3	13.9	--	--	--	--	--	--	--	--	15.1	11.5	13.7	14.9	12.8	14.2	
Type III		14.2	12.9	17.3	8.3	16.4	--	--	--	--	--	--	--	--	15.0	13.3	14.0	14.1	13.7	13.8	
Type I	1050° ±60°	--	--	14.1	5.5	10.2	--	--	--	--	--	--	--	--	--	--	--	--	--	--	--
Type II		16.6	14.2	16.2	15.8	16.0	16.7	16.4	16.6	18.1	14.8	16.4	15.5	14.8	15.5	14.8	16.4	15.5	14.8	15.2	
Type III		--	--	16.6	15.5	15.7	13.7	13.2	13.3	--	--	--	--	--	--	--	--	--	--	--	--
Type I	1150° ±75°	18.8	12.9	15.0	13.8	14.2	--	--	--	--	--	--	--	--	--	--	--	13.6	6.8	10.6	
Type II		18.0	15.1	16.3	14.3	15.2	17.7	16.9	17.2	--	--	--	--	--	--	--	--	13.6	12.5	13.1	
Type III		--	--	14.1	13.4	13.8	18.1	14.5	15.9	--	--	--	--	--	--	--	--	15.9	8.2	11.1	
Type I	1250° ±75°	19.6	15.9	14.2	8.0	10.7	--	--	--	--	--	--	--	--	--	--	--	12.7	3.3	9.5	
Type II		15.8	14.9	18.4	11.6	15.0	20.6	15.3	18.2	--	--	--	--	--	--	--	--	19.4	14.3	16.7	
Type III		--	--	15.9	15.0	15.3	16.5	16.5	16.5	--	--	--	--	--	--	--	--	12.3	11.9	12.0	
Type I	1400° ±75°	--	--	--	--	--	--	--	--	--	--	--	--	--	--	--	--	--	--	--	
Type II		15.5	11.7	12.7	11.7	12.0	9.9	8.0	8.6	12.4	10.0	11.8	13.1	9.6	11.5	11.5	11.8	13.1	9.6	11.5	
Type III		--	--	--	--	--	--	--	--	--	--	--	--	--	--	--	--	--	--	--	--

Surface Treaters

Type I: Open component hot filament apparatus (Paragraph 3.1.1a)

Type II: Enclosed component hot filament apparatus (Paragraph 3.1.1b)

Type III: Radiation heating-resistance tube furnace (Paragraph 3.1.1c)

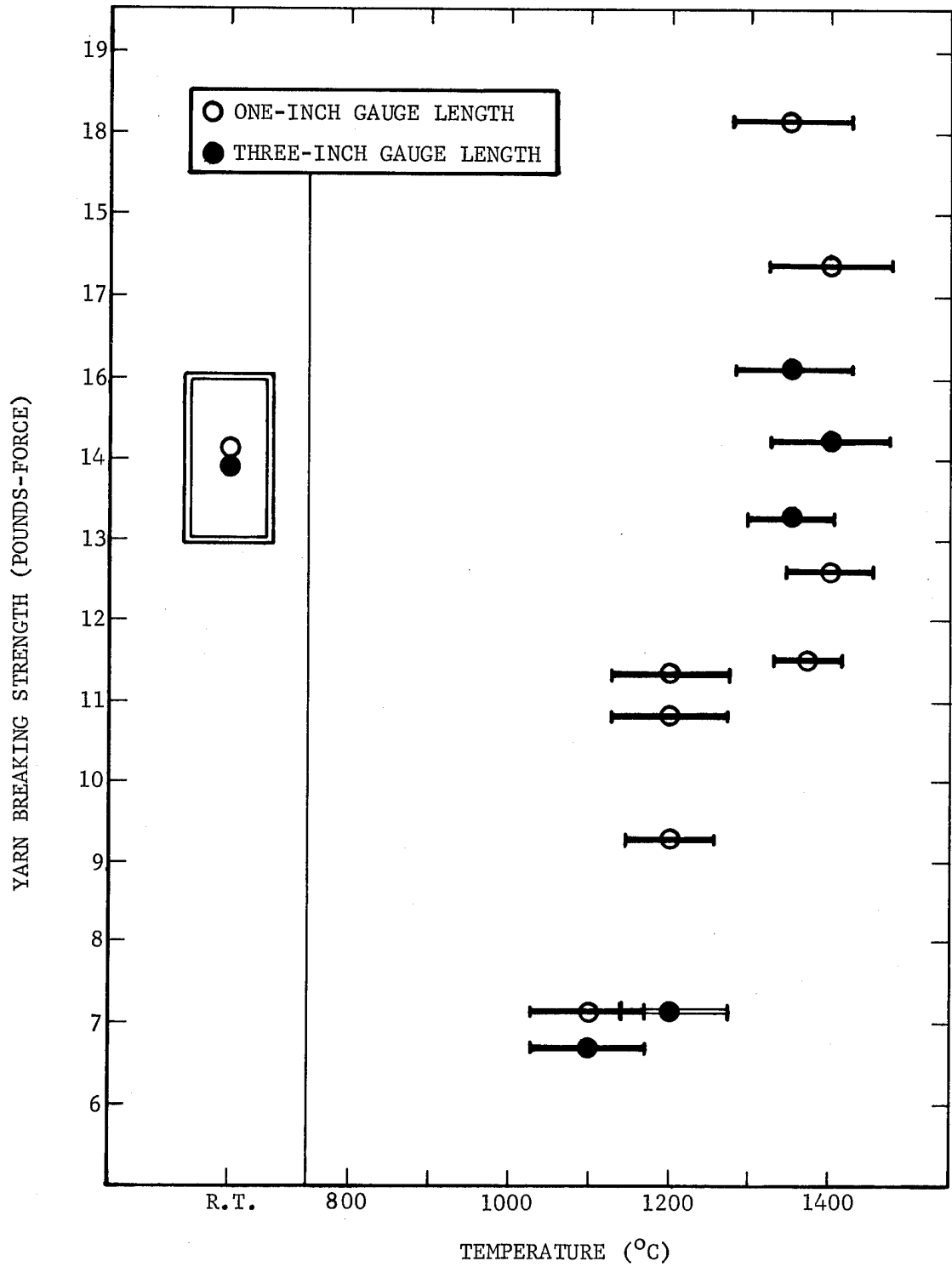


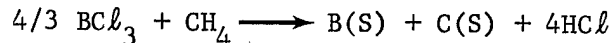
FIGURE 44. EFFECT OF SURFACE DEPOSITED BORON ON YARN BREAKING STRENGTH AS FUNCTION OF DEPOSITION TEMPERATURE

TABLE VIII. THE EFFECT OF BORON DOPING ON THORNEL 75S YARN BREAKING STRENGTH FOR SOME DEPOSITION TEMPERATURES

Temperature (°C)	Breaking Strength, Pounds											
	Pull Rate = 0.05 Inch/Minute						Pull Rate = 0.25 Inch/Minute					
	1 in. Gauge		3 in. Gauge		Ave		1 in. Gauge		3 in. Gauge		Ave	
	High	Low	Ave	High	Low	Ave	High	Low	Ave	High	Low	Ave
1100° ±50°	7.5	6.6	7.3	8.4	5.2	7.3	--	--	--	9.6	5.8	7.0
1100° ±75°	7.8	6.7	7.1	7.0	6.4	6.7	--	--	--	--	--	--
1200° ±50°	12.0	9.6	11.3	9.7	5.8	7.1	9.9	7.9	9.3	10.5	6.3	9.2
1200° ±75°	11.5	9.3	10.8	7.4	5.6	6.6	--	--	--	11.4	8.7	10.5
1350° ±40°	--	--	--	16.3	12.4	13.2	--	--	--	--	--	--
1350° ±75°	--	--	--	17.7	13.8	15.1	18.4	16.9	18.1	--	--	--
1400° ±50°	--	--	--	16.7	12.5	14.0	13.2	10.1	12.5	14.0	9.4	12.1
1400° ±75°	18.8	12.6	16.4	15.3	13.0	14.2	--	--	--	--	--	--

All data were derived from specimens which were processed with the Type II - Enclosed Hot Filament (Paragraph 3.1.1b) surface treater.

conditions of boron content in the reaction chamber during processing. Availability of boron was effected through the controlled reduction of boron trichloride by the combined reactions



and



In general, the strength of Thornel 75S yarn was substantially impaired in the presence of boron for all three types of processing apparatus at temperatures below 1300°C. Above 1300°C, the enclosed hot filament surface treater (Paragraph 3.1.1b) which was developed during this program appears capable under ideal conditions of doping Thornel yarn with boron to improve the tensile properties. However, those conditions are in large randomly governed. Thus, results are inconsistent as to the effect of boron doping on the tensile properties (or yarn breaking strength).

#### 3.2.4 SUMMARY AND CONCLUSIONS

In general, the objectives of Task II were realized. Breaking strength of treated Thornel 75S yarn was shown to be directly related to the temperature of the yarn during surface treatment. A temperature dependency upon the effect of heat cleaning Thornel yarn in Argon was established for the surface treatment apparatus utilized in these investigations. Surface treatment apparatus was shown to govern the efficacy of boron doping as a method of surface treatment. A temperature dependency was also established for the boron treatment independent of surface treatment apparatus.

Figures 45 and 46 best summarize the above conclusions. Figure 45 presents the apparent effect on resultant breaking strength over the temperature range of investigation for the three surface treatment units utilized in this task. The figure was derived by analysis of the data and by arbitrarily weighing very slightly the curves to reflect the probability of success as based on investigative experience over several years. As such, the curves in the figure are intended to serve as suggestive of the chance of successful utilization of some concepts and components of the respective surface treatment apparatus. With that qualification in mind the following general observations are in order regarding surface treatment apparatus:

- (1) Enclosing the entire surface treatment process inside an ambient atmosphere is beneficial.
- (2) Heat cleaning the yarn before entering boron deposition chamber enhances the chance of improved tensile properties.

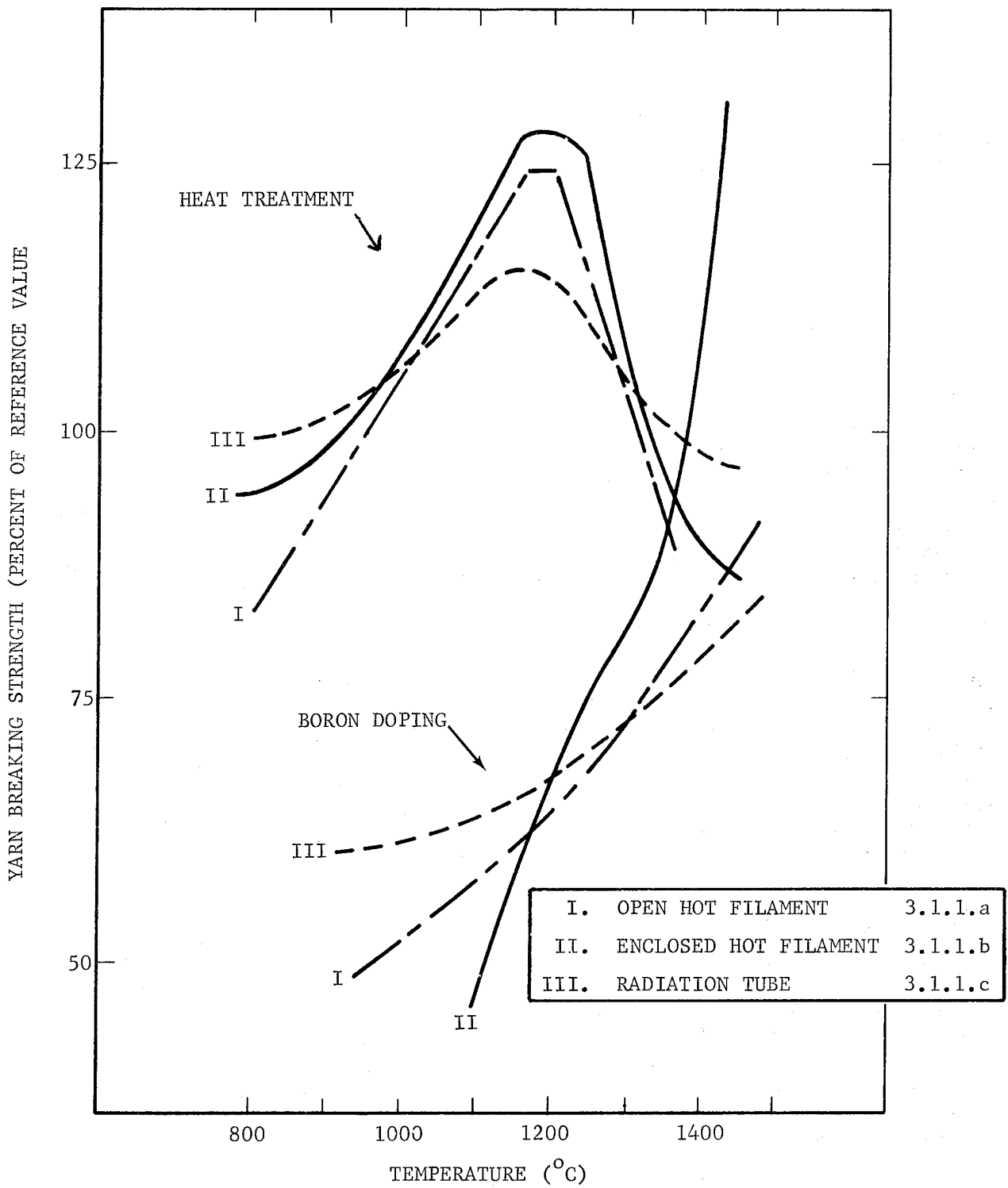


FIGURE 45. APPARENT EFFECT OF SURFACE TREATMENT APPARATUS ON RESULTANT BREAKING STRENGTH FOR TWO SURFACE TREATMENTS

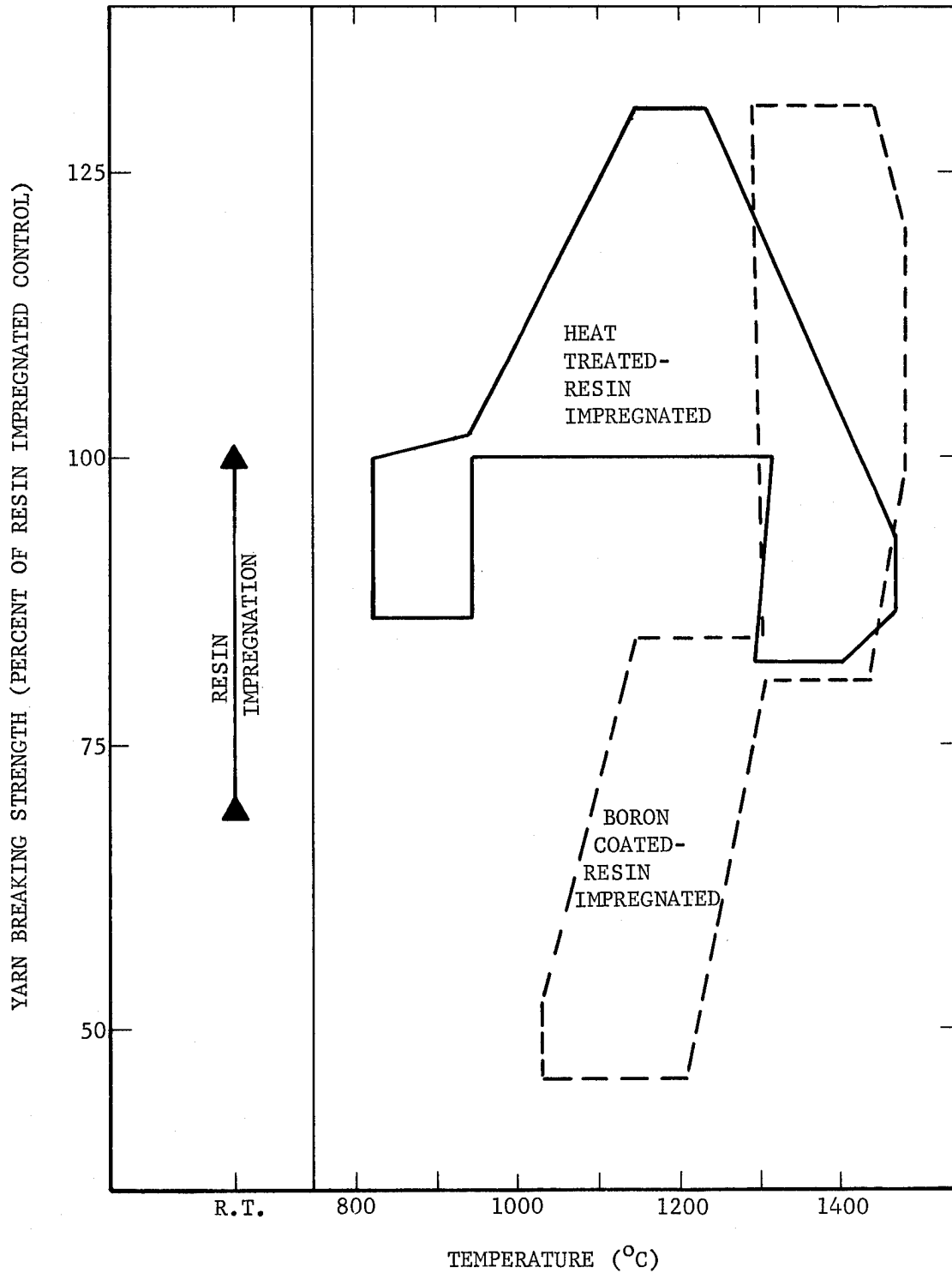


FIGURE 46. SUMMARY AND PATTERN OF THE VARIATION IN YARN BREAKING STRENGTH RESULTING FROM DIFFERENT SURFACE TREATMENTS

- (3) In the hot filament type of apparatus, continual cleaning of the current contacts increase the probability of process completion and reduces the probability of physical degradation.
- (4) Indirect heating such as radiation heating (Type III - Figure 45) reduces the probability of physical degradation, but concurrently reduces the probability of enhancement of the tensile property (see Paragraph 3.1.1c).
- (5) The area which inflicts the most physical abuse on the yarn is always at the point of heat initiation (the lead electrode in the hot filament technique; the entrance into the hot zone in the radiation type heating).

Figure 46 is a summary of the variation in yarn breaking strength as a function of temperature for the two types of surface treatment investigated. The temperature dependency of both treatments is graphically illustrated. Based on the summation presented in Figures 45 and 46, the following observations seem appropriate:

- (1) Retention of breaking strength was generally greater in the heat cleaning treatment.
- (2) Retention of strength was greatest in treatments at lower temperatures.
- (3) With improvements in surface treatment apparatus, boron doping may enhance the tensile strength of yarn at deposition temperatures greater than 1400°C.

#### REFERENCES

1. Quackenbush, N. E. and Doner, D. R., "Graphite Filament Reinforced Plastics," V-4648, N00019-68-C-0475, May 1969, Philco-Ford Corporation, Aeronutronic Division.
2. Quackenbush, N. E. and Doner, D. R., "Graphite Filament Reinforced Plastics," V-4798, N00019-69-C-0135, January 1970, Philco-Ford Corporation, Aeronutronic Division.
3. Bridges, D. W. and Pope, J. P., "Development of Surface Treatments for High-Modulus Graphite Filaments," N00019-70-C-0301, Philco-Ford Corporation, Aeronutronic Division, July 1971.
4. Penton, A. P. and Perry, J. L., "Investigation of Graphite Filament Reinforced Plastic Composites," N00019-70-C-0439, June 1971, Philco-Ford Corporation, Aeronutronic Division.
5. Mullin, J. V. and Mazzio, V. F., "Basic Failure Mechanisms in Advanced Composites, Final Report," NASA Contract NASW-2093, April 1971.
6. Epreman, E., "Thornel, A New Graphite Reinforcement," pp 139-144 of Applied Polymer Symposium No. 15, John Wiley & Sons, Inc., 1970.
7. Talley, C. P., et al., "Boron Reinforcements for Structural Composites," in Air Force Technical Documentary Report No. ASD-TDR-63-396, April 1963, p. 434.
8. Brown, A. R. G. and Watt, W., "The Preparation and Properties of High-Temperature Pyrolytic Carbon," pp. 86-100 in Industrial Carbon and Graphite, Paper read at the Conference held in London 24-26 September 1957, published by the Society of Chemical Industry, and printed by Metchim and Sons, Ltd., London, 1958.
9. Friedlander, H. N. and Calfee, J. D., "The Importance of Fabrication Technology in Translation of Fiber and Matrix Properties to Advanced Composites," pp. 9-50 in Applied Polymer Symposium No. 15, John Wiley and Sons, 1970.

REFERENCES (Continued)

10. Markenovic, S., "Simultaneous Pyrolytic Deposition of Carbon and Boron," Carbon, 7, pp. 185-193 (1969).
11. Katz, B. N. and Gazzara, C. P., "The Influence of Boron Content on the Fine Structure of Pyrolytic Carbon," Journal of Material Sciences, 3, pp. 61-69 (1968).
12. Allen, S., et al., "Carbon Fibres of High Modulus," National Physical Laboratory, England, IMS Report 7 (November 1969).

## SECTION 4

### CONCLUSIONS AND RECOMMENDATIONS FOR FUTURE WORK

Following are the conclusions that resulted from the investigations discussed in Section 2, Hybrid or Mixed Fiber Composites:

- (1) Significant increases in impact fracture toughness result through the incorporation of supplemental interply reinforcements unidirectionally to Modulite 5206 material (Modmor II fiber and Narmco 1004 epoxy resin). The incorporation of 25 percent S2 glass fiber volume increased the longitudinal impact resistance 550 percent while 10 percent S2 glass increased the longitudinal impact resistance 258 percent compared to a laminate composed solely of Modulite 5206. By using 25 percent and 10 percent PRD-49 III as supplemental reinforcement, the impact resistance increased 283 percent and 149 percent, respectively. Increases in impact efficiency were also realized by using boron and Nomex nylon as supplemental reinforcement. However, their effect was not as pronounced as the S2 glass and PRD-49 materials.
- (2) The particular combination of Thornel 400 and PRD-49 III proved to be of interest for increased impact efficiency. By alternating plies of the two materials, longitudinal impact resistance appears to be synergistically altered so that higher energy levels can be absorbed. This energy

absorbing capability is higher in combination than the capability of a laminate fabricated solely of either constituent material. Evidently, additional or a greater degree of impact fracture modes are occurring in the hybrid than occur in the basic material laminates. The longitudinal impact strength is 385 percent greater than a laminate composed solely of Modulite 5206. Longitudinal tensile properties of this material were very nearly identical to Modulite 5206.

- (3) Of significance is the fact that higher impact strength were realized by those fibers which exhibited lower transverse strength and interlaminar shear strength. Reduced fiber to matrix bonding evidently allows stresses to distribute along the fiber in the general area of impact as opposed to having the stresses localized to the area of impact. In the PRD-49 composite, smooth resin interfaces and complete catastrophic failure of the fiber result in significantly higher impact strengths. The fluted nature of the graphite fibers result in higher transverse and interlaminar shear strengths which confine the energy of impact to the immediate area, thus resulting in definite planes of failure. The fibers are then sheared in a cleavage-type fracture. In unidirectional composites, significant strain energy is stored in the filaments. By lowering fiber to matrix bonding, better utilization of available energy can be made. Controlling fiber to matrix bonding is an important parameter involved in achieving less brittle fiber composites. However, this must be controlled without undue sacrifice of other structural properties.
- (4) From the investigations carried out in Appendix D using an instrumented Charpy apparatus to obtain impact failure information, it was determined that hybrid panels undergo initial fracture at very low energy levels when compared to the "brittle" Modulite 5206. However, initial fracture for a hybrid panel does not correspond to catastrophic failure as it does in the case of Modulite 5206. The principal failure mode of a hybrid Charpy specimen is delamination. Further

investigations should be carried out to better define the test parameters, material variables and responses, and significance of test results to specific materials applications.

- (5) Higher yarn breaking strengths were realized for Thornel 75S graphite yarn when the yarn was subjected to surface treatment. Heat cleaning (1000°C to 1300°C) in an inert environment was shown to be a more reproducible method of yarn strengthening than boron deposition. Boron doping as a method of yarn strengthening appears to be strongly governed by the deposition temperature; enhancement of strength occurring at and beyond 1300°C. The temperature dependency of both surface treatment methods concur with previous research wherein the strength of graphite composites of surface treated yarn were the criteria. However, in general, the extent of strengthening was greater for these treated yarn measurements than for the treated graphite yarn composites. Whereas significant improvement (130 percent) to the individual in yarn breaking strength were realized, similarly treated yarn resulted in degraded strengths (longitudinal tensile) for composites of treated yarn in the previous efforts. This contradiction underlies the random nature of surface treatment effects on yarn strength and is directly attributable to surface treatment apparatus. Physical abuse and mechanical degradation is induced in the yarn by the apparatus and randomly and increasingly develop weak links in otherwise strengthened yarn. Thus, the probability of incorporating several tensile weakened short gauge lengths of treated yarn into reinforced graphite composites increases with the length of processing.

APPENDIX A

MATERIAL SUMMARY

MATERIAL PROPERTY MATRIX

<u>Property</u>	<u>PRD-49 Type III</u>	<u>Thornel 400</u>	<u>Modmor II</u>	<u>Nomex Nylon</u>	<u>S-2 CG Glass</u>
Tensile Strength, psi	400, 000	425, 000	360, 000	94, 000	665, 000
Tensile Modulus psi x 10 <sup>6</sup>	19	32	39	2.3	12.6
Elongation, %	2.0	1.3	0.92	22	5.4
Denier gm/9000 M	195	698	7830	200	304
Density <sub>3</sub> gm/CM <sup>3</sup>	1.45	1.78	1.71	1.38	2.49
Description	High Modulus Organic Yarn	1,000 Filament Pan Based Yarn	10,000 Filament Pan Based TOW	100 Filament Polyamide Yarn	204 Filament S Glass Yarn

MODULITE 5206 DMS 1936B MATERIAL REQUIREMENTS

<u>Property</u>	<u>Requirement</u>
Type 2	Broadgoods
Class 2	$35 \times 10^6$ psi modulus graphite filaments
Resin Content	$42 \pm 3\%$ by weight
Volatile Content	3.0% by weight maximum
<u>Gell Time @ 350°F</u>	18-26 minutes
Filament	Modmor II
Resin	Narmco 1004 epoxy

3M SP-272 EPOXY-BORON FILAMENT PREPREG PROPERTIES

<u>Property</u>	<u>Requirement</u>
Filament	Boron, 0.004 inch diameter, 450,000 psi tensile strength, $55 \times 10^6$ psi tensile modulus
Resin	Scotchply SP-272
Resin Content	29 to 34 weight %
Volatile Content	< 2%

APPENDIX B

MATERIAL PROCESSING PARAMETERS



TABLE B.1. LAMINATE PROCESSING PARAMETERS (Continued)

PANEL NO.	MATERIALS	CONSTRUCTION	BULK DENSITY, g/cc	TOTAL FIBER VOLUME, %	CONSTITUENT VOLUME, %	PREPREG RESIN CONTENT, WT %	PREPREG VOLATILE CONTENT, WT %	THICKNESS, MILLS	REMARKS
6	<ul style="list-style-type: none"> <li>● Modulite 5206 (I)</li> <li>● PRD-49 III (:) )</li> <li>● 1004 epoxy</li> </ul>	Thin 	1.50	52	= 43 : = 9	42	6.4	33	
		Thick    : : :	1.50	52	= 43 : = 9	42	6.4	94	
7	<ul style="list-style-type: none"> <li>● Modulite 5206 (I)</li> <li>● PRD-49 III (:) )</li> <li>● 1004 epoxy</li> </ul>	Thin None							Impact specimens only
		Thick : : : : : :	1.58	62	= 51 : = 11	39	1.1	87	
8	<ul style="list-style-type: none"> <li>● Fabricated small piece only. No data recorded.</li> <li>● Modulite 5206</li> <li>● PRD-49 III</li> </ul>	Thin None							Impact specimens only
		Thick ~10% PRD-49 uniformly distributed							
9	<ul style="list-style-type: none"> <li>● Modulite 5206 (I)</li> <li>● Boron (:) )</li> </ul>	Thin-  : :  Data not determined							
		Thick  : : : : : :	1.61	53	= 27 : = 26	30	1.2	99	
10	<ul style="list-style-type: none"> <li>● Modulite 5206 (I)</li> <li>● Boron (:) )</li> </ul>	Thin  : :  Data not determined							
		Thick   : : : : : :	1.56	52	= 42 : = 10	34	1.1	98	

TABLE B.1. LAMINATE PROCESSING PARAMETERS (Continued)

PANEL NO.	MATERIALS	CONSTRUCTION	BULK DENSITY, g/cc	TOTAL FIBER VOLUME, %	CONSTITUENT VOLUME, %	PREPREG RESIN CONTENT, WT %	PREPREG VOLATILE CONTENT, WT %	THICKNESS, MILS	REMARKS
11 (11A)	<ul style="list-style-type: none"> <li>• Thornel 400 (I)</li> <li>• PRD-49 III (:)</li> <li>• 1004 epoxy</li> </ul>	Thin 	1.50 (1.43)	69 (66)	= 33(31) : = 36(35)	39 (39)	3.5 (3.5)	33 (31)	High fiber volume
12	<ul style="list-style-type: none"> <li>• Thornel 400 (I)</li> <li>• PRD-44 III (:)</li> <li>• 1004 epoxy</li> </ul>	Thin 	1.53	73	= 57 : = 16	37	3.1	32	High fiber volume
14	<ul style="list-style-type: none"> <li>• Modulite 5206 (I)</li> <li>• S2 glass (:)</li> <li>• 1004 epoxy</li> </ul>	Thin 	1.73	59	= 32 : = 27	36	1.3	30	
15	<ul style="list-style-type: none"> <li>• Modulite 5206 (I)</li> <li>• S2 glass (:)</li> <li>• 1004 epoxy</li> </ul>	Thin 	1.58	55	= 45 : = 10	37	1.1	31	
16	<ul style="list-style-type: none"> <li>• Modulite 5206 (I)</li> <li>• PRD-49 III (:)</li> <li>• 1004 epoxy</li> </ul>	Thin None made	1.59	60	= 43 : = 17	40	1.3	96	Impact specimens only
2A	<ul style="list-style-type: none"> <li>• PRD-49 III</li> <li>• 1004 epoxy</li> </ul>	Thin-7 plies	1.29	78	41	41	3.7	4.3/ply	High fiber volume

TABLE B.1. LAMINATE PROCESSING PARAMETERS (Continued)

PANEL NO.	MATERIALS	CONSTRUCTION	BULK DENSITY, g/cc	TOTAL FIBER VOLUME, %	CONSTITUENT VOLUME, %	PREPREG RESIN CONTENT, WT %	PREPREG VOLATILE CONTENT, WT %	THICKNESS, MILS	REMARKS
17	<ul style="list-style-type: none"> <li>Modulite 5206 (I)</li> <li>PRD-49 III (:)</li> <li>1004 epoxy</li> </ul>	Thin-none made							
		Thick-     :	1.59	58	= 43 : = 15	42	1.1	95	
		Thin-none made							
18	<ul style="list-style-type: none"> <li>Modulite 5206 (I)</li> <li>S2CG (:)</li> </ul>	Thick-     :	1.61	54	= 44 : = 10	40	0.7	91	
		Thin-5 plies	1.61	68		42	2.5	7.0/ply	
3A	<ul style="list-style-type: none"> <li>Thornel 400 (I)</li> <li>1004 epoxy</li> </ul>	Thick-15 plies	1.60	64		42	2.2	7.2/ply	
		Thin-  : :	1.76	64	= 35 : = 29	38	1.8	40	
19	<ul style="list-style-type: none"> <li>Thornel 400 (I)</li> <li>S2CG (:)</li> <li>1004 epoxy</li> </ul>	Thick-     :	1.75	60	= 33 : = 27	38	1.8	105	
		Thin-none made							
20	<ul style="list-style-type: none"> <li>Thornel 400 (I)</li> <li>PRD-49 III (:)</li> <li>1004 epoxy</li> </ul>	Thick-     :	1.57	67	= 51 : = 16	37	2.5	97	
		Thin-  : :	1.41	60	= 25 : = 35	44	2.1	34	
22	<ul style="list-style-type: none"> <li>Modulite 5206 (I)</li> <li>Nomex (:)</li> <li>1004 epoxy</li> </ul>	Thick-     :	1.43	62	= 26 : = 36	44	2.1	98	
		Thin-  : :	1.45	56	= 42 : = 14	43	1.2	33	
23	<ul style="list-style-type: none"> <li>Modulite 5206 (I)</li> <li>Nomex (:)</li> <li>1004 epoxy</li> </ul>	Thick-     :	1.51	58	= 43 : = 15	43	1.2	94	
		Thin-none made							
24	<ul style="list-style-type: none"> <li>Modulite 5206 (I)</li> <li>Nomex (:)</li> <li>1004 epoxy</li> </ul>	Thick-     :	1.48	56	= 42 : = 14	43	1.2	95	
		Thin-none made							

APPENDIX C

CROSS-SECTIONAL PHOTOMICROGRAPHS  
PHOTOMACROGRAPHS OF IMPACT FRACTURE AREAS

CROSS-SECTIONAL PHOTOMICROGRAPHS

FIGURES C-1 TO C-24

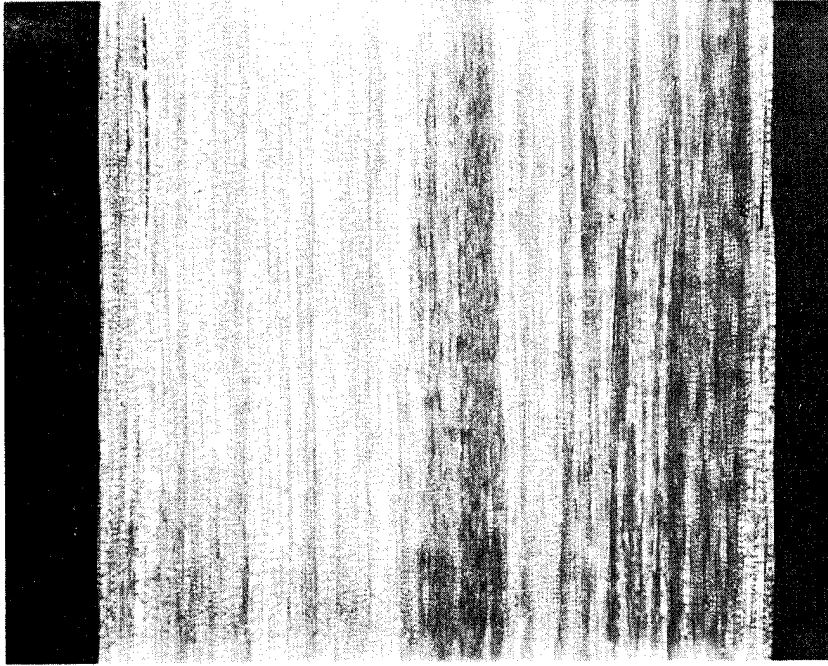


FIGURE C-2. 40X CROSS-SECTION OF PANEL #2  
PRD-49, TYPE III

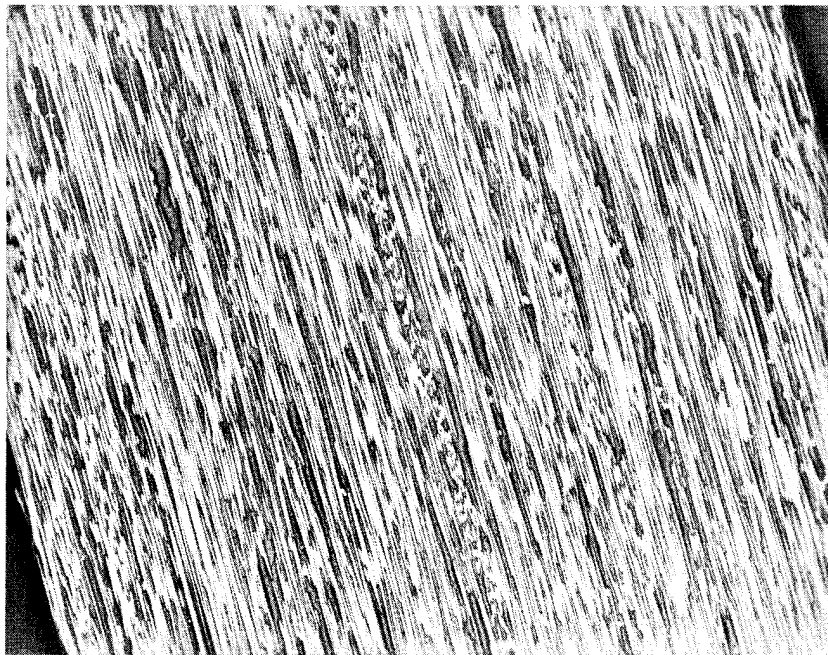


FIGURE C-1 40X CROSS-SECTION OF PANEL #1  
MODULITE 5206

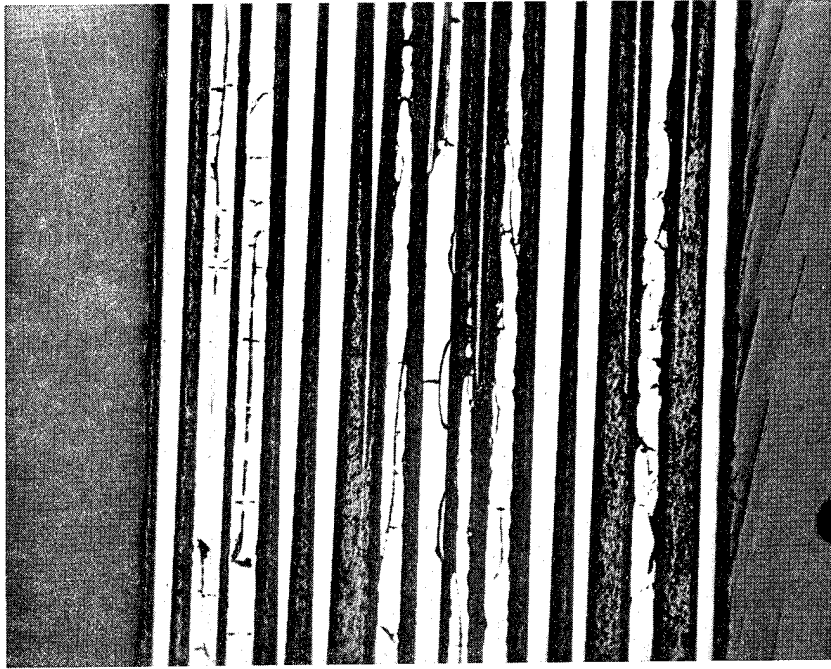


FIGURE C-4. 40X CROSS-SECTION OF PANEL #4  
BORON

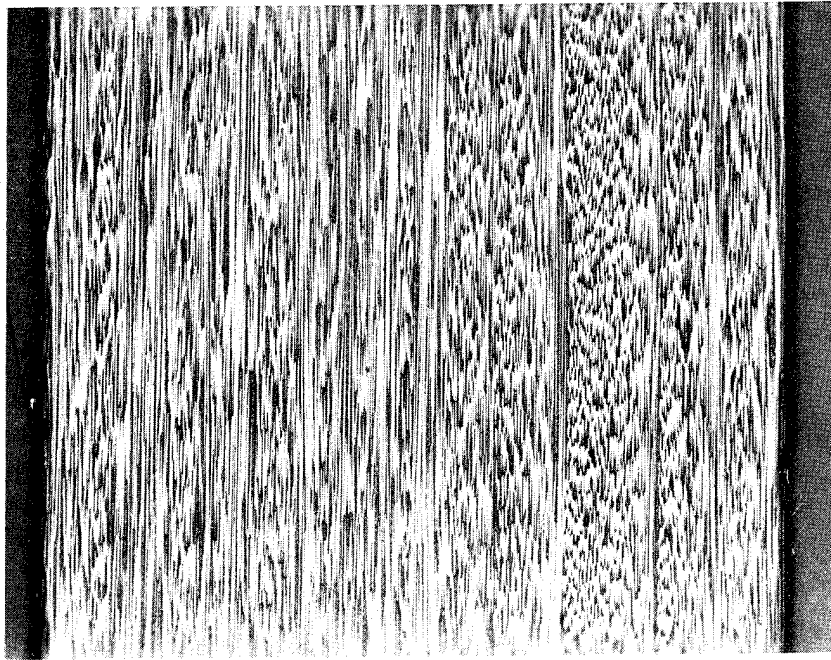


FIGURE C-3. 40X CROSS-SECTION OF PANEL #3  
THORNEL 400

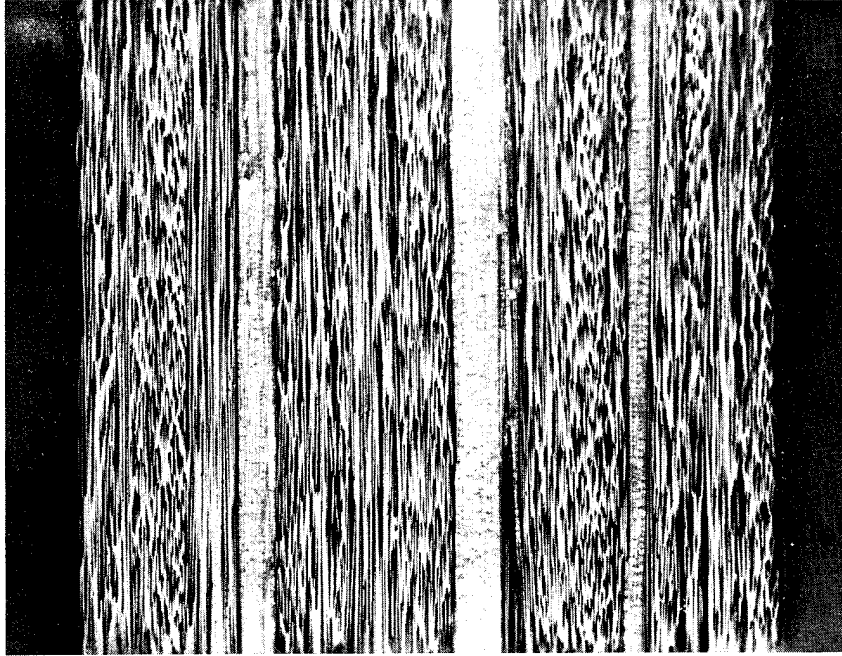


FIGURE C-6. 40X CROSS-SECTION OF PANEL #6  
MODULITE 5206/PRD-49

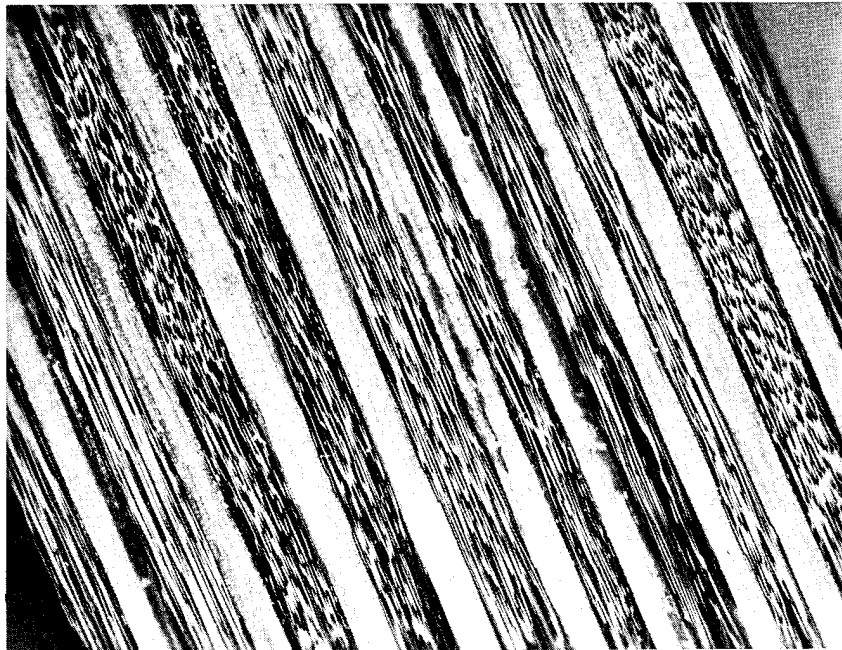


FIGURE C-5. 40X CROSS-SECTION OF PANEL #5  
MODULITE 5206/PRD-49

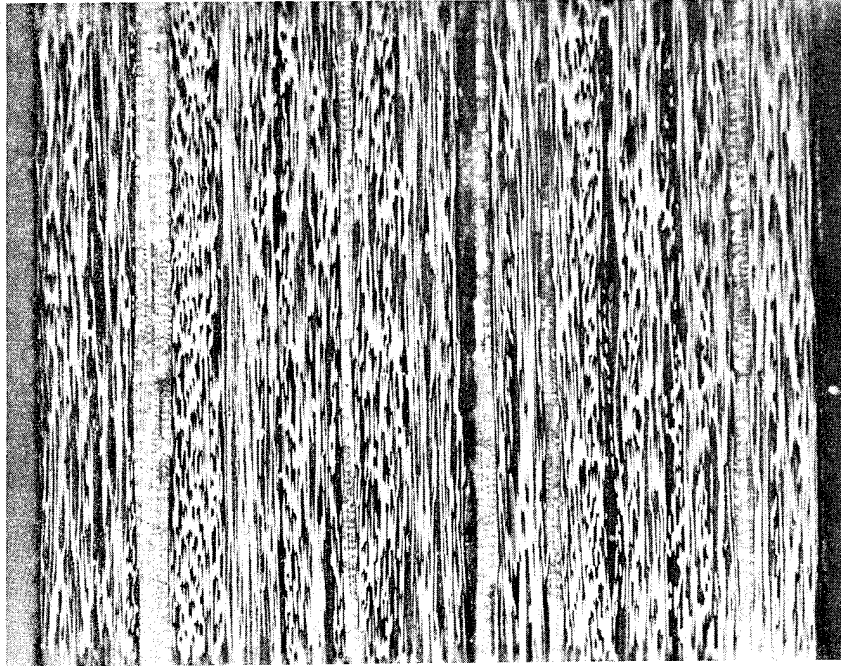


FIGURE C-8. 40X CROSS-SECTION OF PANEL #8  
MODULITE 5206/PRD-49

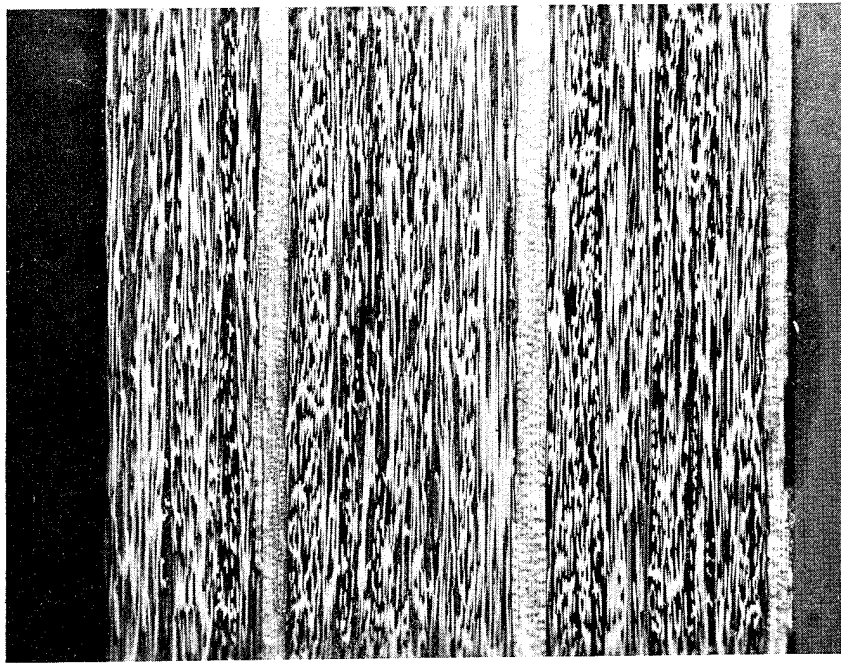


FIGURE C-7. 40X CROSS-SECTION OF PANEL #7  
MODULITE 5206/PRD-49

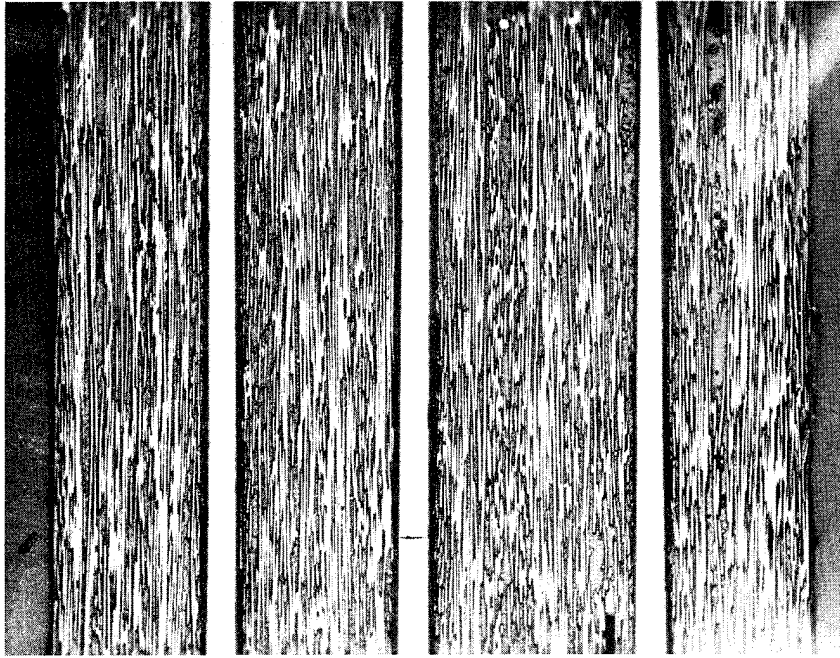


FIGURE C-10. 40X CROSS-SECTION OF PANEL #10  
MODULITE 5206/BORON

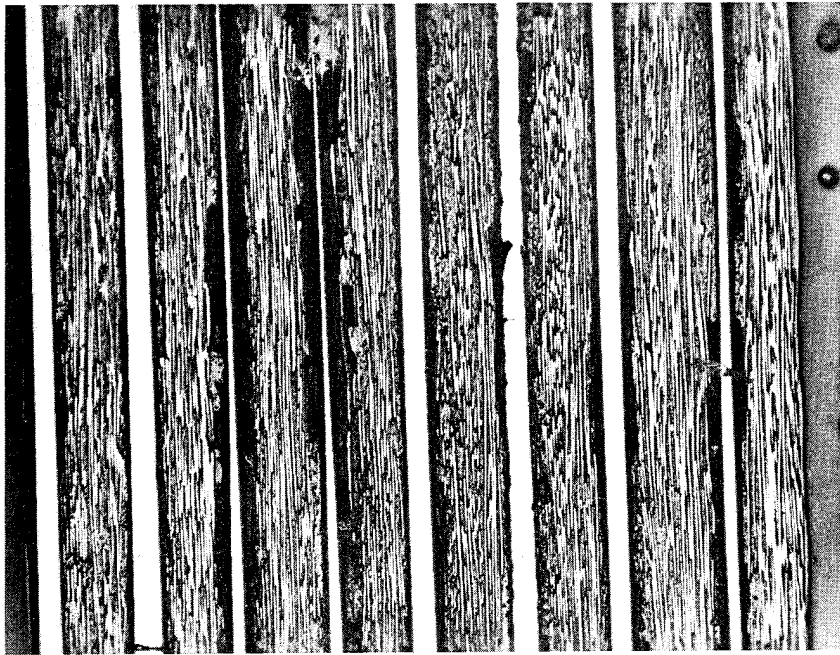


FIGURE C-9. 40X CROSS-SECTION OF PANEL #9  
MODULITE 5206/BORON

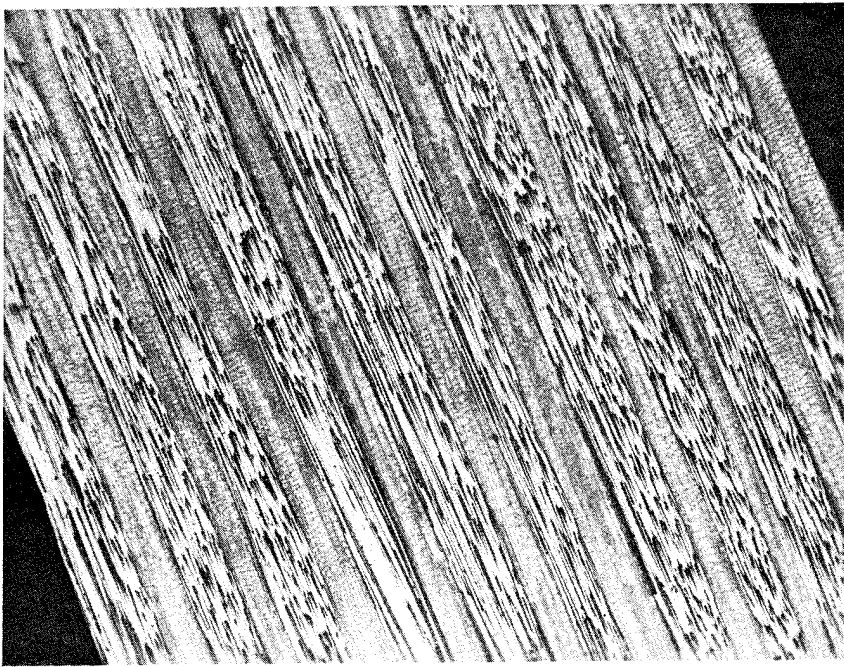


FIGURE C-11. 40X CROSS-SECTION OF PANEL #11  
THORNEL 400/PRD-49

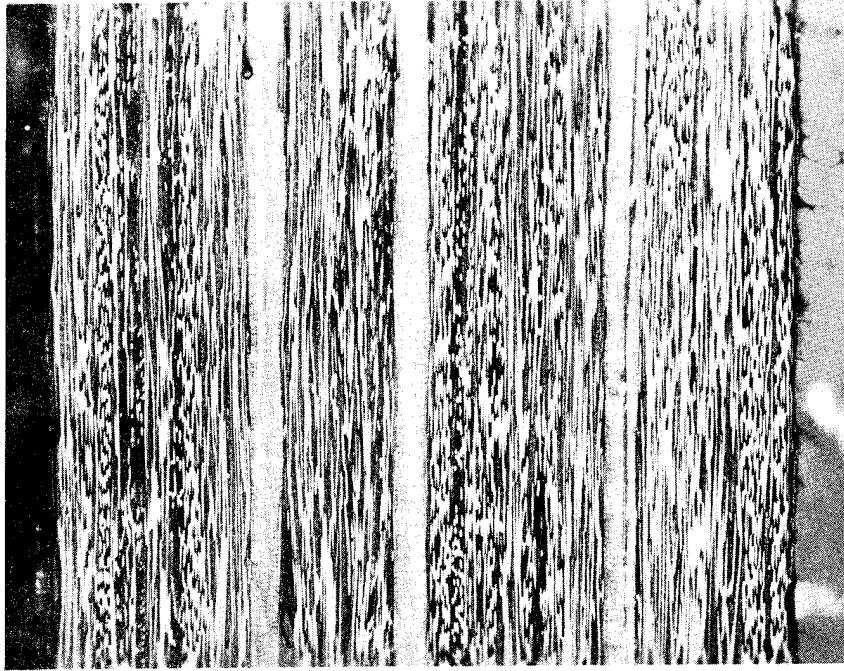


FIGURE C-12. 40X CROSS-SECTION OF PANEL #12  
THORNEL 400/PRD-49

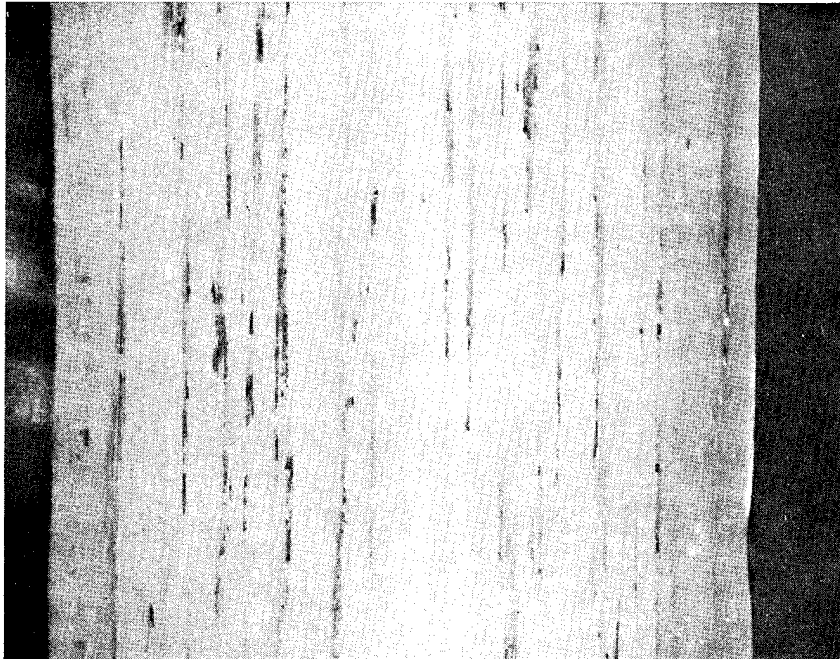


FIGURE C-13. 40X CROSS-SECTION OF PANEL #13  
S2 GLASS

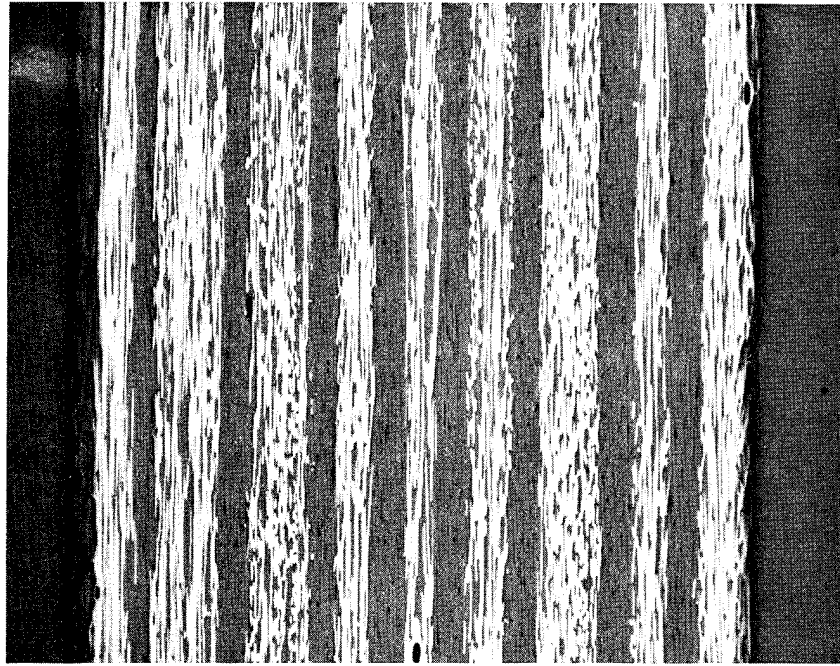


FIGURE C-14. 40X CROSS-SECTION OF PANEL #14  
MODULITE 5206/S2 GLASS

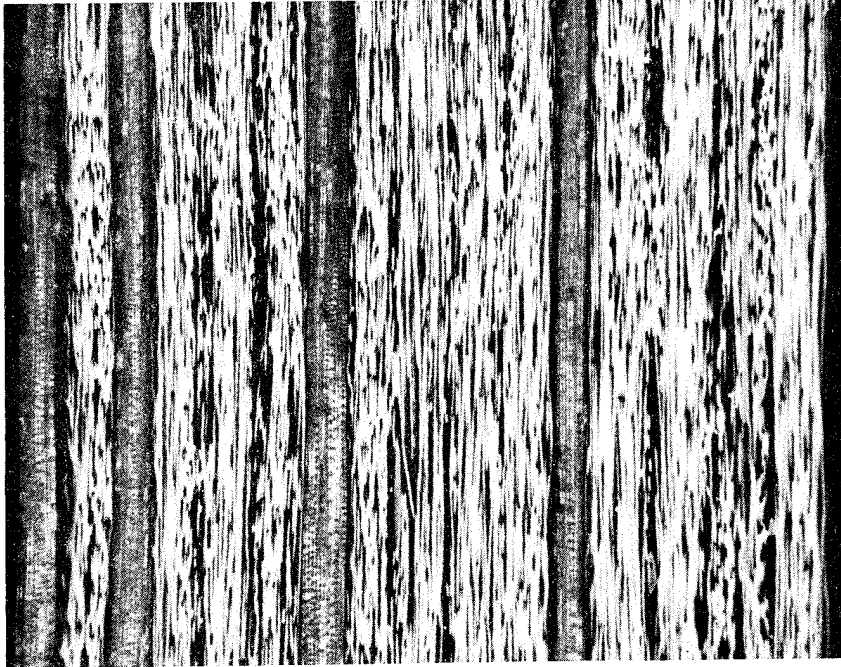


FIGURE C-16. 40X CROSS-SECTION OF PANEL #16  
MODULITE 5206/PRD-49

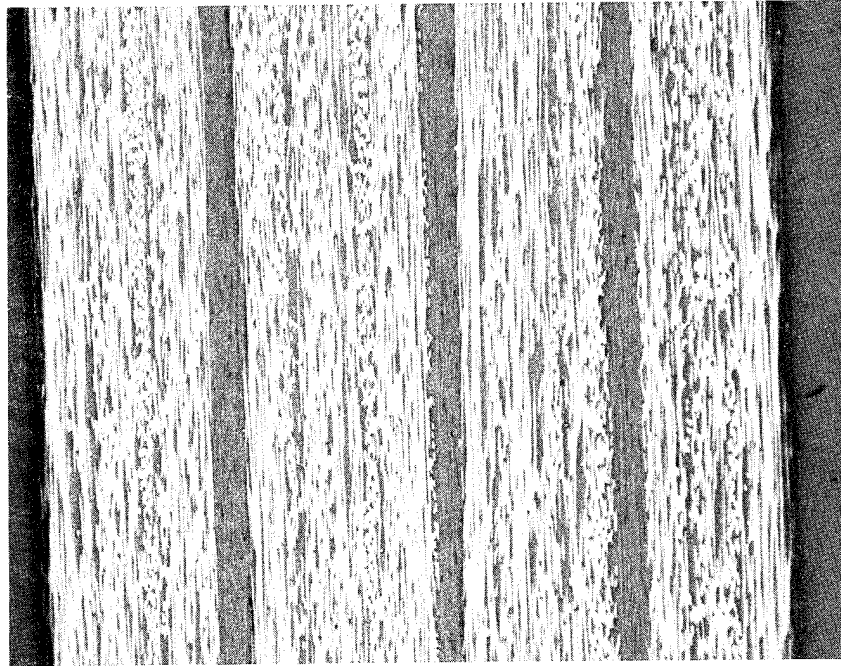


FIGURE C-15. 40X CROSS-SECTION OF PANEL #15  
MODULITE 5206/S2 GLASS

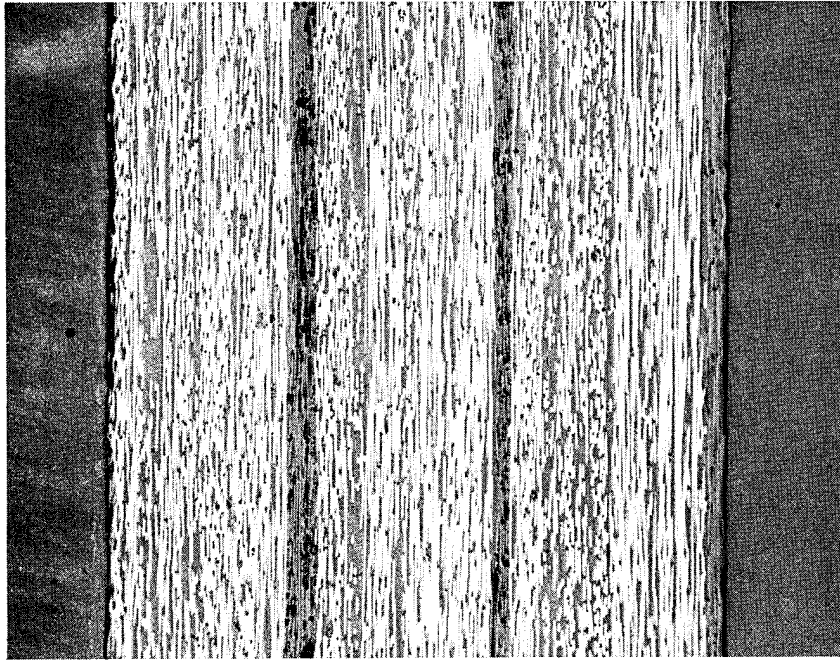


FIGURE C-18. 40X CROSS-SECTION OF PANEL #18  
MODULITE 5206/S2 GLASS

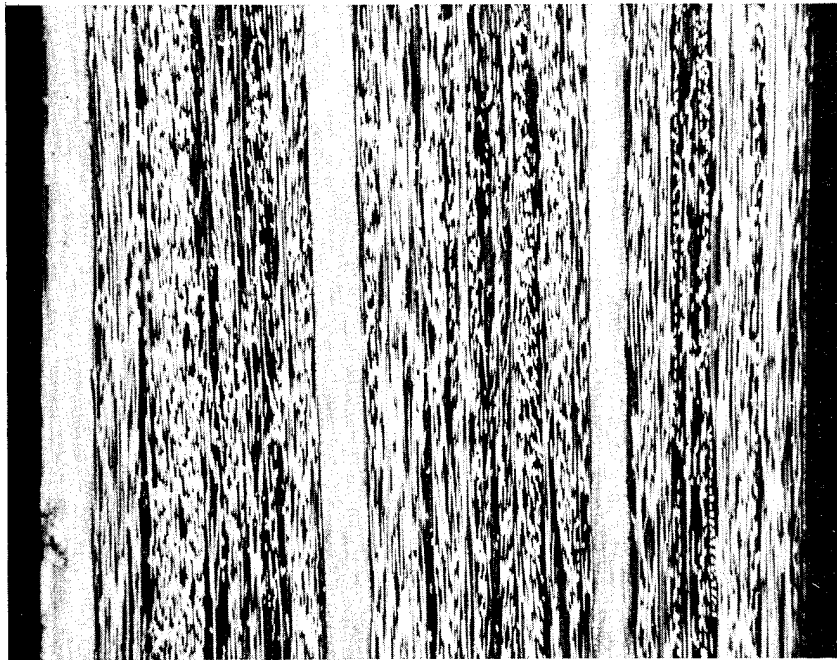


FIGURE C-17. 40X CROSS-SECTION OF PANEL #17  
MODULITE 5206/PRD-49

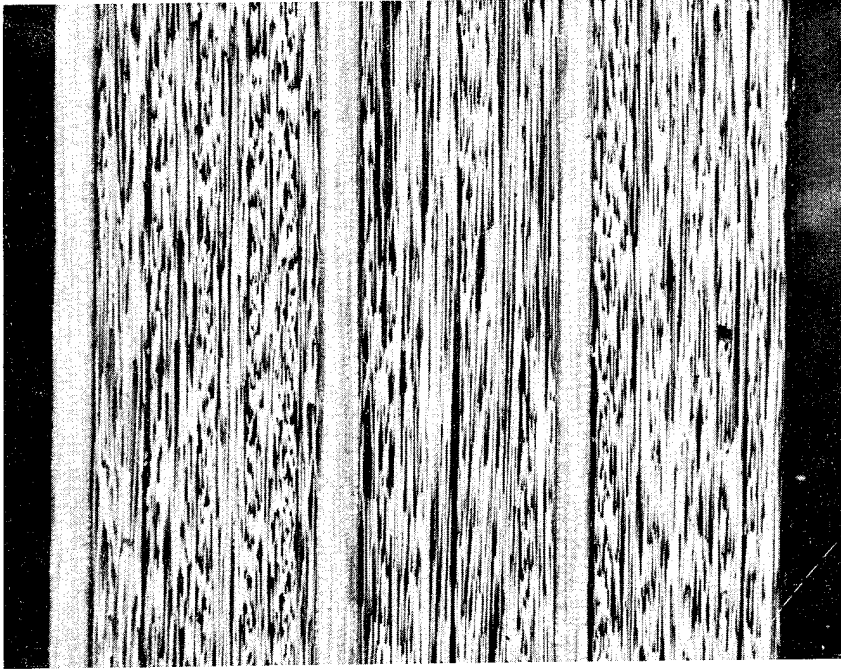


FIGURE G-20. 40X CROSS-SECTION OF PANEL #20  
THORNEL 400/PRD-49

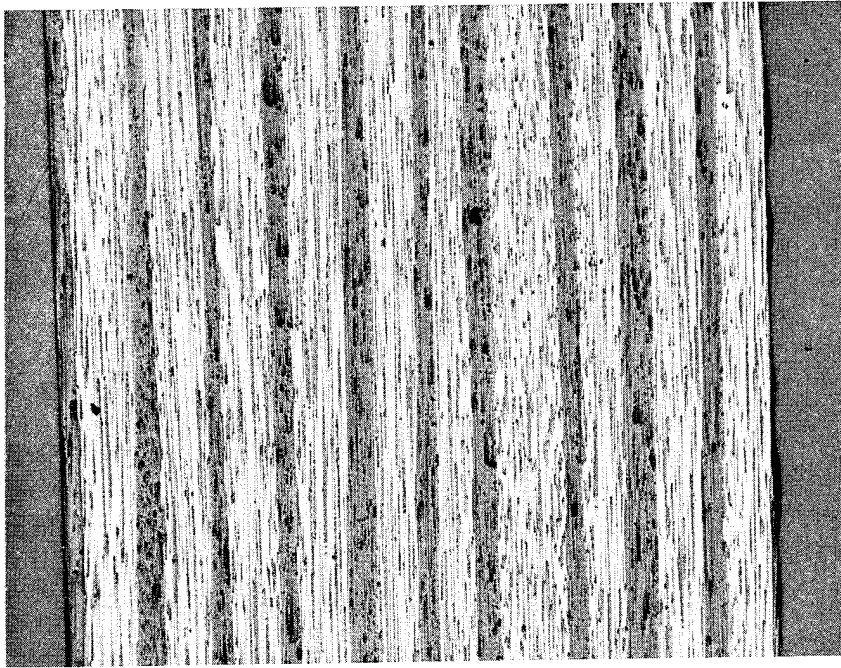


FIGURE G-19. 40X CROSS-SECTION OF PANEL #19  
THORNEL 400/S2 GLASS

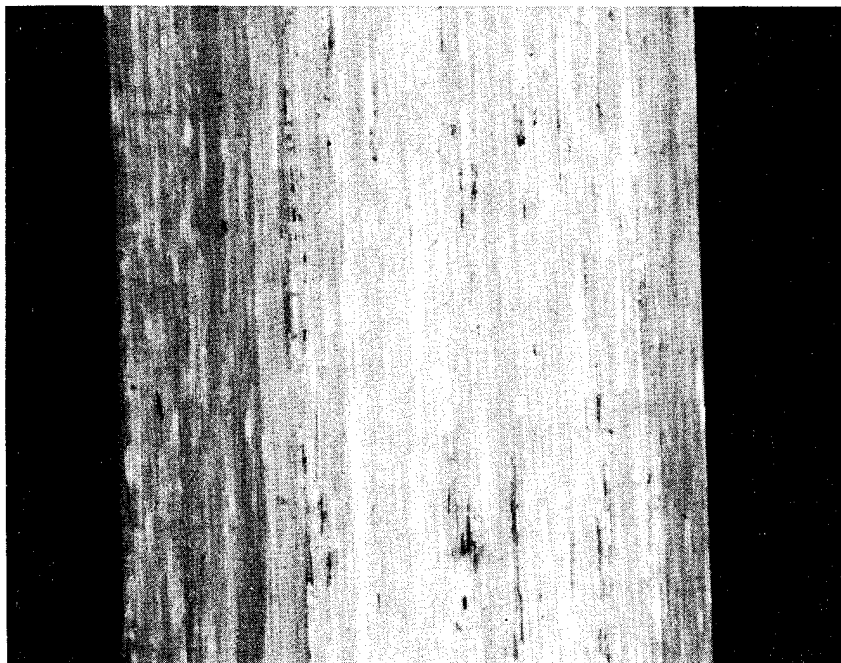


FIGURE C-21. 40X CROSS-SECTION OF PANEL #21  
NOMEX NYLON

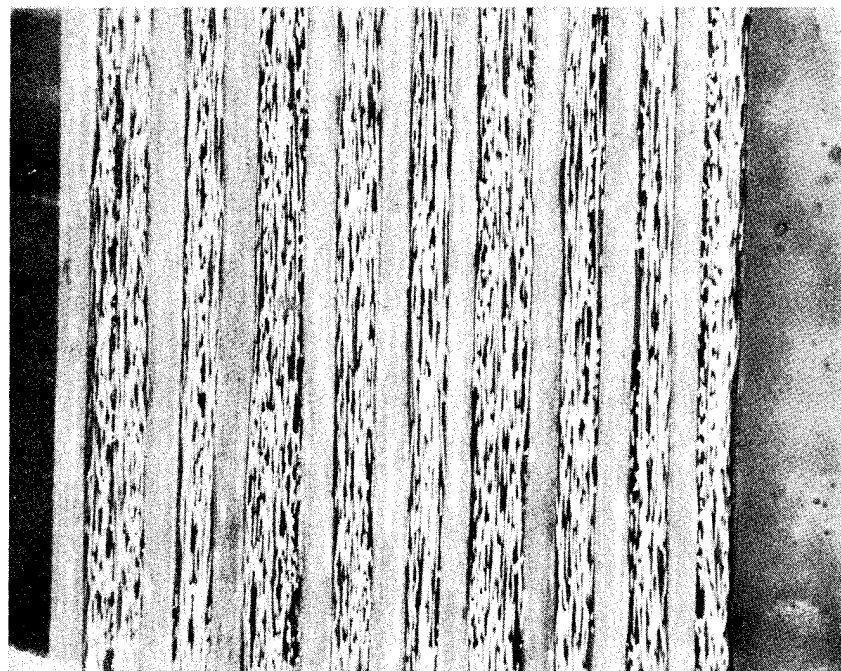


FIGURE C-22. 40X CROSS-SECTION OF PANEL #22  
MODULTE 5206/NOMEX



FIGURE G-24. 40X CROSS-SECTION OF PANEL #24  
MODULITE 5206/NOMEX

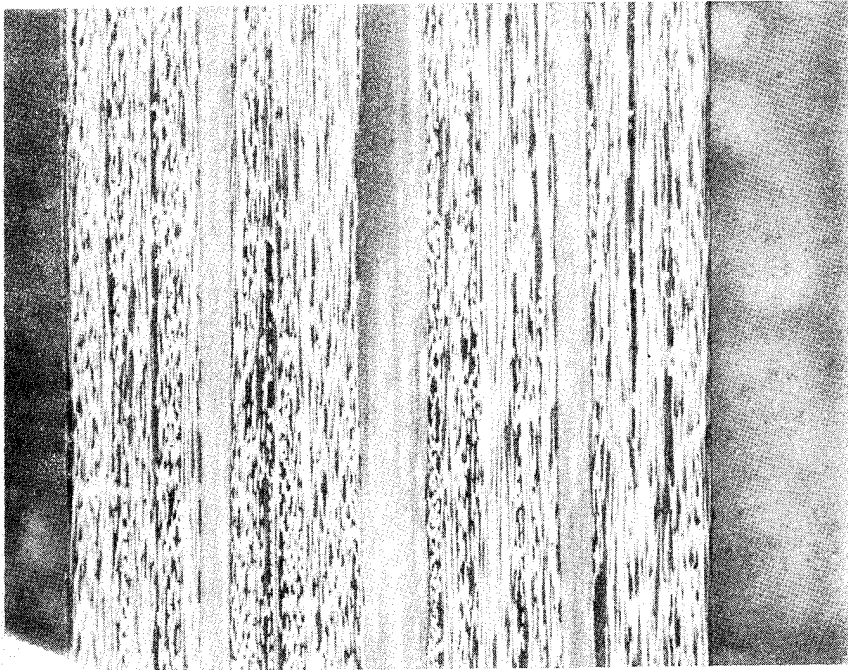
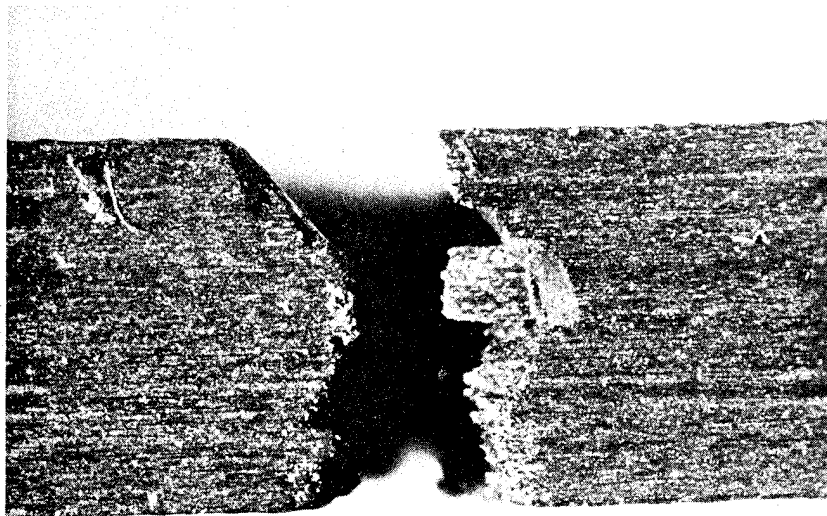


FIGURE G-23. 40X CROSS-SECTION OF PANEL #23  
MODULITE 5206/NOMEX

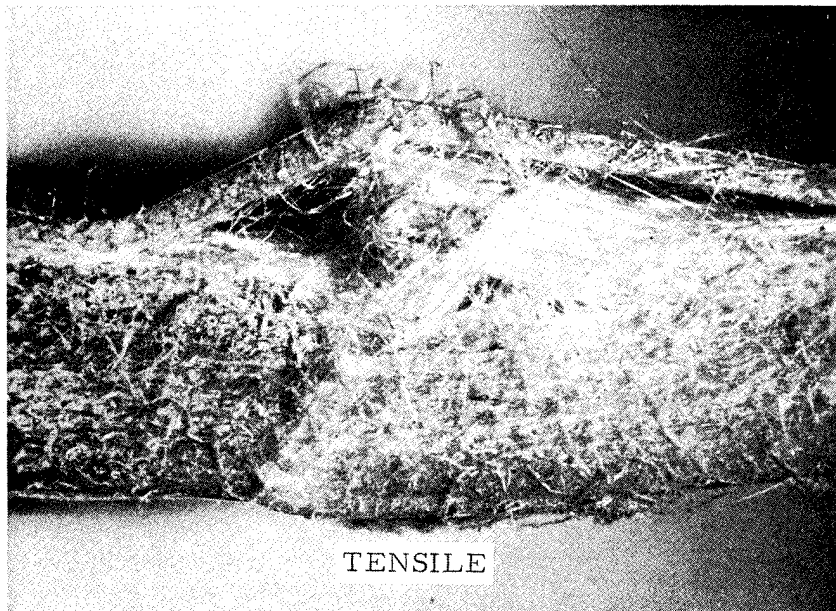
EDGEWISE PHOTOMACROGRAPHS  
OF IMPACT FRACTURE AREAS

FIGURES C-25 TO C-48



TENSILE

FIGURE C-25. 18X EDGE-VIEW OF IMPACT FRACTURE AREA OF PANEL #1 MODULITE 5206



TENSILE

FIGURE C-26. EDGE-VIEW IMPACT FRACTURE AREA OF PANEL #2 PRD-49, TYPE III

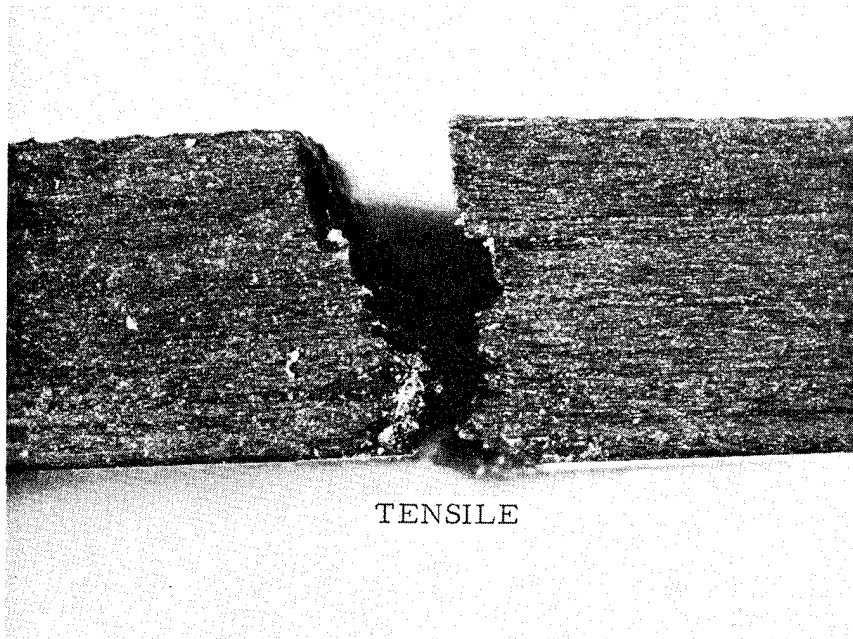


FIGURE C-27. 18X EDGE-VIEW OF IMPACT FRACTURE AREA OF PANEL #3 THORNEL 400

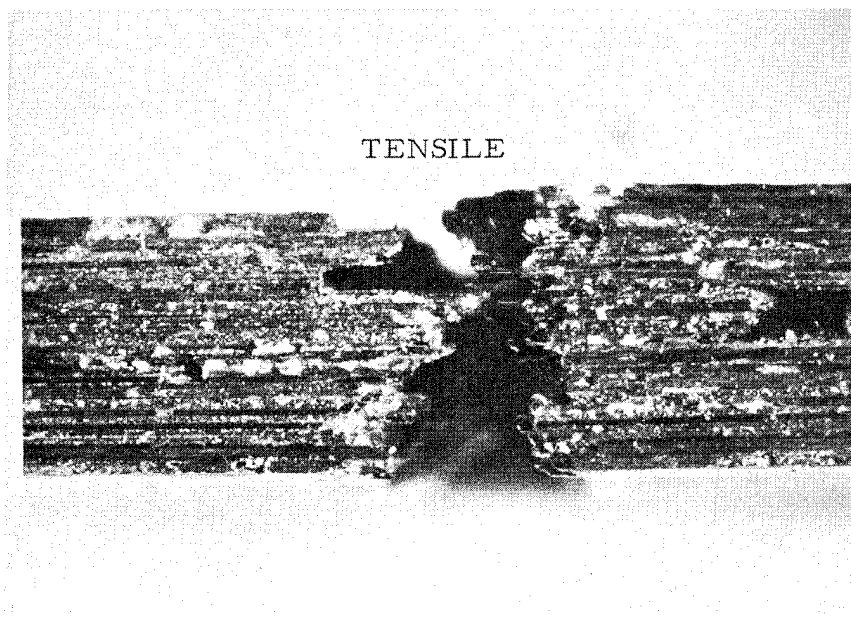


FIGURE C-28. 18X EDGE-VIEW OF IMPACT FRACTURE AREA OF PANEL #4 BORON

TENSILE



FIGURE C-29. 18X EDGE-VIEW OF IMPACT FRACTURE AREA OF PANEL  
#5 MODULITE 5206/PRD-49

TENSILE

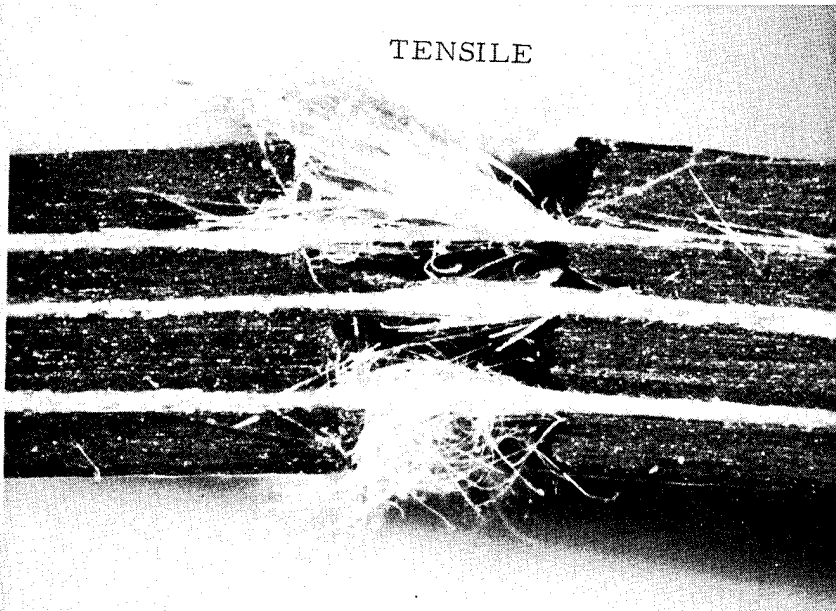


FIGURE C-30. 18X EDGE-VIEW OF IMPACT FRACTURE AREA OF PANEL  
#6 MODULITE 5206/PRD-49

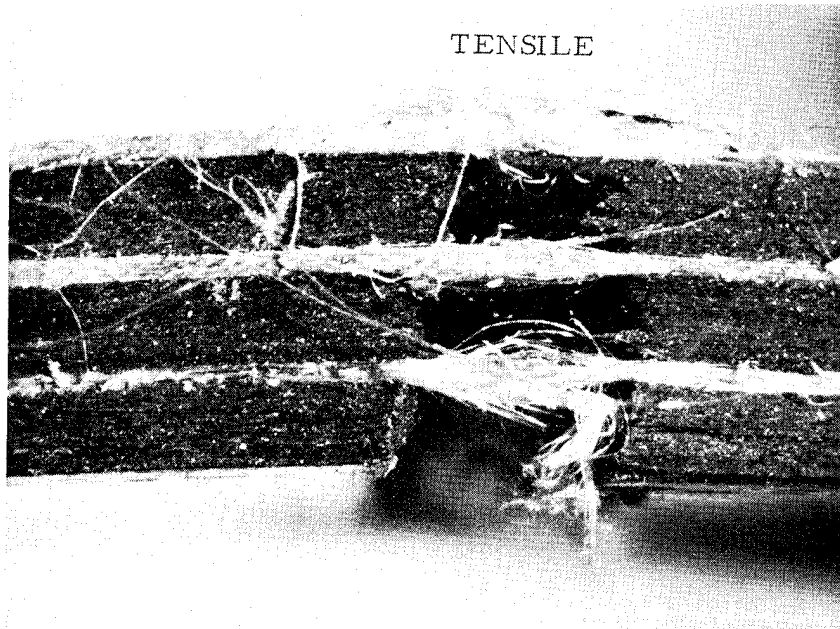


FIGURE C-31. 18X EDGE-VIEW OF IMPACT FRACTURE AREA OF PANEL #7 MODULITE 5206/PRD-49

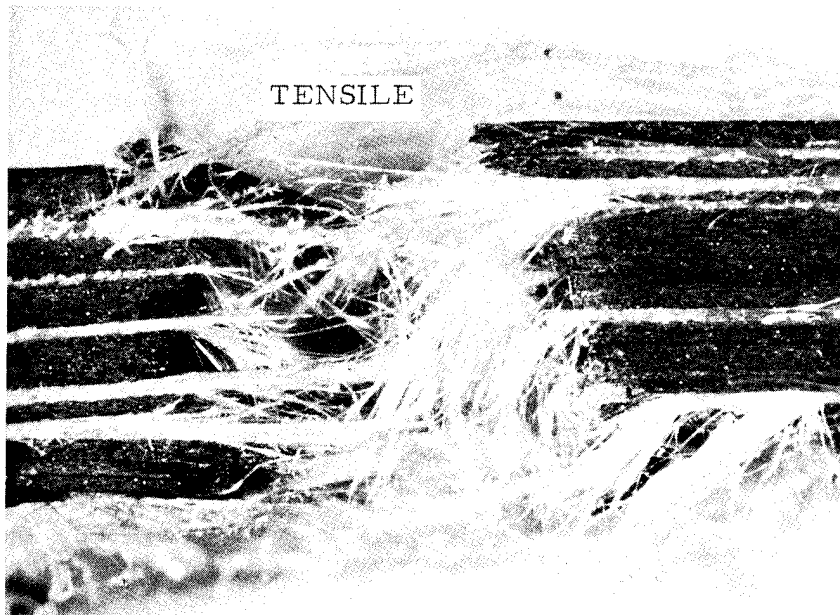


FIGURE C-32. 18X EDGE-VIEW OF IMPACT FRACTURE AREA OF PANEL #8 MODULITE 5206/PRD-49

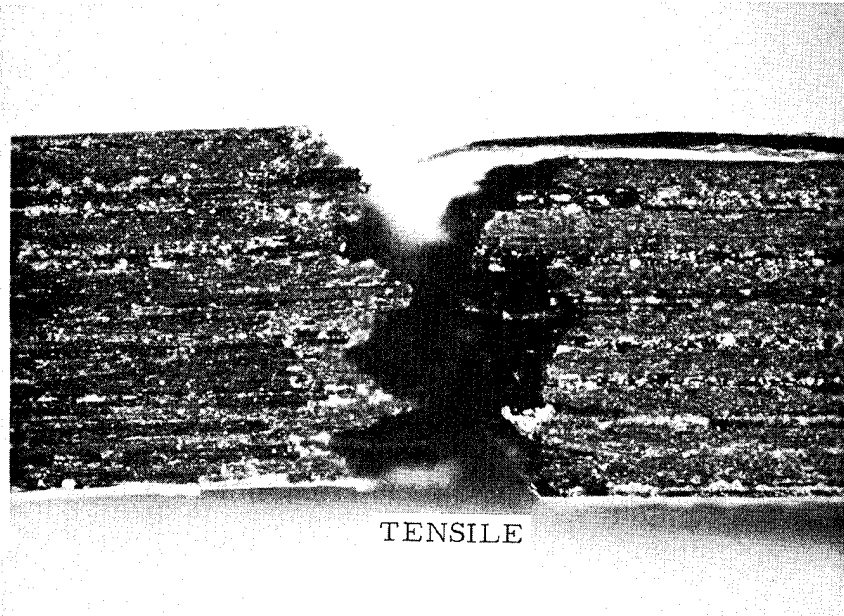


FIGURE C-33. 18X EDGE-VIEW OF IMPACT FRACTURE AREA OF PANEL  
#9 MODULITE 5206/BORON

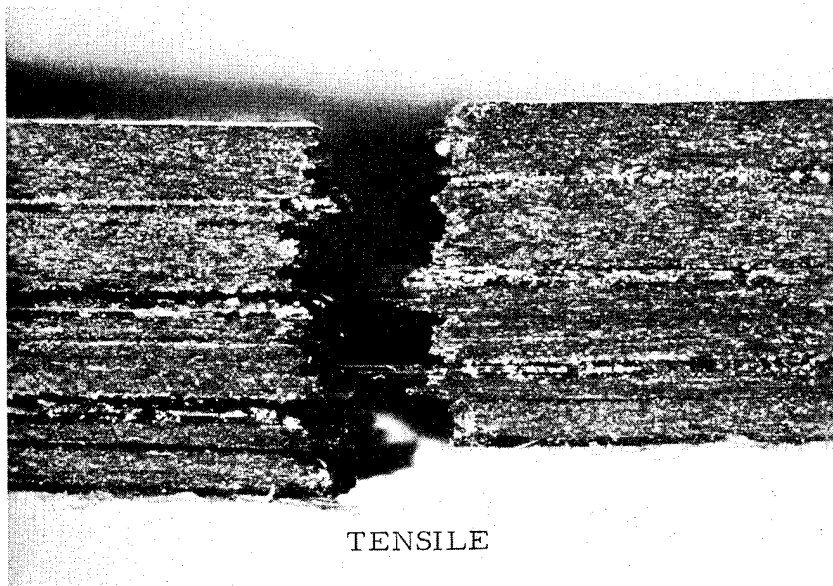


FIGURE C-34. 18X EDGE-VIEW OF IMPACT FRACTURE AREA OF PANEL  
#10 MODULITE 5206/BORON

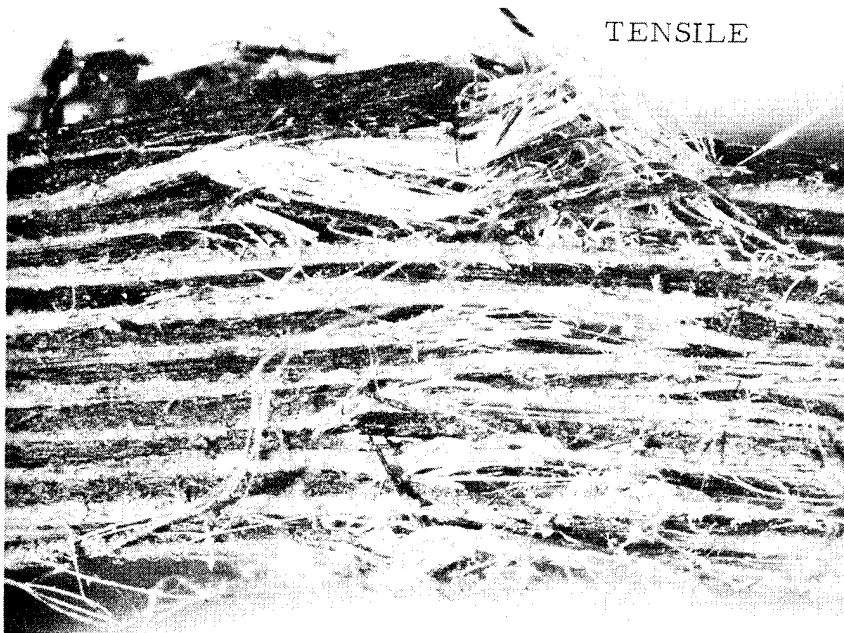


FIGURE C-35. 18X EDGE-VIEW OF IMPACT FRACTURE AREA OF PANEL  
#11 THORNEL 400/PRD-49

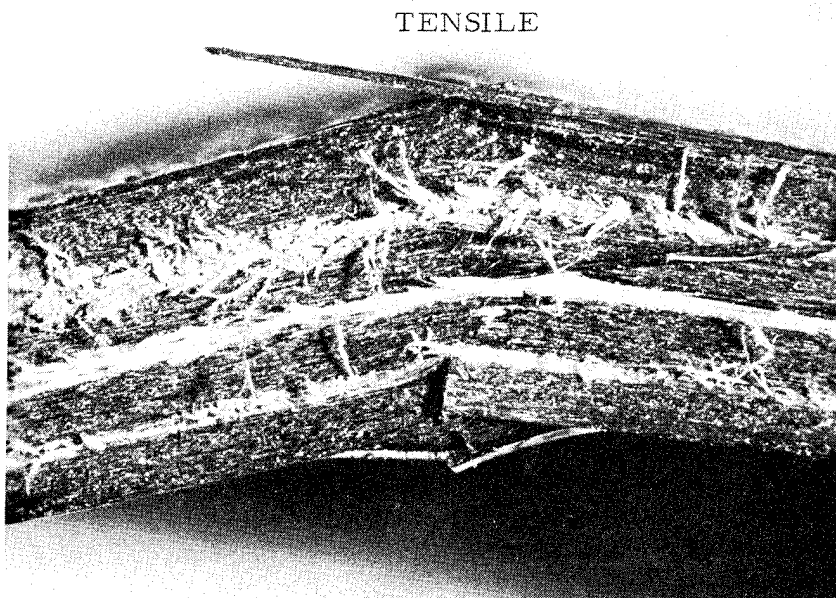


FIGURE C-36. 18X EDGE-VIEW OF IMPACT FRACTURE AREA OF PANEL  
#12 THORNEL 400/PRD-49

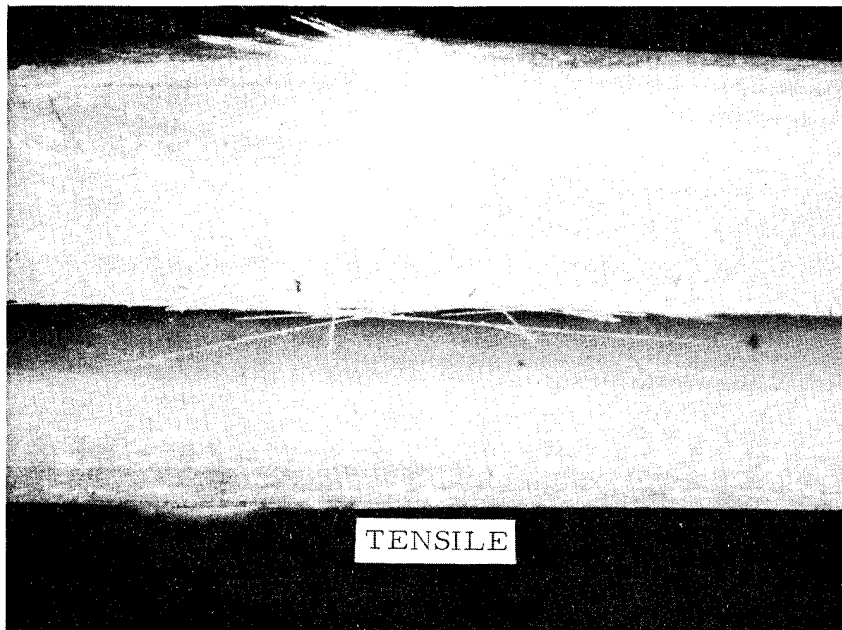


FIGURE C-37. 18X EDGE-VIEW OF IMPACT FRACTURE AREA OF  
PANEL #13 S2 GLASS

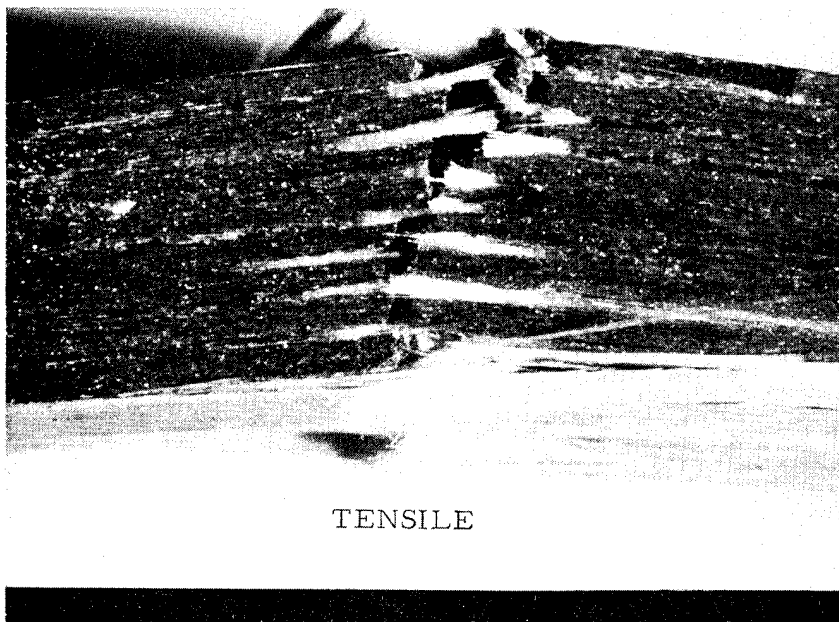


FIGURE C-38. 18X EDGE-VIEW OF IMPACT FRACTURE AREA OF  
PANEL #14 MODULITE 5206/S2 GLASS

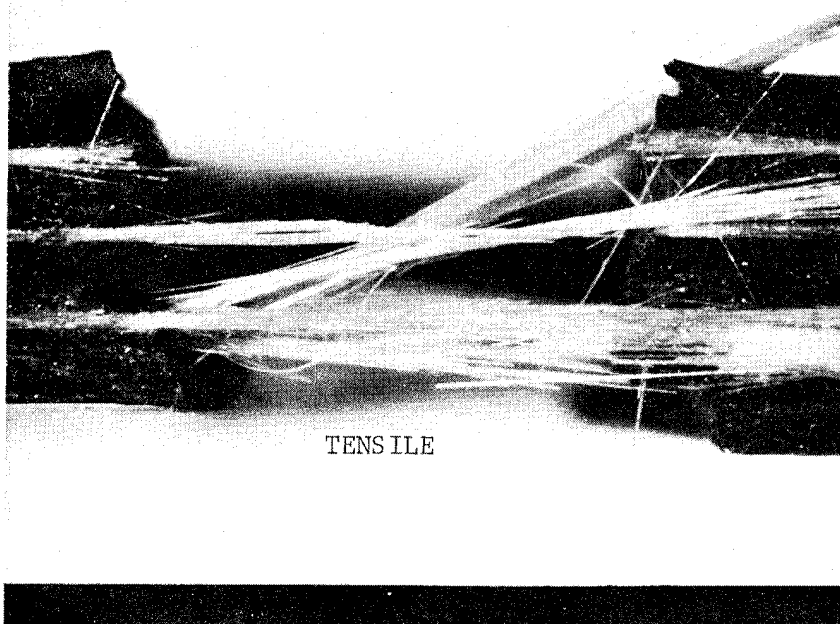


FIGURE C-39. 18X EDGE-VIEW OF IMPACT FRACTURE AREA OF  
PANEL #15 MODULITE 5206/S2 GLASS

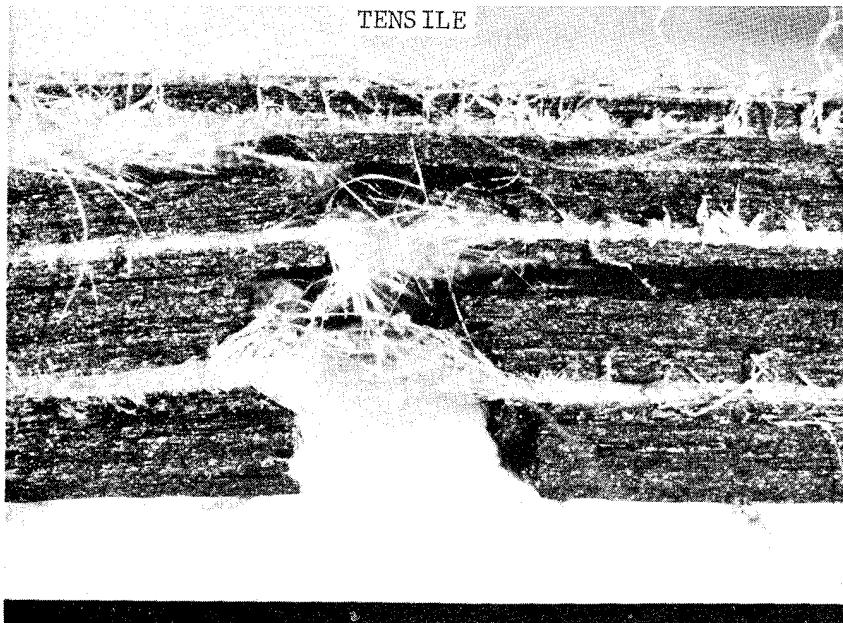


FIGURE C-40. 18X EDGE-VIEW OF IMPACT FRACTURE AREA  
OF PANEL #16 MODULITE 5206/PRD-49

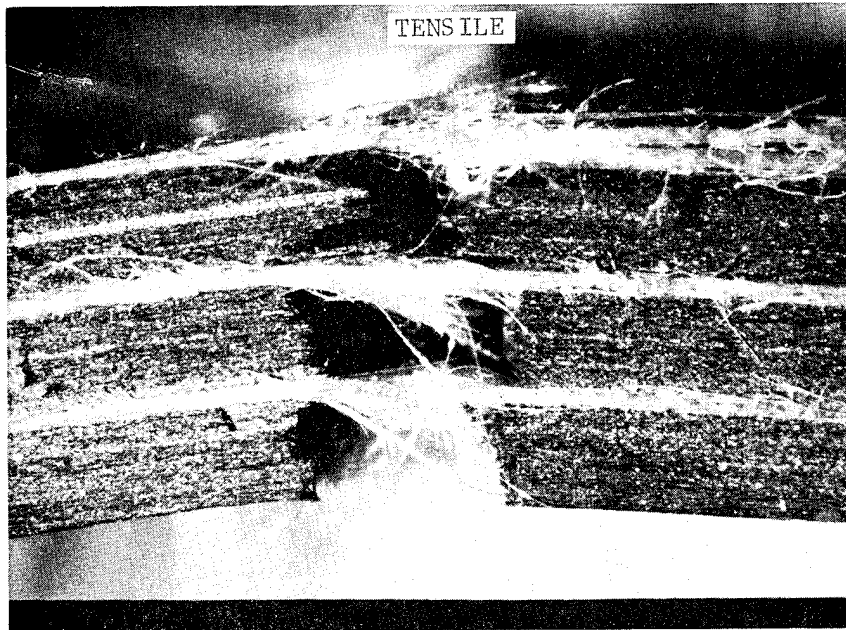


FIGURE C-41. 18X EDGE-VIEW OF IMPACT FRACTURE AREA OF PANEL #17 MODULITE 5206/PRD-49

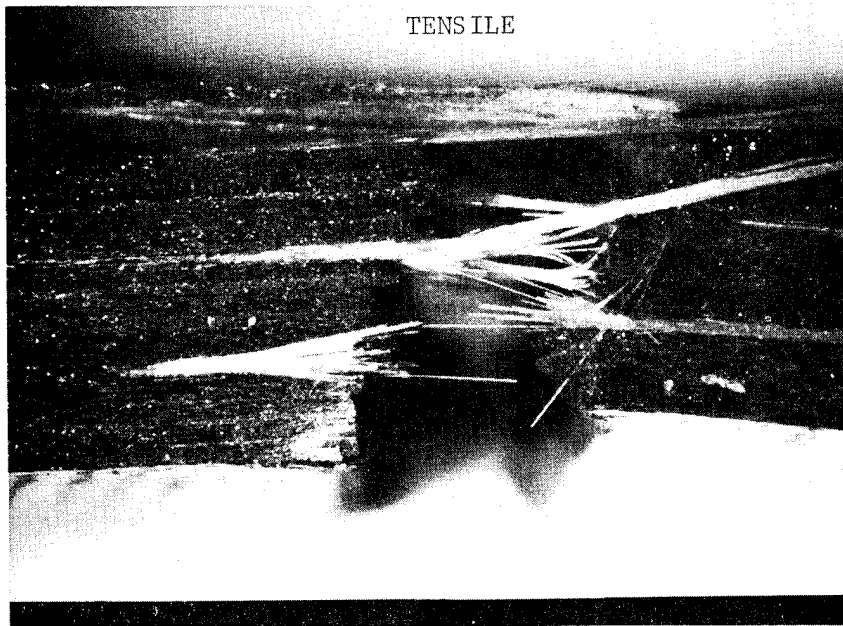


FIGURE C-42. 18X EDGE-VIEW OF IMPACT FRACTURE AREA OF PANEL #18 MODULITE 5206/S2 GLASS

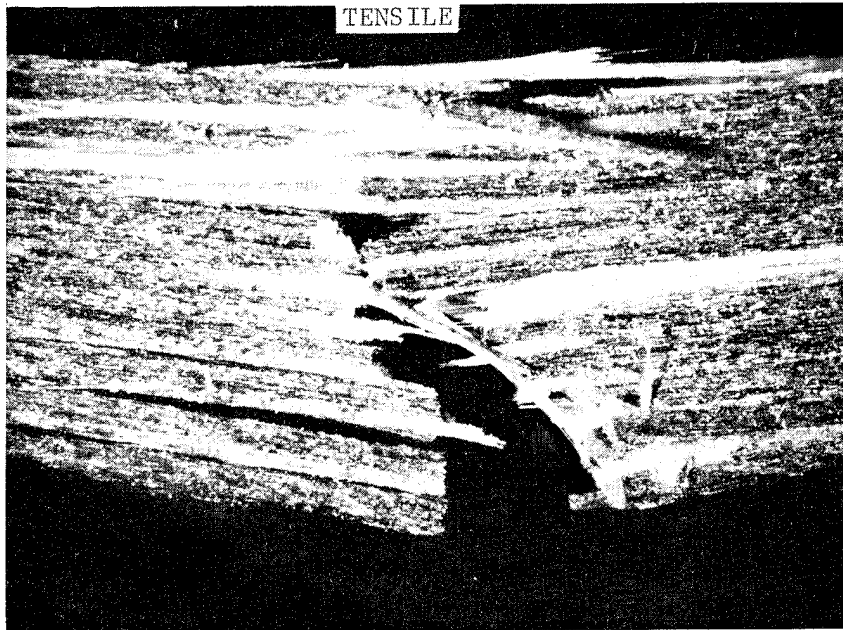


FIGURE C-43. 18X EDGE-VIEW OF IMPACT FRACTURE AREA OF PANEL #19 THORNEL 400/S2 GLASS

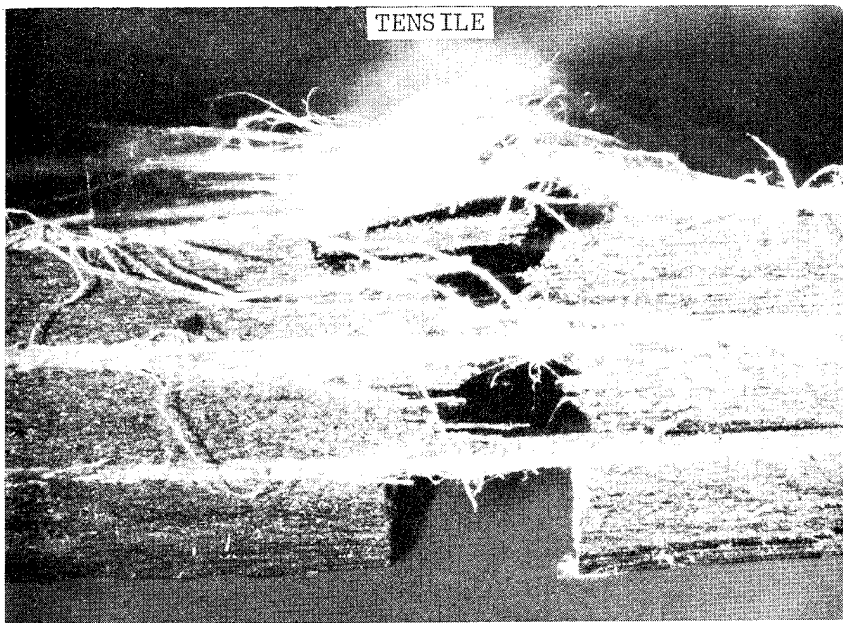


FIGURE C-44. 18X EDGE-VIEW OF IMPACT FRACTURE AREA OF PANEL #20 THORNEL 400/PRD-49

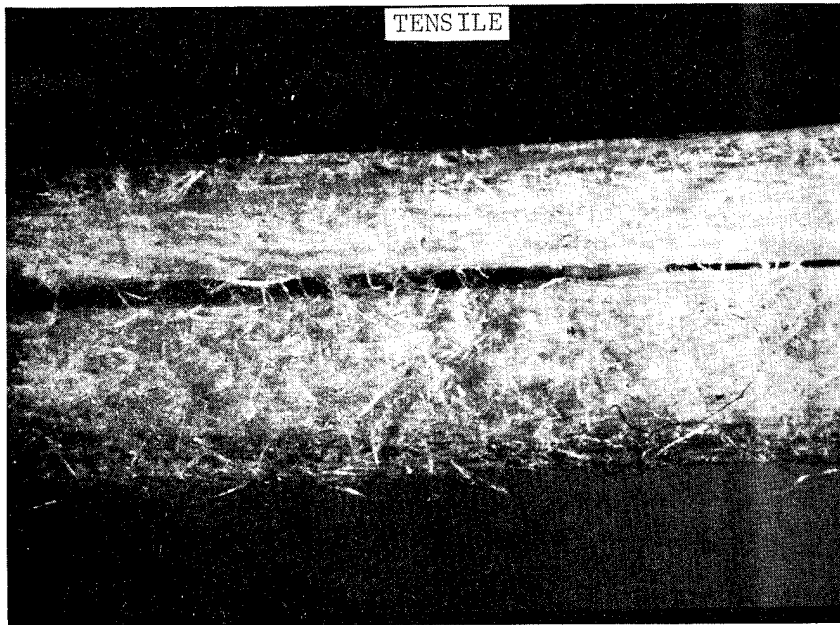


FIGURE C-45. 18X EDGE-VIEW OF IMPACT FRACTURE AREA OF PANEL #21 NOMEX NYLON

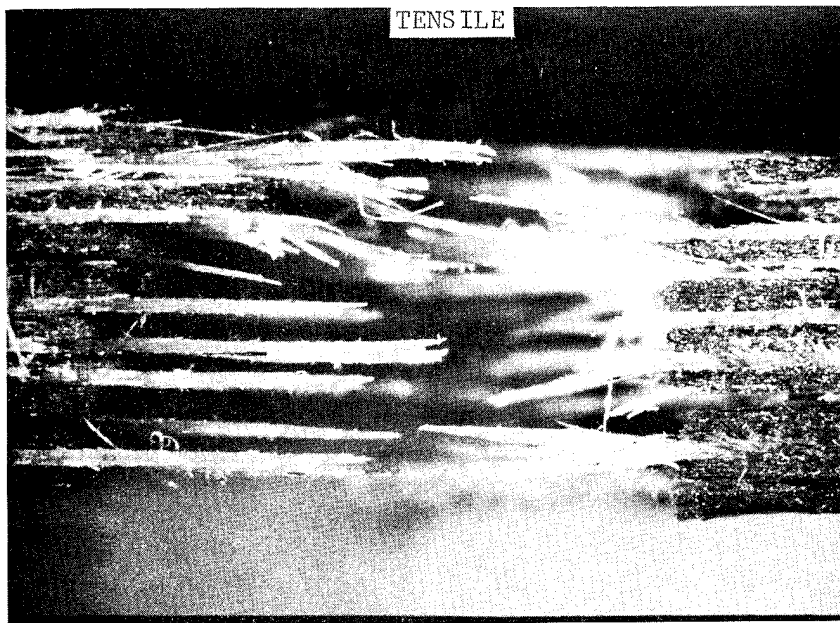


FIGURE C-46. 18X EDGE-VIEW OF IMPACT FRACTURE AREA OF PANEL #22 MODULITE 5206/NOMEX NYLON

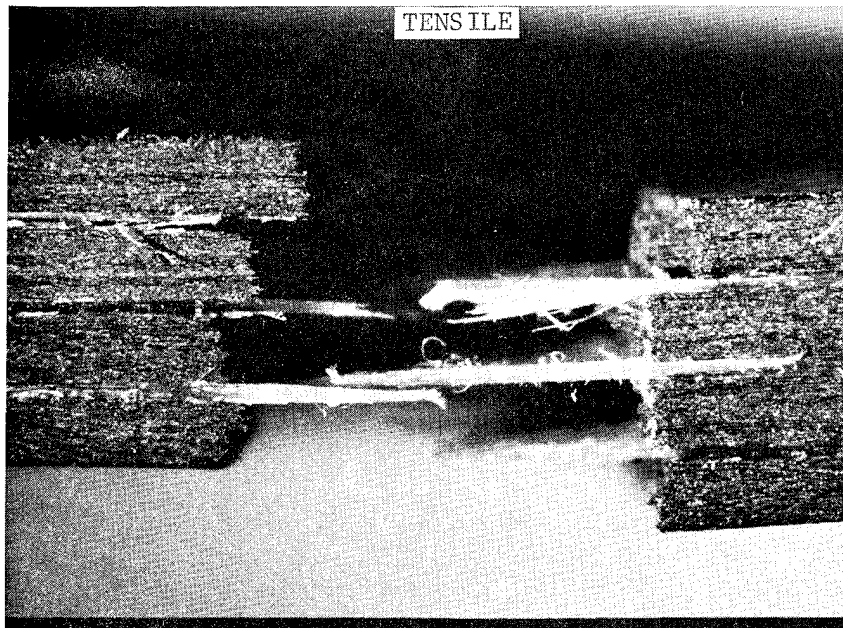


FIGURE C-47. 18X EDGE-VIEW OF IMPACT FRACTURE AREA OF PANEL #23 MODULITE 5206/NOMEX NYLON

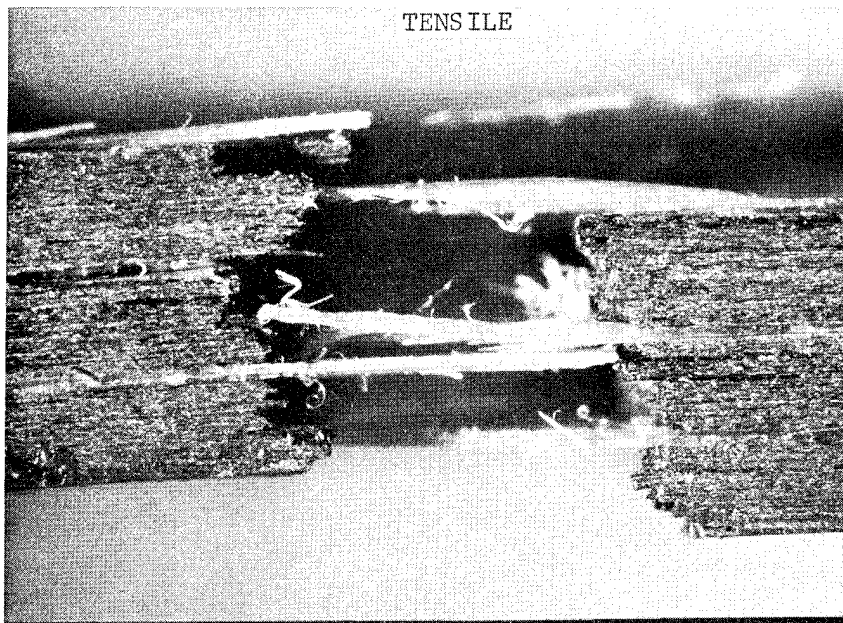


FIGURE C-48. 18X EDGE-VIEW OF IMPACT FRACTURE AREA OF PANEL #24 MODULITE 5206/NOMEX NYLON

APPENDIX D

CHARPY TEST RESULTS AND INTERPRETATION

Supplementary to the planned program, a study was conducted to determine the relative impact characteristics of selected panel configurations utilizing an instrumented Charpy impact testing apparatus. Although conceived and designed for metals fracture toughness characterization, the Charpy impact test has found its way into the area of toughness investigations of nonmetallic materials. With proper definition of test parameters, it is conceivable that valid conclusions as to nonmetallic materials toughness behavior may be reached using this method. The study was conducted only to investigate and recognize those parameters and not to arrive at preconceived conclusions.

The Charpy impact test is essentially a rapid three point bend test and provides a means of determining the relative differences in fracture toughness between two different materials. A "normal" Charpy impact test provides only information as to the total amount of impact energy absorbed. By instrumenting the Charpy striker head with a suitable transducer and providing proper amplification and recording equipment, load-time behavior can be obtained in addition to the energy absorbed. The load-time trace yields additional information about the various energies associated with the initiation and propagation of fracture.

The test apparatus is illustrated in Figure D-1. Aeronutronic Division of Philco-Ford has purchased the instrumented impact test equipment as developed and marketed by Effects Technology, Inc., and has installed it on a Reihle impact test machine. Schematically, the test instrumentation is diagrammed in Figure D-2. The striker head of the hammer is strategically instrumented with strain gages. The strain gage output is amplified and recorded on an oscilloscope triggered as the hammer interrupts the light source to the photo cell. The gages are statistically and dynamically calibrated to provide known outputs for known inputs. The striker head then acts essentially as a load cell.

Four panel configurations were selected and fabricated. The panel processing parameters are given in Table D.1. The panels were composed of Modulite 5206 (control), alternating plies of Modulite 5206 and S2CG glass (27 percent of total laminate volume), alternating plies of Modulite 5206 and PRD-49 (36 percent of total laminate volume), and alternating plies of Thornel 400 and PRD-49 (36 percent of total laminate volume). All the panels were unidirectional with all fibers aligned in the same direction.

The test results appear in Table D.2. Specimen configuration approximated the standard Charpy specimen dimensions of 0.394 by 0.394 by 2.165 inches. Actual specimen dimensions are shown in Table D.2. All specimens were impacted perpendicular to the fibers in an unnotched condition, at an impact velocity of 16.2 feet per second. Available energy at impact was 240 foot-pounds. The representative oscilloscope traces for each panel type appear as Figures D-3 through D-10. Figures D-4, D-6, D-8, and D-10 were obtained by attaching an auxiliary oscilloscope into the system and expanding the time base to obtain a clearer and more exacting picture of the initial

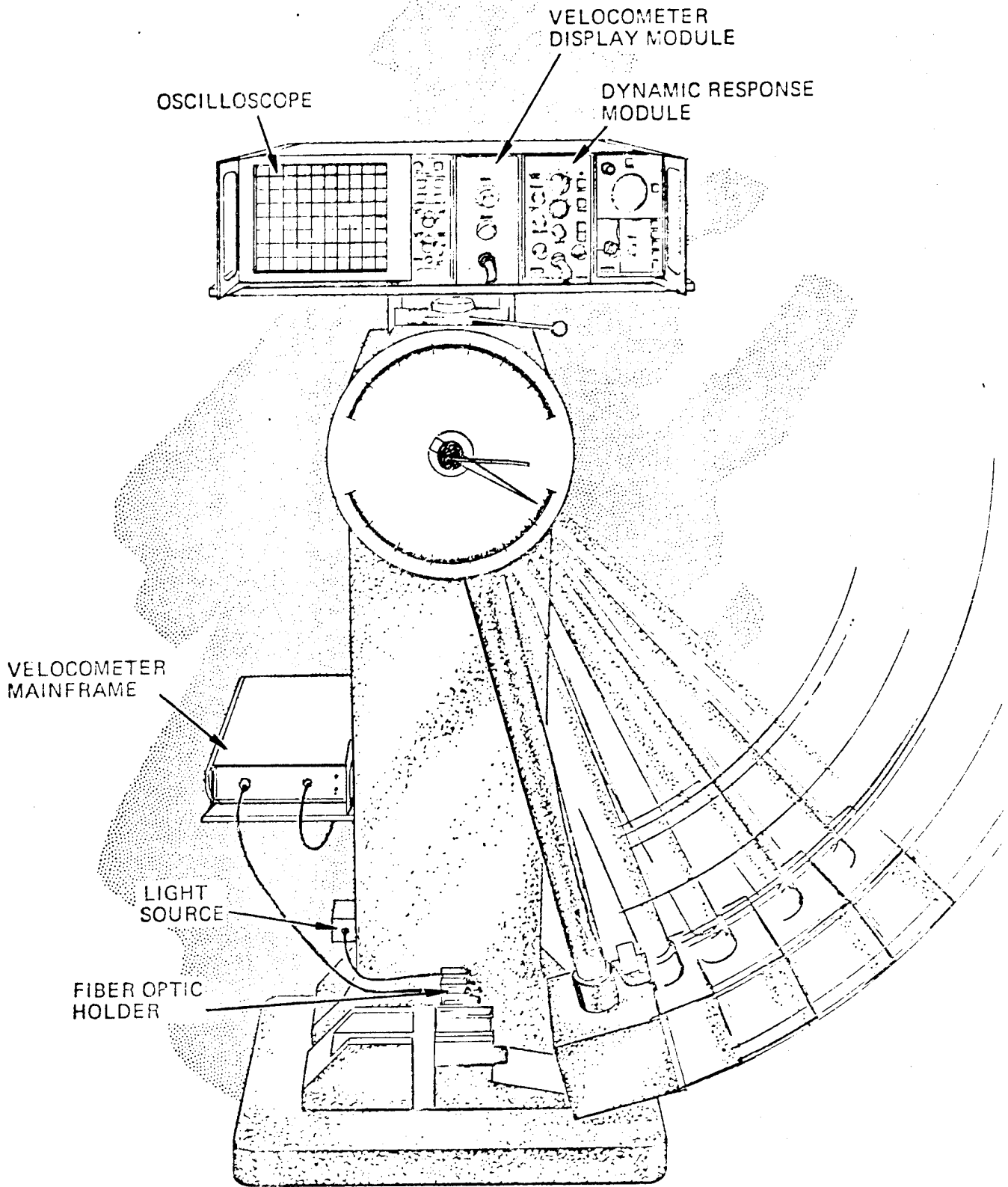
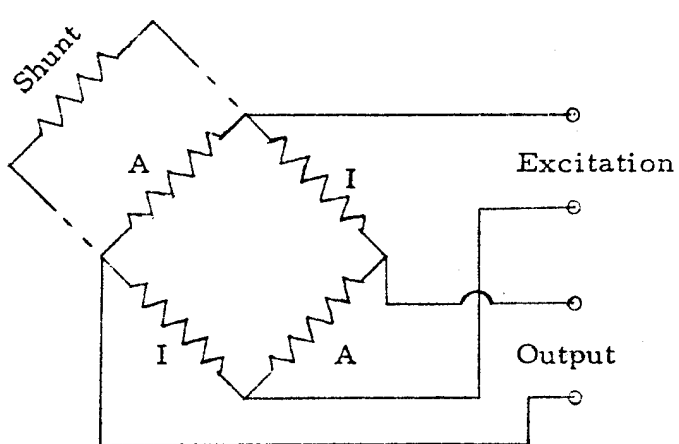
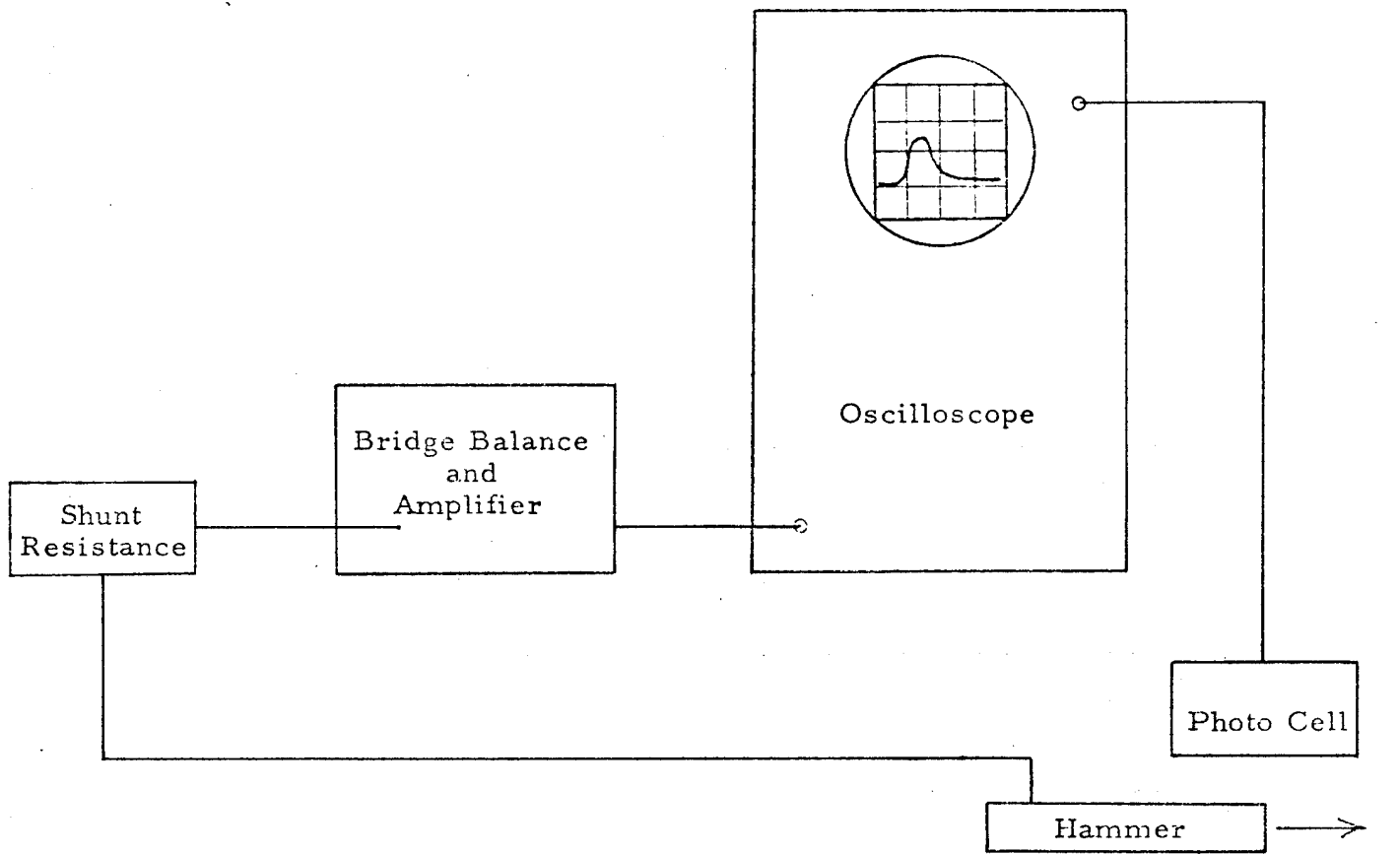


FIGURE D-1. CHARPY TESTING APPARATUS



I = Inactive Gage  
 A = Active Gage

FIGURE D-2. SCHEMATIC DIAGRAM OF THE INSTRUMENTATION FOR THE INSTRUMENTED CHARPY TEST

TABLE D.1. CHARPY TEST PANEL PROCESSING PARAMETERS

Panel Number	Panel Materials	Panel Construction	Bulk Density, g/cc	Total Fiber Volume, %	Constituent Volume, %	Prepreg Resin Content, W %	Prepreg Volatile Content, W %	Thickness, mils
26	Modulite 5206	53 plies	1.58	52	52	43	0.7	375
27	Modulite 5206 S2 Glass	40 alternating plies each	1.70	57	30 (M5206) 27 (S2)	39	1.2	389
28	Modulite 5206 PRD-49	35 alternating plies each	1.47	62	26 (M5206) 36 (PRD)	43	2	381
29	Thornel 400 PRD-49	40 alternating plies each	1.50	68	32 (T400) 36 (PRD)	42	3	419

TABLE D.2. CHАРY TEST RESULTS

Panel Number	Panel (1) Description	Specimen	Dimensions		Peak Load P <sub>max</sub> , lbs	Time to Initial Fracture LI, msec	Energy At Initial Fracture EI, ft-lbs	Total Impact Energy E <sub>T</sub> , ft-lbs	Normalized Energy at Initial Fracture ENI, ft-lbs/in W/in T	Normalized Total Impact Energy ENT, ft-lbs/in W/in T
			Width W, inches	Thickness T, inches						
26	Modulite 5206 F.V. = 52%	1	0.359	0.373	2910	0.29	6.4	11.3	47.8	84.4
		2	0.360	0.369	2590	0.27	5.7	8.3	42.9	62.5
		3	0.359	0.375	2640	0.26	5.1	8.1	37.9	60.1
		AVG			2713	0.27	5.7	9.2	42.9	69.0
27	M5206 30% S2 Glass 27% F.V. = 57%	1	0.360	0.393	1510	0.16	3.0	22.1	21.2	156.0
		2	0.361	0.389	1500	0.17	1.8	25.1	12.8	178.0
		3	0.361	0.390	1420	0.16	2.1	21.2	14.9	150.0
		AVG			1479	0.16	2.3	22.8	16.3	161.0
28	M5206 26% PRD-49 36% F.V. = 62%	1	0.378	0.385	773	0.18	1.0	19.4	6.9	133.0
		2	0.378	0.380	680	0.16	1.0	16.5	7.0	115.0
		3	0.376	0.376	770	0.16	1.0	18.3	7.1	129.0
		AVG			741	0.17	1.0	18.1	7.0	126.0
29	T400 32% PRD-49 36% F.V. = 68%	1	0.392	0.410	681	0.15	1.2	21.5	7.5	134.0
		2	0.391	0.419	685	0.15	1.0	23.3	6.1	142.0
		3	0.391	0.403	660	0.14	1.2	21.5	7.6	136.0
		AVG			675	0.15	1.2	22.1	7.1	137.0

(1) See Table D.1.

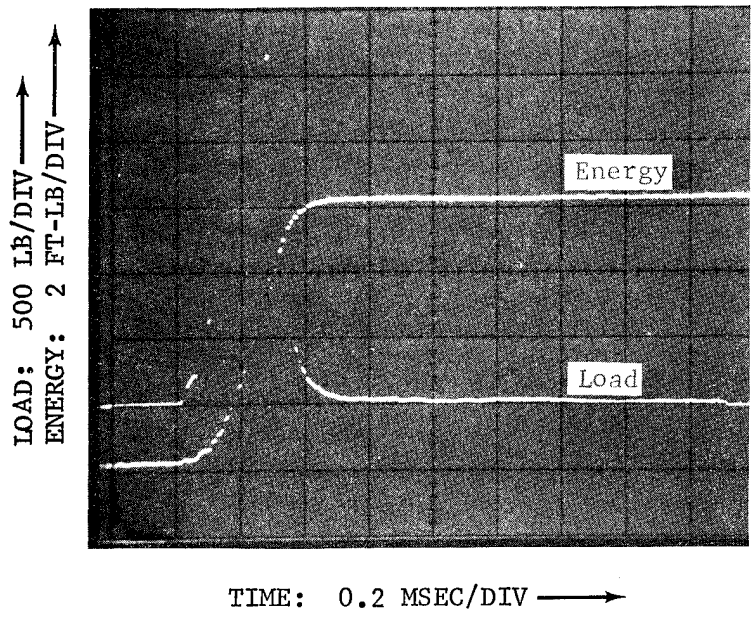


FIGURE D-3. LOAD-TIME AND ENERGY TRACES FOR MODULITE 5206, SPECIMEN 26-3

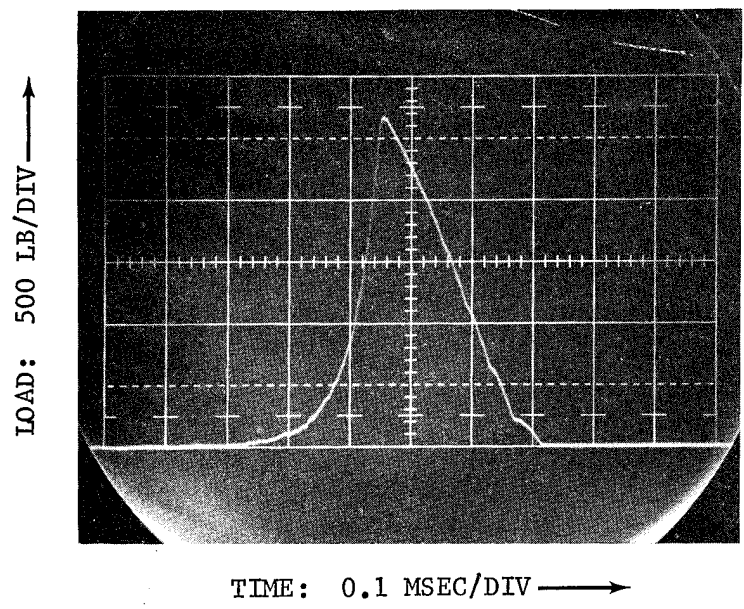


FIGURE D-4. EXPANDED LOAD-TIME TRACE OF SPECIMEN 26-3

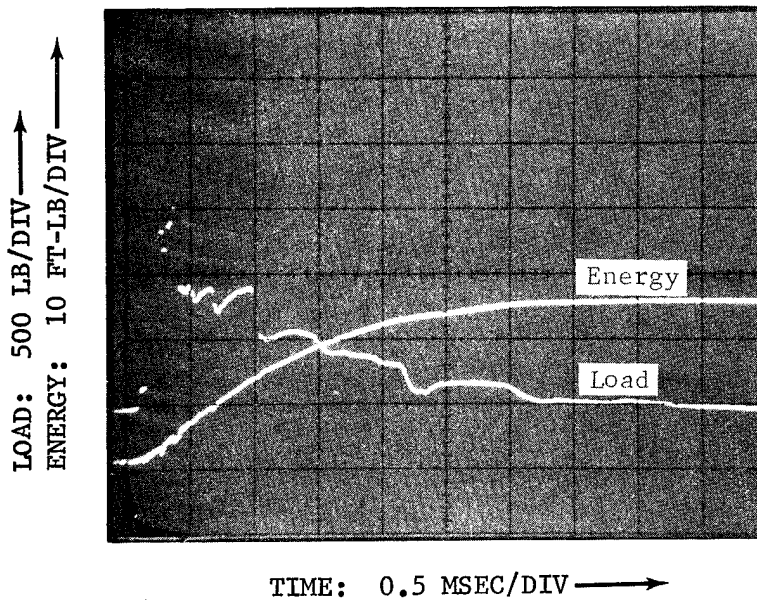


FIGURE D-5. LOAD-TIME AND ENERGY TRACES FOR MODULITE 5206/S2 GLASS, SPECIMEN 27-2

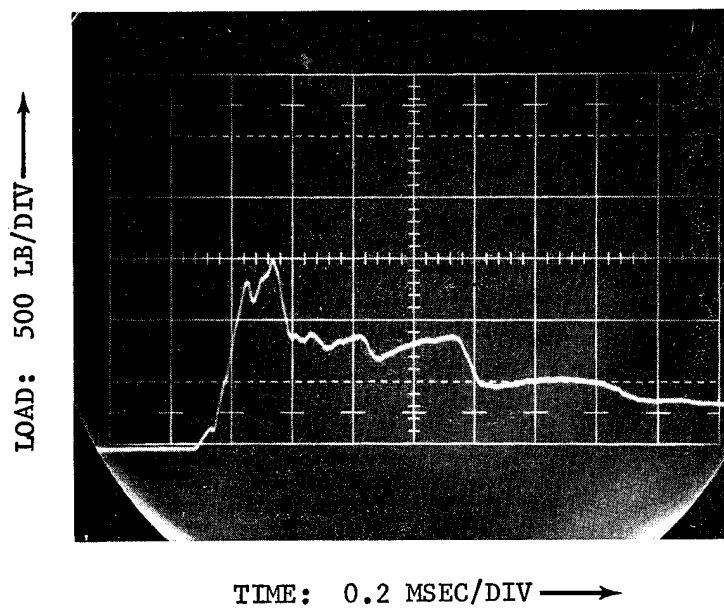


FIGURE D-6. EXPANDED LOAD-TIME TRACE OF SPECIMEN 27-2

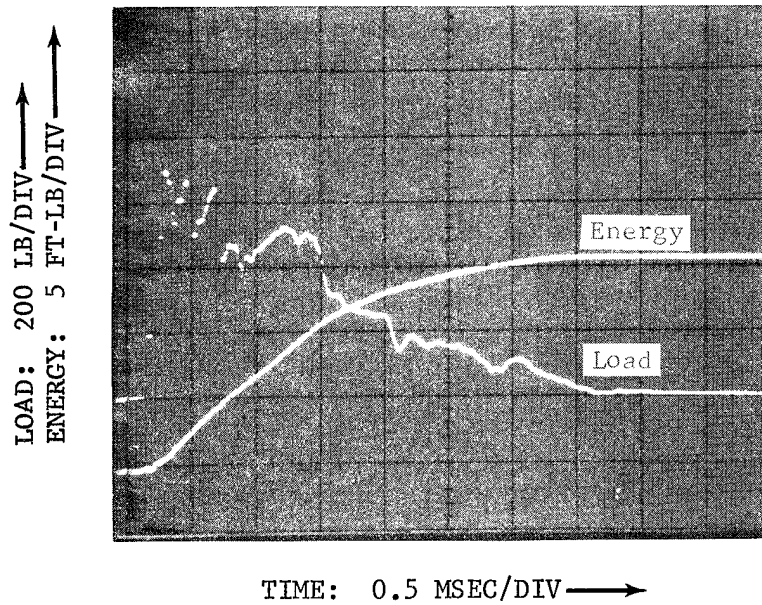


FIGURE D-7. LOAD-TIME AND ENERGY TRACES FOR MODULITE 5206/PRD-49, SPECIMEN 28-2

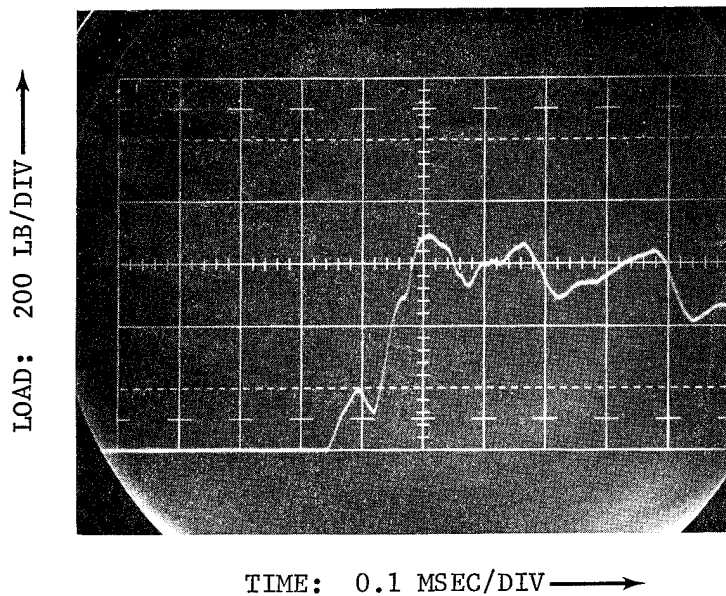


FIGURE D-8. EXPANDED LOAD-TIME TRACE OF SPECIMEN 28-2

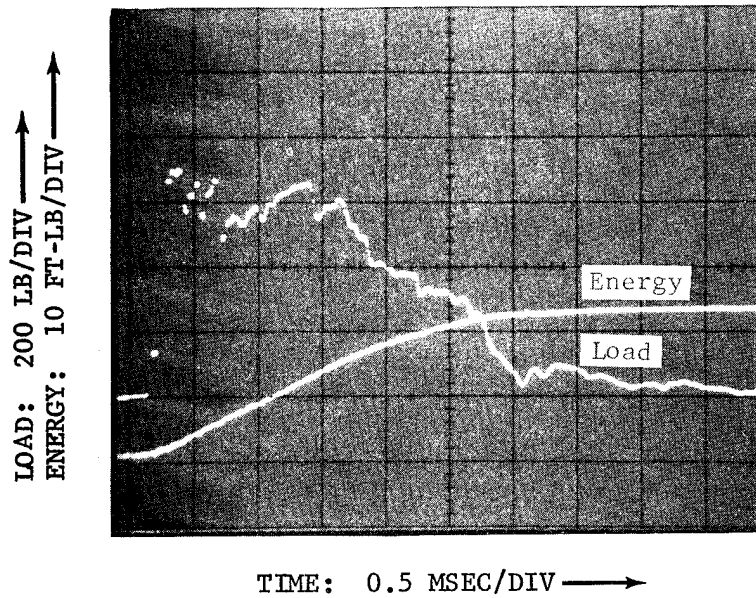


FIGURE D-9. LOAD-TIME AND ENERGY TRACES FOR THORNEL 400/PRD-49, SPECIMEN 29-2

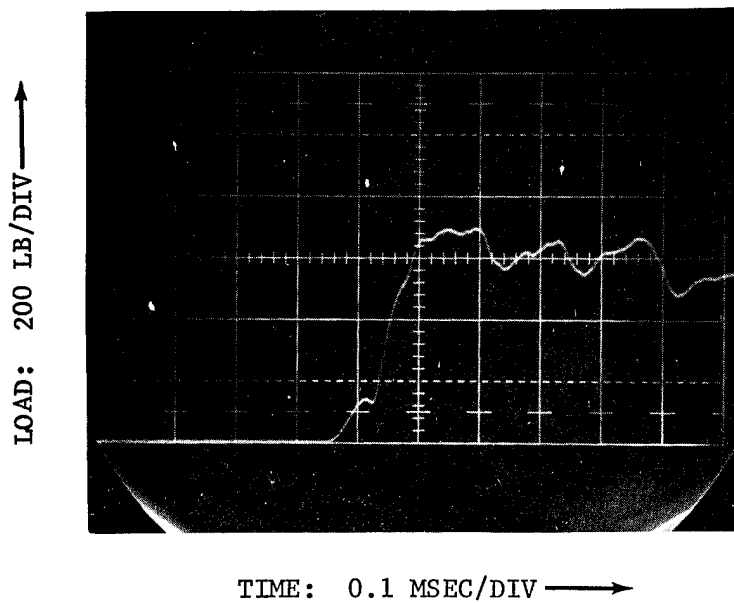


FIGURE D-10. EXPANDED LOAD-TIME TRACE OF SPECIMEN 29-2

impact behavior. The energy curve on Figures D-3, D-5, D-7, and D-9 is simply an instantaneous integration of the load-time trace providing a record of total energy absorbed at any point in time. The initial "glitch" in each load-time trace appearing at approximately 200 pounds is attributed to inertial loading of the head. Representative post-test specimens are shown in Figure D-11.

It is apparent from the load-time trace in Figures D-3 and D-4 that the Modulite 5206 acted in a nearly "brittle" manner. The point of initial fracture corresponds to complete catastrophic failure. This is not the case for any of the hybrid panels whose load-time traces appear in Figures D-5 through D-10. The hybrid panels continue to absorb large amounts of energy after initial fracture. Looking at the normalized energy values given in Table D.2, it can be seen that at initial fracture the Modulite 5206 panel has absorbed over 60 percent of the total impact energy while the hybrid panels are only capable of absorbing 5 to 10 percent of the total impact energy before initial fracture. This is a significant point. The normalized energies at initial fracture for the hybrid panels are significantly lower than the normalized energy at initial fracture for the "brittle" Modulite 5206. It takes a lower amount of energy to initiate fracture of a hybrid panel than it does for a Modulite 5206 panel. The time to initial fracture for the hybrids is approximately half of the time to initial fracture for Modulite 5206. However, it must be remembered that initial fracture for the hybrids does not correspond to catastrophic failure. Specimen integrity would be maintained could a "low-blow" of 16.3 ft-lbs/in W/in T in the case of panel 27 be delivered to the specimen. Initial fracture, however, would occur. This same "low-blow" value could be delivered repeatedly to the Modulite 5206 panel 26 with no effect. But, conversely, a "low-blow" of 42.9 ft-lbs/in W/in T which would cause initial fracture and ultimately complete fracture to the Modulite 5206 panel 26 would not completely fail a specimen made from panel 27. It would only cause initial fracture plus possibly some fracture propagation.

A look at Figure D-11 shows that delamination is the principal failure mode for the hybrid panels while the Modulite 5206 underwent a "brittle" cleavage mode of failure. Any cleavage of the graphite plies in the hybrid panels appears to be arrested by delamination of the supplemental reinforcement/graphite reinforcement interface.

The instrumented Charpy test provides additional information of significant interest about the impact specimen response and failure mechanisms involved. Investigations should be carried out to better define the test parameters involved, material variables and responses, and significance of test results to specific materials applications.

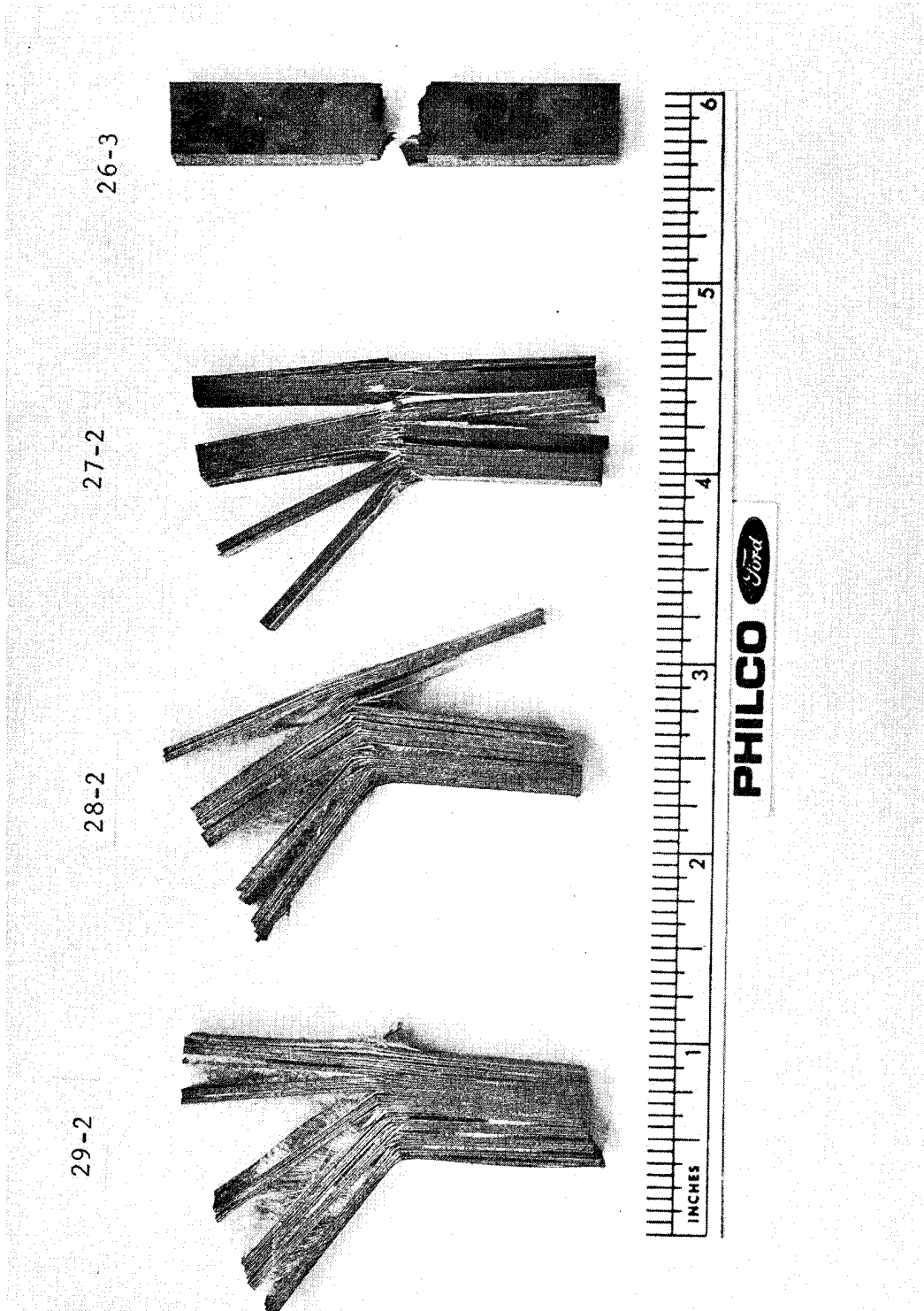


FIGURE D-11. POST TEST SPECIMENS DEPICTING DELAMINATION OF HYBRID PANELS (27, 28, 29) AND BRITTLE BEHAVIOR OF MODULITE 5206 CONTROL PANEL (26)



Unclassified

SECURITY CLASSIFICATION OF THIS PAGE(When Data Entered)

Block 20. Abstract (Continued)

improve interfacial (resin-fiber) bonding properties in the composites.

The most promising third phase additive was S-2 glass yarn which increased the impact strength of a graphite composite 550% for a 25% fiber volume composite and 260% for a 10% fiber volume composite.

Instrumented Charpy impact strengths were determined for selected composites. Ultimate loads and load versus time data demonstrated the large energy absorption characteristics of the hybrid composites and identified and delineated significant and subtle differences in fracture energy levels.

Unclassified

SECURITY CLASSIFICATION OF THIS PAGE(When Data Entered)

(Contract N00019-71-C-0166)

DISTRIBUTION LIST

Naval Air Systems Command  
Washington, D. C. 20361  
Attn: AIR-50174  
(9 copies)  
For distribution as follows:  
AIR-52032D (3 copies)  
AIR-50174 (6 copies)

Office of Naval Research  
Washington, D. C. 20360  
(Code 472)

Naval Research Laboratory  
Washington, D. C. 20360  
(Code 6306)  
(Code 6120)  
(2 copies)

Naval Ordnance Laboratory  
White Oak, Maryland 20910  
(Code 234)

Air Force Materials Laboratory  
Wright-Patterson Air Force Base  
Ohio 45433  
Attn: LC 1, LN 1, LTF 1, LAE 1  
(4 copies)

Air Force Flight Dynamics Lab.  
Wright-Patterson Air Force Base  
Ohio 45433  
Attn: FDTC

Defense Ceramic Information Center  
Battelle Memorial Institute  
505 King Avenue  
Columbus, Ohio 43201

Illinois Institute of Technology  
Research Institute  
10 West 34th Street  
Chicago, Illinois 60616  
Attn: Dr. R. Cornish

Director  
Plastics Technical Evaluation Center  
Picatinny Arsenal  
Dover, New Jersey 07801  
(2 copies)

Hercules Incorporated  
Magna, Utah 84044  
Attn: Mr. E. G. Crossland

Commonwealth Scientific Corporation  
500 Pendelton Street  
Alexandria, Virginia 22314

Northrop Corporation  
3901 W. Broadway  
Hawthorne, California 90250  
Attn: Mr. J. Damman

Naval Air Propulsion Test Center  
Trenton, New Jersey 08628  
Attn: Mr. J. Glatz

Chief of Naval Material  
Deep Submergence Systems  
Project Office  
Washington, D. C. 20360  
Attn: Mr. H. Bernstein PM-11221

Commander  
U. S. Naval Weapons Center  
China Lake, California 92555

Celanese Research Company  
Box 1000  
Summit, New Jersey 07901  
Attn: Mr. R. J. Leal

Naval Ship Engineering Center  
Navy Department  
Washington, D. C. 20360

Brunswick Corporation  
Technical Products Division  
325 Brunswick Lane  
Marion, Virginia 24354

NASA Headquarters  
600 Independence Avenue S. W.  
Washington, D. C. 20546  
Code RV-2 (Mr. N. Mayer)

The Boeing Company  
Aerospace Division  
P. O. Box 3707  
Seattle, Washington 98124  
Attn: Mr. G. E. Hughes

Commanding Officer  
Naval Air Development Center  
Warminster, Pennsylvania 18974  
Attn: Air Vehicle Technology Dept.

Naval Ship Research & Development  
Center  
Washington, D. C.  
Attn: Mr. M. Krenzke, Code 727

NASA  
Lewis Research Center  
21000 Brookpark Road  
Cleveland, Ohio 44135

NASA  
Langley Research Center  
Hampton, Virginia

United Aircraft Corporation  
United Aircraft Research Labs.  
E. Hartford, Connecticut 06108

United Aircraft Corporation  
Pratt & Whitney Aircraft Division  
East Hartford, Connecticut 06108

United Aircraft Corporation  
Pratt & Whitney Aircraft Division  
East Hartford, Connecticut 06108  
Attn: Mr. K. Boll

Naval Ordnance Systems Command  
Navy Department  
Washington, D. C. 20360  
(Code ORD 033)

Union Carbide Corporation  
Carbon Products Division  
P. O. Box 6116  
Cleveland, Ohio 44101

General Dynamics, Convair Division  
P. O. Box 1128  
San Diego, California 92112  
Attn: Mr. W. G. Scheck  
Dept. 572-10

The Rand Corporation  
1700 Main Street  
Santa Monica, California 90406

HITCO  
1600 W. 135th Street  
Gardena, California 90406

AVCO Corporation  
Applied Technology Division  
Lowell, Massachusetts 01851

Department of the Army  
Army Materials & Mechanics  
Research Center  
Watertown, Massachusetts 02172

North American Aviation  
Columbus Division  
4300 E. Fifth Avenue  
Columbus, Ohio 43216

McDonnell-Douglas Corporation  
Douglas Aircraft Company  
3855 Lakewood Blvd.  
Long Beach, California 90801  
Attn: Mr. R. J. Palmer

General Electric Company  
Valley Forge Space Center  
Philadelphia, Pennsylvania 19101

United Aircraft Corporation  
Sikorsky Aircraft Division  
Stratford, Connecticut 06602  
Attn: Dr. M. Salkind

United Aircraft Corporation  
Hamilton-Standard Division  
Windsor Locks, Connecticut  
Attn: Mr. T. Zajac

Monsanto Research Corporation  
1515 Nicholas Road  
Dayton, Ohio 45407

Material Sciences Corporation  
1777 Walton Road  
Blue Bell, Pennsylvania 19422

U. S. Army Air Mobility R&D Lab.  
Fort Eustis, Virginia  
Attn: SAVDL-EU-SS (Mr. J. Robinson)

B. F. Goodrich Aerospace and  
Defense Products  
500 South Main Street  
Akron, Ohio 44318

Great Lakes Research Corporation  
P. O. Box 1031  
Elizabethton, Tennessee

Whittaker Corporation  
Research and Development Division  
3540 Aero Court  
San Diego, California 92123

Washington University  
St. Louis, Missouri 03130

University of Maryland  
College Park, Maryland 20742  
Attn: Dr. W. J. Bailey

**PHILCO**



Philco-Ford Corporation  
Aeronutronic Division  
Newport Beach, Calif. • 92663